



National Library  
of Canada

Bibliothèque nationale  
du Canada

Canadian Theses Service

Service des thèses canadiennes

Ottawa, Canada  
K1A 0N4

## NOTICE

The quality of this microform is heavily dependent upon the quality of the original thesis submitted for microfilming. Every effort has been made to ensure the highest quality of reproduction possible.

If pages are missing, contact the university which granted the degree.

Some pages may have indistinct print especially if the original pages were typed with a poor typewriter ribbon or if the university sent us an inferior photocopy.

Reproduction in full or in part of this microform is governed by the Canadian Copyright Act, R.S.C. 1970, c. C-30, and subsequent amendments.

## AVIS

La qualité de cette microforme dépend grandement de la qualité de la thèse soumise au microfilmage. Nous avons tout fait pour assurer une qualité supérieure de reproduction.

S'il manque des pages, veuillez communiquer avec l'université qui a conféré le grade.

La qualité d'impression de certaines pages peut laisser à désirer, surtout si les pages originales ont été dactylographiées à l'aide d'un ruban usé ou si l'université nous a fait parvenir une photocopie de qualité inférieure.

La reproduction, même partielle, de cette microforme est soumise à la Loi canadienne sur le droit d'auteur, SRC 1970, c. C-30, et ses amendements subséquents.

UNIVERSITY OF ALBERTA

THE EFFECT OF LIGHT ON SELECTED PROPERTIES OF  
PARYLENE C-COATED SILK FABRICS

BY  
BONNIE G. HALVORSON



A THESIS  
SUBMITTED TO THE FACULTY OF GRADUATE STUDIES AND RESEARCH IN  
PARTIAL FULFILLMENT OF THE REQUIREMENTS FOR THE DEGREE OF

MASTER OF SCIENCE  
DEPARTMENT OF CLOTHING AND TEXTILES

EDMONTON, ALBERTA  
FALL, 1991



National Library  
of Canada

Bibliothèque nationale  
du Canada

Canadian Theses Service    Service des thèses canadiennes

Ottawa, Canada  
K1A 0N4

The author has granted an irrevocable non-exclusive licence allowing the National Library of Canada to reproduce, loan, distribute or sell copies of his/her thesis by any means and in any form or format, making this thesis available to interested persons.

The author retains ownership of the copyright in his/her thesis. Neither the thesis nor substantial extracts from it may be printed otherwise reproduced without his/her permission.

L'auteur a accordé une licence irrévocable et non exclusive permettant à la Bibliothèque nationale du Canada de reproduire, prêter, distribuer ou vendre des copies de sa thèse de quelque manière et sous quelque forme que ce soit pour mettre des exemplaires de cette thèse à la disposition des personnes intéressées.

L'auteur conserve la propriété du droit d'auteur qui protège sa thèse. Ni la thèse ni des extraits substantiels de celle-ci ne doivent être imprimés ou autrement reproduits sans son autorisation.

ISBN 0-315-69919-1

Canada

Bonnie Halvorson  
301 Printing Services Building  
University of Alberta  
Edmonton, Alberta  
June 5, 1991

AMD

Elsevier Science Publishing Company Inc.  
Journal Information Centre

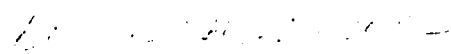
To Whom it may Concern:

I am a student at the University of Alberta, Canada, presently completing my Master of Science thesis in textile conservation. I would like to obtain permission to reprint a diagram illustrating the structure of silk fibroin as part of my literature review.

The diagram I would like to reprint originally appeared in the publication The Symposia of the Society for Experimental Biology, Number XXXIV, published by the Press Syndicate of the University of Cambridge. However, when I wrote to them requesting permission, their reply indicated I should write to you, as the diagram was based on diagrams originally published in Biochimica et Biophysica Acta (1955) in an article entitled "An Investigation of the Structure of Silk Fibroin" by Marsh, Corey and Pauling beginning on page 1 of volume 16. I enclose a copy of the diagram in question and also of the letter I sent to Cambridge, and their reply. §

The diagram would be a valuable addition to my literature review, if you can grant permission for me to use it. Clearly, the original sources of the diagram would be acknowledged in my thesis. I look forward to your reply. My office phone number is (403) 492-7216 if you would like to contact me by phone. Thank you for considering my request.

Sincerely,

  
Bonnie Halvorson

Permission granted subject to  
permission from the author(s)  
and to full acknowledgement of  
the source.  
Elsevier Science Publishers

24 June 1991





University of Alberta  
Edmonton

Department of Clothing and Textiles  
Faculty of Home Economics

Canada T6G 2N1

361 Printing Services Building, Telephone (403) 432-2479

Press Syndicate of the University of Cambridge  
The Pitt Building  
Trumpington Street  
Cambridge, CB2 1RP  
April 18, 1991

To Whom it May Concern:

I am a student at the University of Alberta, Canada, presently completing my Master of Science thesis in textile conservation. I would like to ask for permission to reprint a diagram which appeared in your publication The Symposia of the Society for Experimental Biology, Number XXXIV, "The Mechanical Properties of Biological Materials", edited by J.F V. Vincent and J. D. Curry (1980). The diagram was part of the chapter "Silks- Their Properties and Functions" by Mark W. Denny and appeared on page 258. A photocopy of this page has been enclosed.

This diagram is the best I have seen in illustrating the complex structure of silk clearly, and would be an important addition to the portion of my thesis literature review devoted to silk structure. Clearly, the original source of the diagram would be acknowledged in my thesis. Thankyou for considering this request.

Sincerely,

*Bonnie Halvorson*

Bonnie Halvorson

bgh  
encl:1

cc 32 East 57th Street  
New York City, NY

*I was not sure who to  
mail this letter to, so  
I sent it to both the  
Cambridge and NY offices  
SEND TO ~~LEFE~~  
N.Y. ONLY!*

Permission is granted provided full  
acknowledgements are given to the author,  
title of the book, and ourselves as  
publisher.

*Mark F. Anderson*  
Subsidiary Rights Department  
Cambridge University Press

*8/5/91*

 **NOVA TRAN** CORPORATION

100 Deposition Drive  
Phone (715) 263-2333

• Clear Lake, WI 54005  
FAX (715) 263-3189

May 3, 1991

Ms. Bonnie Halvorsen  
University of Alberta  
Dept. of Clothing & Textiles  
301 Printing Services Bldg.  
Edmonton, Alberta T6G 2N1

Dear Bonnie,

Sorry to take so long getting back to you. You know how it goes!

In regard to the Windover Fabric, you may summarize as you wish from this paper. It has finally been published and I am enclosing the source information for you.

The source of the U.V. data is probably from a U.C.C. internal report or Spivak's paper which I also enclose for your reference.

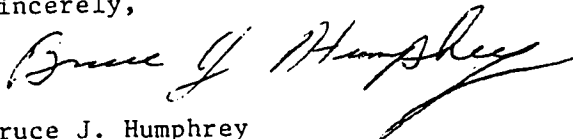
[ You may use any of the diagrams and tables in your paper, that's what they are for.

If you would like to have a U.C.C. scientist proofread your draft and comment, I as well as Dr. Beach, would be willing to assist. Just let me know.

In any case, we would like to have copies of your work.

I hope all goes well with your work, and hope to see you at some future date.

Sincerely,



Bruce J. Humphrey  
Conservation Specialist

BJH:ras

Enclosures



A Subsidiary of  
Union Carbide Corporation

# CANADIAN TEXTILE

JOURNAL • LA REVUE DU

# TEXTILE CANADIEN

August 13, 1991

Bonnie Halvorson  
Department of Clothing and Textiles  
University of Alberta  
Edmonton, AB T6G 2N1

Dear Ms. Halvorson:

In answer to your request of August 4, I am happy to say you are welcome to make use in your thesis of the diagram on page 50 of the May 15, 1969 **Canadian Textile Journal**. All we require is that you credit the magazine when this material is reproduced.

If I can be of further help to you, please let me know. Good luck with your thesis.

Yours sincerely,



Kathryn Hanley  
Editor

1 page total

UNIVERSITY OF ALBERTA  
RELEASE FORM

NAME OF AUTHOR: BONNIE G. HALVORSON  
TITLE OF THESIS: THE EFFECT OF LIGHT ON SELECTED  
PROPERTIES OF PARYLENE C-COATED SILK  
FABRICS  
DEGREE: MASTER OF SCIENCE  
YEAR THIS DEGREE GRANTED: 1991

PERMISSION IS HEREBY GRANTED TO THE UNIVERSITY OF ALBERTA  
LIBRARY TO REPRODUCE SINGLE COPIES OF THIS THESIS AND TO LEND  
OR SELL SUCH COPIES FOR PRIVATE, SCHOLARLY OR SCIENTIFIC  
RESEARCH PURPOSES ONLY.

THE AUTHOR RESERVES OTHER PUBLICATION RIGHTS, AND NEITHER  
THE THESIS NOR EXTENSIVE EXTRACTS FROM IT MAY BE PRINTED OR  
OTHERWISE REPRODUCED WITHOUT THE AUTHOR'S WRITTEN PERMISSION.



77 Calder Crescent  
Regina, Saskatchewan  
Canada, S4S 4A5

August 28 , 1991



UNIVERSITY OF ALBERTA  
FACULTY OF GRADUATE STUDIES AND RESEARCH

THE UNDERSIGNED CERTIFY THEY HAVE READ, AND RECOMMEND TO THE FACULTY OF GRADUATE STUDIES AND RESEARCH FOR ACCEPTANCE, A THESIS ENTITLED THE EFFECT OF LIGHT ON SELECTED PROPERTIES OF PARYLENE C-COATED SILK FABRIC SUBMITTED BY BONNIE G. HALVORSON IN PARTIAL FULFILLMENT OF THE REQUIREMENTS FOR THE DEGREE OF MASTER OF SCIENCE IN CLOTHING AND TEXTILES.

*Nancy Kerr*  
\_\_\_\_\_  
Dr. N. Kerr (supervisor)

*Betty Crown*  
\_\_\_\_\_  
Dr. E. Crown

*M. Hollingsworth*  
\_\_\_\_\_  
Dr. M. Hollingsworth

Date: *August 15, 1991*

## ABSTRACT

Consolidation of highly degraded silk artifacts is problematic for the textile conservator because there is no entirely satisfactory treatment method. One option recently introduced to the field of conservation is parylene C, a polymer whose unique gas-phase deposition method allows extremely thin (below 1  $\mu\text{m}$ ), highly conformal coatings to be applied.

For parylene C to be used successfully as a conservation treatment, the coating must not only have a positive initial effect, but must also resist degradation over time. In order to evaluate the long-term effect of light on parylene C-coated silk fabrics, the change in colour, flexural rigidity, tensile properties, and moisture regain after accelerated photochemical aging was measured, and the fabrics analyzed with SEM. The samples were aged by placing them in a xenon-arc Weather-Ometer: some samples were masked from the light, or protected by a UV filter (which excluded radiation with wave-lengths below 400 nm), while others were exposed to the full simulated daylight spectrum emitted by the xenon arc lamp.

The effect of the parylene C coating was found to depend on several factors including fabric construction, colour of dye, and the initial strength of the fabric. A thin coating (< 1  $\mu\text{m}$ ) on naturally aged silk fabric made highly deteriorated fabrics easier to handle, even though statistically significant differences in tensile properties could not be established in some cases. This thin coating also caused a noticeable stiffening of all fabrics tested, and a slight iridescent sheen was apparent on smooth-surfaced, dark-coloured samples.

The parylene coating retained its beneficial consolidating properties with exposure to visible light, but was not capable of slowing down the degradation of silk if wave-lengths below 400 nm were present. With exposure to UV

light, the thin coating yellowed noticeably, and became embrittled as revealed by SEM. It is therefore of paramount importance that artifacts consolidated with parylene C be protected from harmful ultraviolet radiation. Because parylene is an irreversible technique, the decision to coat a textile artifact with this polymer must be made carefully; however, for highly degraded silk artifacts for which there is no other viable option, this treatment may be appropriate.

## ACKNOWLEDGEMENTS

Many people assisted me throughout the course of this research. I would like to thank Dr. Nancy Kerr for all her helpful suggestions along the way, and many hours of editing and proofreading. I also appreciate the advice and support I received from Dr. Betty Crown and Dr. Mark Hollingsworth, my other two committee members.

I wish to acknowledge the financial support of Union Carbide Corporation in providing funds for me to travel to the Nova Tran Laboratory in Clear Lake WI. Many thanks are due to Bruce Humphrey for his assistance in coating my samples, and for providing me with excellent resource material (and parylene-coated Big Bird feathers). Thanks also to Mr. Henry Yetter for taking the time to dig up answers to my questions.

The assistance provided by Elaine Bitner in operating the Weather-Ometer and countless other activities was greatly appreciated, as was the help of Linda Turner. I am also grateful for the assistance I received from the people in the statistical consulting office, especially Terry Taerum for his invaluable help in running the statistics on my data and thus making sense of all those numbers. Thanks also to George Braybrook for working his magic on the scanning electron microscope to produce such terrific photographs.

In addition, I need to extend heartfelt thanks to Joan, Nikki, Aileen, and the other CLTX grad students for always being there to 'talk textiles' or whatever else, and to the friendly folks in the geology department for their wonderful sense of fun. A very special thank-you goes to Stephen Prevec for his never-ending support and encouragement, and for always knowing the right thing to do or say. Finally, I wish to thank my parents for always encouraging me in whatever I decided to do.

## TABLE OF CONTENTS

|  |    |
|--|----|
| CHAPTER 1 INTRODUCTION . . . . .                       | 1  |
| Justification and Statement of Purpose . . . . .       | 1  |
| Objectives . . . . .                                   | 3  |
| Definitions . . . . .                                  | 4  |
| CHAPTER 2 REVIEW OF THE LITERATURE . . . . .           | 5  |
| Introduction . . . . .                                 | 5  |
| Silk . . . . .   | 5  |
| Structure of Proteins . . . . .                        | 5  |
| Structure of Silk . . . . .                            | 6  |
| Fibroin Chemical Composition . . . . .                 | 6  |
| Fibroin Structure . . . . .                            | 9  |
| Primary structure . . . . .                            | 9  |
| Secondary structure . . . . .                          | 11 |
| Tertiary structure . . . . .                           | 11 |
| Fine structure . . . . .                               | 12 |
| Summary . . . . .                                      | 13 |
| Sericin . . . . .                                      | 14 |
| Properties of Silk . . . . .                           | 14 |
| Morphology . . . . .                                   | 14 |
| Physical Properties . . . . .                          | 14 |
| Chemical Properties . . . . .                          | 16 |
| Hydrolytic effects . . . . .                           | 16 |
| Oxidative effects . . . . .                            | 17 |
| Cross-linking effects . . . . .                        | 20 |
| Degradation of Silk . . . . .                          | 20 |
| Causes of Degradation . . . . .                        | 20 |
| Chemical degradation . . . . .                         | 20 |
| Thermal degradation . . . . .                          | 22 |
| Photochemical degradation . . . . .                    | 24 |
| Weighting agents . . . . .                             | 28 |
| Summary and Comparison of Degradative Forces . . . . . | 29 |
| Accelerated Aging of Silk . . . . .                    | 30 |
| Parylene . . . . .                                     | 32 |
| Parylene Structure and Nomenclature . . . . .          | 32 |
| Polymerization and Deposition of Parylene . . . . .    | 33 |
| History . . . . .                                      | 33 |
| Gas Phase Polymerization . . . . .                     | 34 |
| The Structure of Parylene Coatings . . . . .           | 38 |
| Properties of Parylene . . . . .                       | 39 |
| Electrical Properties . . . . .                        | 42 |
| Barrier Properties . . . . .                           | 42 |
| Optical Properties . . . . .                           | 42 |
| Solubility . . . . .                                   | 42 |
| Degradation of Parylene . . . . .                      | 43 |
| Hydrolytic Degradation . . . . .                       | 43 |
| Oxidative Degradation . . . . .                        | 43 |
| Exposure to Heat . . . . .                             | 44 |
| Exposure to Light . . . . .                            | 46 |

|   |     |
|---|-----|
| Exposure to Chemicals . . . . .                     | 47  |
| Uses of Parylene . . . . .                          | 47  |
| General Uses . . . . .                              | 47  |
| Uses in Artifact Conservation . . . . .             | 48  |
| Miscellaneous artifacts . . . . .                   | 48  |
| Paper and books . . . . .                           | 49  |
| Textiles . . . . .                                  | 51  |
| Reversibility . . . . .                             | 53  |
| CHAPTER 3 MATERIALS AND METHODS . . . . .           | 55  |
| Fabrics . . . . .                                   | 55  |
| Sampling Procedure . . . . .                        | 56  |
| Accelerated Aging . . . . .                         | 58  |
| Measurement of Physical Properties . . . . .        | 60  |
| Rationale . . . . .                                 | 60  |
| Colour Change . . . . .                             | 61  |
| Flexibility . . . . .                               | 63  |
| Tensile Properties . . . . .                        | 64  |
| Moisture Regain . . . . .                           | 65  |
| SEM Analysis . . . . .                              | 66  |
| Statistical Analysis . . . . .                      | 67  |
| CHAPTER 4 RESULTS AND DISCUSSION . . . . .          | 69  |
| Colour Change . . . . .                             | 69  |
| Flexural Rigidity . . . . .                         | 75  |
| Tensile Properties . . . . .                        | 79  |
| Tensile Strength . . . . .                          | 79  |
| Extension at Break . . . . .                        | 86  |
| Energy to Break . . . . .                           | 91  |
| Moisture Regain . . . . .                           | 96  |
| Scanning Electron Microscopy . . . . .              | 101 |
| Summary of Results . . . . .                        | 106 |
| Initial Effect of Parylene C Coating . . . . .      | 106 |
| Effect of Light on Parylene Coated Silk             |     |
| Fabric . . . . .                                    | 108 |
| UV Filtered Light . . . . .                         | 108 |
| Simulated Daylight . . . . .                        | 109 |
| Artificially vs Naturally Aged Fabrics . . . . .    | 112 |
| CHAPTER 5 CONCLUSIONS AND RECOMMENDATIONS . . . . . | 113 |
| Summary . . . . .                                   | 113 |
| Conclusions . . . . .                               | 116 |
| Recommendations for Future Research . . . . .       | 118 |
| REFERENCES . . . . .                                | 119 |
| APPENDIX A-1: Additional Procedures . . . . .       | 131 |
| APPENDIX A-2: Cutting Diagram for Artificially Aged |     |
| Specimens . . . . .                                 | 134 |
| APPENDIX A-3: Summary of Raw Data . . . . .         | 137 |
| APPENDIX A-4: Summary Tables of F-Ratios . . . . .  | 161 |

## LIST OF TABLES

|          |   |    |
|----------|---|----|
| Table 1  | Amino Acid Composition of <i>Bombyx mori</i> Fibroin  | 7  |
| Table 2  | Properties of Silk Fibres . . . . .   | 15 |
| Table 3  | Properties of Parylene . . . . .  | 40 |
| Table 4  | Descriptions of Naturally and Artificially Aged Silk Samples . . . . .  | 56 |
| Table 5  | Parylene-C Coating of Silk Fabric Specimens .   | 58 |
| Table 6  | Light Exposure Conditions Assigned to Treatment Groups . . . . .  | 59 |
| Table 7  | Samples Analyzed With SEM . . . . .   | 66 |
| Table 8  | Initial Effect of Parylene C Coating on the Colour of Silk Fabrics . . . . .  | 70 |
| Table 9  | Change in Colour ( $\Delta E^a$ and $YI^b$ ) of Silk Fabrics After Exposure . . . . .   | 73 |
| Table 10 | Initial Effect of Parylene C Coating on the Flexural Rigidity of Silk Fabrics . . . . .   | 76 |
| Table 11 | Fraction of Flexural Rigidity Retained by Parylene C-Coated Silk Fabrics After Exposure to Simulated Daylight: Normalized Data <sup>a</sup> . . . | 77 |
| Table 12 | Initial Effect of Parylene C Coating on the Tensile Strength of Silk Fabrics . . . . .  | 81 |
| Table 13 | Fraction of Tensile Strength Retained by Parylene C-Coated Silk Fabrics After Exposure to Simulated Daylight: Normalized Data . . .               | 84 |
| Table 14 | Initial Effect of Parylene C Coating on the Extension at Break of Silk Fabrics . . . . .  | 86 |
| Table 15 | Fraction of Extension at Break Retained by Silk Fabrics After Exposure to Simulated Daylight: Normalized Data . . . . .                           | 89 |
| Table 16 | Initial Effect of Parylene C Coating on the Energy to Break of Silk Fabrics . . . . .   | 93 |
| Table 17 | Fraction of Energy to Break Retained by Silk Fabrics After Exposure to Simulated Daylight: Normalized Data . . . . .                              | 95 |

|          |  |     |
|----------|--|-----|
| Table 18 | Initial Effect of Parylene C Coating on the<br>Moisture Regain of Silk Fabrics . . . . .                                   | 98  |
| Table 19 | Fraction of Moisture Regain Retained by Silk<br>Fabrics After Exposure to Simulated Daylight:<br>Normalized Data . . . . . | 100 |



## LIST OF FIGURES

|            |   |    |
|------------|---|----|
| Figure 1.  | The antiparallel $\beta$ -pleated tertiary structure of <i>Bombyx mori</i> silk fibroin . . . . .                   | 13 |
| Figure 2.  | Spectral distributions of daylight and a filtered xenon arc lamp. . . . .   | 31 |
| Figure 3.  | The parylene deposition process . . . . .   | 34 |
| Figure 4.  | Total colour change of parylene C-coated silk fabric after exposure to simulated daylight . . . . .                 | 72 |
| Figure 5.  | Flexural rigidity of parylene C-coated silk fabric after exposure to simulated daylight . . . . .                   | 78 |
| Figure 6.  | Tensile strength of parylene C-coated silk fabrics after exposure to simulated daylight . . . . .                   | 80 |
| Figure 7.  | Extension to break of parylene C-coated silk fabrics exposed to simulated daylight . . . . .                        | 87 |
| Figure 8.  | Energy to break of parylene C-coated silk fabrics after exposure to simulated daylight . . . . .                    | 92 |
| Figure 9.  | Moisture regain of parylene C-coated silk fabric after exposure to simulated daylight . . . . .                     | 97 |
| Figure 10. | Relationship between change in mass per unit area and change in moisture regain, after coating application. . . . . | 99 |

LIST OF PHOTOGRAPHIC PLATES

|          |   |     |
|----------|---|-----|
| Plate 1. | Combination of undamaged and fibrillated fibres in uncoated fabric 2 after exposure to UV-filtered light (1000x) . . . . .  | 103 |
| Plate 2. | Parylene C-coated fabric 2 before exposure to light showing smooth coating on some fibres, irregular on others depending on state of fibre surface prior to coating (1000x) . . | 103 |
| Plate 3. | Overall surface debris, and fibrils extending across neighbouring fibres on uncoated fabric 8 exposed to UV-filtered light (1600x) . .  | 104 |
| Plate 4. | Thickened fibrils bonded to neighbouring fibres, and irregular coated surface due to underlying debris on coated fabric 8 exposed to UV-filtered light (1500x). . . . .         | 104 |
| Plate 5. | Coated fibres bonded together (spot welded), and debris on coated fibre surface of fabric 5 after exposure to the full simulated daylight spectrum (1500x). . . . .             | 105 |
| Plate 6. | Cracking of parylene C coating on fabric 8 after exposure to the full xenon arc spectrum and stress (1500x) . . . . .   | 105 |
| Plate 7. | Coated fibrils forming bridges between fibres, and cracking of parylene coating on fabric 7 after exposure to the full xenon arc spectrum and stress . . . . .                  | 105 |

## CHAPTER 1 INTRODUCTION

## Justification and Statement of Purpose

Many museum collections contain artifacts made from silk. The conservation of highly degraded "shattered" silk is problematic and as yet there is no entirely satisfactory approach to treatment (Bogle, 1979). Often conventional stitching techniques cannot be utilized because the needle and sewing thread may break the fragile textile yarns. The use of adhesives for lamination, impregnation or application of a support backing increases the stiffness of the fabric, which may be unacceptable in some cases. The application of such a backing may also obscure important structural and historical information.

Recently, a vapour-polymerized coating called parylene C has shown promise in the field of artifact conservation. The coating is colourless, transparent, flexible, strong, highly conformal, and its method of application causes minimal stress to most substrates (Humphrey, 1984). The literature on its conservation applications reports sufficient success to warrant further research. "We are convinced that Parylene provides a means of dealing with the most fragile of materials so that they become effectively consolidated and strengthened" (Grattan, 1989, p. 16).

For parylene C to be used successfully as a conservation treatment, however, the coating must not only be beneficial initially, but must also be stable over long periods of time. The effects of photochemical aging on parylene-coated objects is especially important, as artifacts must be exposed to a certain amount of light for research or exhibit purposes. States Grattan, "The effect of light has not been studied so much and there is much we would like to know" (Grattan, 1989, p. 16). In the case of silk artifacts, the problem is compounded as the fibres themselves are highly sensitive to light, especially if weighting agents are present (Bogle,

1979).

In the area of textile conservation, parylene's effect on the flexibility, colour, tensile strength, and moisture absorbency of fabrics has only been partially analyzed. The work on parylene-coated silk done by Hansen and Ginell (1989) at the Getty Institute addresses some of these questions, but leaves room for expanded research. Their study tested parylene coated modern and naturally aged silk, as well as unsupported parylene films. Because Hansen and Ginell (1989) did extensive testing on modern silk, this fabric will not be included in the present study; artificially aged silk and naturally aged silk will be used.

The Getty research studied the effects of filtering out UV light on the colour of unsupported parylene films. The present study will determine the effect of these filters on change in colour and tensile properties of coated silk.

The historic silk used in the Getty study underwent accelerated aging before the coating was applied, but not after; change in properties were measured before and after coating only. Both the naturally and artificially aged coated samples in the present study will be exposed to simulated daylight, and the changes due to accelerated photochemical aging measured. In addition, this study will measure changes in moisture absorption and flexibility, properties not covered by the research at the Getty Institute.

The purpose of this research project is to determine the initial effects of the parylene-C coating on selected silk properties, and how these properties change after photochemical aging through exposure to simulated daylight of varying wave-lengths.

### Objectives

The objectives of this study were:

1. to apply the parylene C coating to naturally and artificially-aged silk fabric;
2. to study the initial effects of the coating on selected silk properties: tensile strength, flexibility, colour, and moisture absorption;
3. to determine whether the selected properties change after exposure to simulated daylight, using a xenon-arc Weather-Ometer;
4. to determine whether the presence of a UV filter affects the change in properties of xenon-arc exposed coated silk; and
5. to observe the appearance of the parylene coating using scanning electron microscopy.

### Definitions

For the purpose of this study:

**Degradation:** refers to gradual impairment with respect to some property, quality, or capability, or to the chemical breakdown of polymeric material into a less complex compound (Miller, 1986).

**chemical degradation:** refers to "processes which are induced under the influence of chemicals (eg. acids, bases, solvents, reactive gases etc.) brought into contact with polymers" (Schnabel, 1981, p. 14)

**thermal degradation:** occurs when "the polymer, at elevated temperatures, starts to undergo chemical changes without the simultaneous involvement of another compound" (Schnabel, 1981, p. 14)

**photodegradation:** "concerns the physical and chemical changes caused by irradiation of polymer with ultraviolet or visible light" (Schnabel, 1981, p. 14)

**Parylene:** the generic name for a series of poly-paraxylylene polymers, both substituted and nonsubstituted varieties, except when used in reference to conservation studies, where **parylene** refers to the parylene N and parylene C only.

**parylene C:** the chlorinated variation of parylene polymer, also known by the chemical name 'polychloro-p-xylylene'.

**parylene N:** the nonsubstituted variation of the parylene polymer, also known by the chemical name 'poly-paraxylylene'

**Silk:** refers to the fibroin protein fibres extruded by the *Bombyx mori* moth larvae, with the sericin gum removed.

## CHAPTER 2 REVIEW OF THE LITERATURE

## Introduction

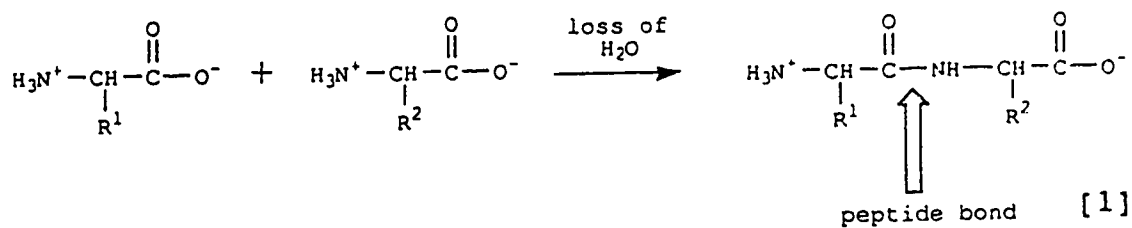
In order to preserve silk artifacts, many of which are unique and of historic value, it is necessary to have an understanding of the factors involved in the degradation of this fibre, and a familiarity with various methods of measuring degradation. The following literature review begins by summarizing silk fibre structure, morphology, and properties. The causes and measurement of silk degradation are then addressed. The polymerization process, properties and uses of the parylene polymer coating will then be discussed.

## Silk

Structure of Proteins

Proteins are natural polymers which are characterized by the specific amino acids from which they are built. Each of these  $\alpha$ -amino acid units contains a side chain (R), an amino group and a carboxyl group. The side chain, which can be neutral, basic, or acidic, small or bulky, is instrumental in determining the physical and chemical properties of the resultant protein.

The positively charged amino group and the negatively charged carboxyl group give rise to a zwitterionic, or dipolar structure. Amide bonds are formed through a condensation reaction between the amino and carboxyl groups of adjacent residues, as shown:



These amide links between amino acid residues are called peptide bonds. Polymers formed in this manner are called peptides; proteins are peptides with molecular weights from approximately 6000 to 40,000,000 (Wade, 1987).

Proteins can be classified as either globular or fibrous. Globular protein molecules, such as haemoglobin and insulin, form coils and are roughly spherical in shape. Fibrous protein chains are extended and are usually insoluble in water. Wool and silk are examples of fibrous proteins.

### Structure of Silk

Raw silk is composed of two types of protein, fibroin and sericin. The pairs of filaments, or brins, extruded by the *Bombyx mori* moth larvae are made from fibroin, and are bound together by gum-like sericin (Otterburn, 1977).

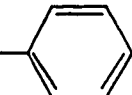
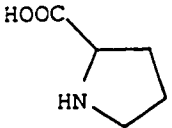
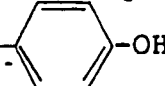
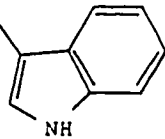
### Fibroin Chemical Composition

Fibroin contains approximately 16  $\alpha$ -amino acids which are listed in Table 1. Most frequently occurring are the small and simple residues glycine, alanine and serine, which together account for 80% to 85% of all the residues in the protein (Robson, 1985). The number of acidic residues (glutamic and aspartic acid) is low, as is the number of basic residues (lysine, histidine and arginine). The majority of polar amino acids are serine, threonine and tyrosine, all of which contain hydroxyl groups (Otterburn, 1977). A very small amount of cystine (0.23%) is also present (Lucas, 1966).

The molecular weight of fibroin is still uncertain. Estimates have ranged from 33,000 daltons using osmotic pressure determination (cited in Otterburn, 1977, p.58) to 1,000,000 (Mercer, 1954) using light scattering measurements. Some more recent studies employing solubilization of gland fibroin extracts using urea or guanidine-HCl have given more consistent values, from 350 000 (Sprague, 1975) to 370 000 (Tashiro, Otsuki, & Shimadzu, 1972).

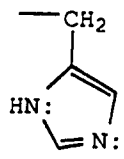


Table 1  
Amino Acid Composition of Bombyx mori Fibroin

| Amino Acid                               | N <sup>a</sup> | R <sup>b</sup> | Side Chain Structure   |
|--|----------------|----------------|--|
| Side Chain is Neutral                    |                |                |  |
| Glycine (Gly)                            | 43.74          | 445            | -H   |
| Alanine (Ala)                            | 28.78          | 293            | -CH <sub>3</sub>   |
| Valine (Val)                             | 2.16           | 22             | -CH(CH <sub>3</sub> ) <sub>2</sub>   |
| Leucine (Leu)                            | 0.52           | 5              | -CH <sub>2</sub> CH(CH <sub>3</sub> ) <sub>2</sub>   |
| Isoleucine (Ile)                         | 0.65           | 7              | -CH(CH <sub>3</sub> )CH <sub>2</sub> CH <sub>3</sub>   |
| Phenylalanine (Phe)                      | 0.62           | 6              | -H <sub>2</sub> C-    |
| Proline (Pro)                            | 0.35           | 3              |                      |
| Side Chain Contains a Hydroxyl Group     |                |                |  |
| Serine (Ser)                             | 11.88          | 121            | -CH <sub>2</sub> OH  |
| Threonine (Thr)                          | 0.89           | 9              | -CH(OH)CH <sub>3</sub>   |
| Tyrosine (Tyr)                           | 5.07           | 52             | -H <sub>2</sub> C-  |
| Side Chain Contains a Non-Basic Nitrogen |                |                |  |
| Tryptophan (Trp)                         | 0.33           | 2              | -H <sub>2</sub> C-  |

Continued

Table 1 (Continued)  
Amino Acid Composition of *Bombyx mori* Fibroin

| Amino Acid                 | N <sup>a</sup> | R <sup>b</sup> | Side Chain Structure   |
|----------------------------|----------------|----------------|--|
| Side Chain is Acidic       |                |                |  |
| Aspartic Acid (Asp)        | 1.28           | 13             | -CH <sub>2</sub> COOH  |
| Glutamic Acid (Glu)        | 1.00           | 10             | -CH <sub>2</sub> CH <sub>2</sub> COOH  |
| Side Chain is Basic        |                |                |  |
| Lysine (Lys)               | 0.63           | 3              | -(CH <sub>2</sub> ) <sub>4</sub> -NH <sub>2</sub>                                    |
| Arginine (Arg)             | 1.83           | 5              | -(CH <sub>2</sub> ) <sub>3</sub> -NH-C-NH <sub>2</sub><br>  <br>NH                   |
| Histidine (His)            | 0.53           | 2              |  |
| Side Chain Contains Sulfur |                |                |  |
| Cystine (Cys)<br>(half)    | 0.15           | 2              | -CH <sub>2</sub> -SH   |
| Methionine (Met)           | 0.07           | 1              | -CH <sub>2</sub> CH <sub>2</sub> -S-CH <sub>3</sub>                                  |

Note. Adapted from Lucas and Rudall, 1968, p. 484; Wade, 1987, p. 1218-1219.

<sup>a</sup>amino acid nitrogen as % of total nitrogen.

<sup>b</sup>Number of amino acid residues per 1000 residues estimated.

## Fibroin Structure

### Primary structure.

The primary structure is the covalently bonded structure of the protein molecule, and refers to the sequence in which the amino acid residues are combined (Wade, 1987). The precise sequence of amino acids in silk has yet to be determined. The residues at the N-terminus (the end of the protein terminating in an amino group) are glycine, alanine, and serine (Truter, 1973). Glycine, alanine, serine, as well as tyrosine, valine and proline (Shaw & Smith, 1954) have all been postulated for the C-terminus residues.

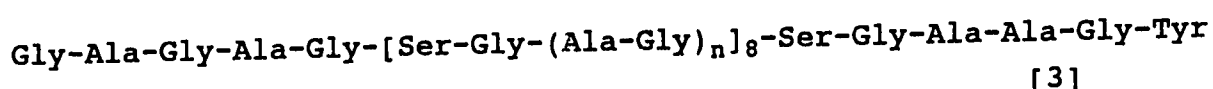
Because several different terminal residues have been isolated, it is possible fibroin has a multi-chain primary structure composed of several polypeptides linked by inter-chain bonds (Shaw, 1964). Research by Sprague (1975) concluded the protein was made up of equal amounts of two distinct polypeptides, each of which appeared to contain the same proportions of the major amino acids (glycine, alanine and serine). Sasaki and Noda (1973) proposed that fibroin is made from one long and three short polypeptides linked by disulphide bonds. Disulphide bonds between chains are theoretically possible because fibroin contains a small amount of cystine (Shaw, 1964), but Otterburn (1977) states there is no direct evidence of cystine forming these bonds between the polymer chains. Ester linkages have also been suggested by Zuber (cited in Robson, 1985, p. 682).

In order to determine its sequence of amino acids, the fibroin must be broken into smaller segments and the composition of these analyzed. The sequence of the fragments must then be found. Partial acid hydrolysis breaks the chain in a random manner. Using this technique, the following minimum repeating unit for fibroin was suggested by Levy and Slobodian (1952):

X-Ala-Gly-Ala-Gly-Y

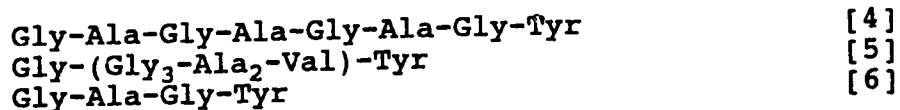
[2]

where X and Y are residues other than alanine and glycine. The use of enzymes rather than acids for hydrolysis is a more selective technique, causing breakage at known points along the chain (Wade, 1987). Lucas, Shaw and Smith (1957) digested fibroin with chymotrypsin, which cleaves the chain at the carboxyl group of the tyrosine, phenylalanine and tryptophan residues (Wade, 1987). A solution (Cs) and a precipitate (Cp) were obtained. An analysis of Cp, which accounted for 60% of the fibroin's total nitrogen, yielded the following structure:



where n usually equals 2. Similar structures were confirmed by Fraser, Macrae and Stewart (1966). Drucker, Hainsworth and Smith, (1953) found the X-ray pattern given by Cp was identical to that of the original fibroin, but indicated a higher crystallinity. They concluded the Cp portion represented the crystalline regions of the unbroken molecule.

The remaining 40% of the fibroin contained in the solution (Cs) was also studied, but many questions remain. The different polypeptides found by several researchers are listed by Otterburn (1977) and Robson (1985). The predominant peptides shown as structures 4, 5, and 6 were those isolated by Lucas, Shaw and Smith (1962). These three peptides make up about 75% of the Cs fibroin residues.



Other studies have employed the use of the trypsin enzyme to cause cleavage at the carboxyl group of lysine and arginine residues (Wade, 1987). The results of such a study by Shaw (1964) combined with the results from the chymotrypsin studies

led Shaw to propose a three phase primary structure for fibroin. Phase I is composed of the Cp sequence corresponding to the crystalline regions of the molecule (60%). Phase II, 30%, contains sequences of glycine, alanine, valine and tyrosine. Phase III, contains the remaining 10% of the residues, including those with acidic, or bulky side chains. How these phases are related to the multi-chain structure of fibroin is not certain. Each polypeptide may be a combination of phases, or limited to one phase (Shaw, 1964). Many of the fibre's properties are dictated by the fact that fibroin is composed of 80% to 85% glycine, alanine and serine, all of which lack bulky side chains.

#### Secondary structure.

Individual protein molecules tend to be held by hydrogen bonds in coiled ( $\alpha$ -helix) or folded ( $\beta$ -pleated sheet) structures. This orderly arrangement is called the secondary structure (Wade, 1987).

Through X-ray diffraction techniques, silk fibroin has been found to have a  $\beta$ -pleated sheet structure. According to Meyer and Mark (cited in Robson, 1985, p.667), extended protein chains parallel to the fibre axis are linked by hydrogen bonds between carbonyl and amino groups on adjacent chains. Because silk is composed primarily of residues which lack bulky side groups, the fibroin molecules can pack closely together allowing hydrogen bonding to occur, thus producing a highly crystalline fibre (Peters, 1963).

#### Tertiary structure.

The way by which the protein chain forms 3-dimensional arrangements is called the tertiary structure (Wade 1987). The tertiary structure includes both ordered, crystalline regions, and regions of disorder.

The three phase model postulated by Shaw (1964) can also be applied to the tertiary structure. Phase I forms a crystalline  $\beta$ -structure (pleated sheets). Phase II is not as well ordered, but is not entirely amorphous, and Phase III,

with its bulky side chains, constitutes the amorphous regions (Shaw, 1964). Drucker et al. (1953) and Peters (1963) also relegated larger residues to amorphous regions. However, Marsh, Corey, and Pauling (1955) stated these bulkier residues may be incorporated within the crystalline areas, causing deformations in the crystal structure. Robson (1985) also warns against the assumption that bulky groups occur exclusively in amorphous areas.

Marsh et al. (1955) and Warwicker (1960) have postulated a three dimensional antiparallel  $\beta$ -structure as the crystalline tertiary structure. Extended chains of amino acids, with glycine alternating with the larger alanine or serine residues, are hydrogen bonded laterally to form pleated sheets. These sheets are then stacked in an antiparallel manner, meaning the sheets are stacked back to back; the glycine side chains from one sheet lie next to the glycine chains of the adjacent sheet (Figure 1). In this manner, 3-dimensional crystalline regions are formed. Lim and Steinberg (1981) proposed an entirely different tertiary structure, consisting of several fibroin proteins forming a parallel-chain, tape-like structure, which then coils into a flat helix.

#### Fine structure.

A fibre's fine structure "is a complex combination of long-chain molecules in crystalline and non-crystalline regions, which may in turn be aggregated into fibrils or other supra-molecular structures" (Hearle, 1963a, p.209). As previously mentioned, silk is approximately 60% crystalline, the remaining 40% being more random in arrangement and likely containing the bulkier residues. The crystalline regions are oriented parallel to the fibre axis, whereas chains in the amorphous regions are more randomly arranged (Robson, 1985).

Electron microscopy has shown the fine structure of silk to consist of ribbon-like filaments, or microfibrils lying parallel to the fibre axis (Dobb, Fraser, & Macrae, 1967;

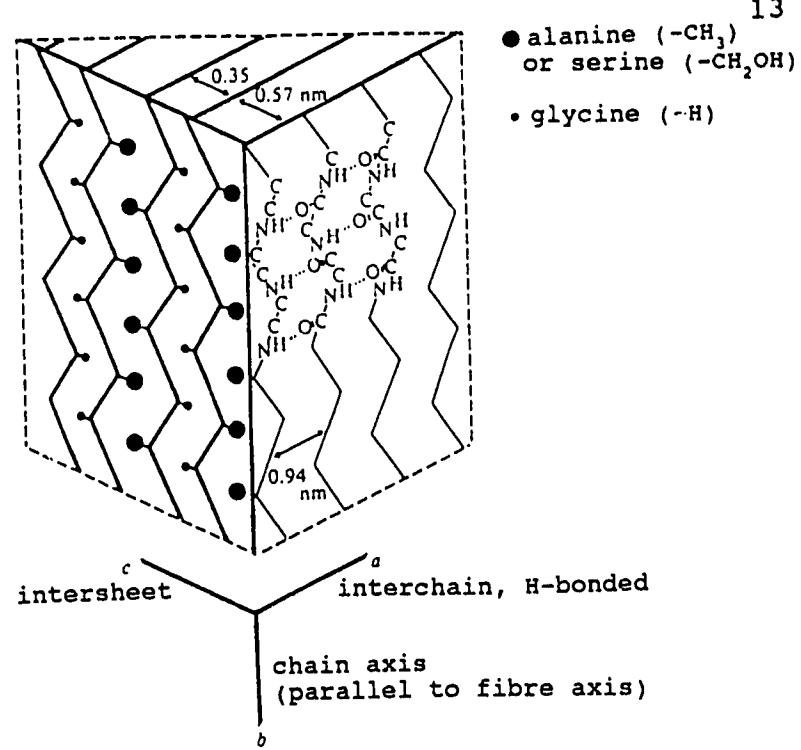


Figure 1. The antiparallel  $\beta$ -pleated tertiary structure of *Bombyx mori* silk fibroin.

Note. From "Silks- Their Properties and Functions" by M. W. Denny, 1980, *Symposia of the Society for Experimental Biology*, 34, p. 258. After Marsh et. al, 1955, "An Investigation of Silk Fibroin", 1955, *Biochimica et Biophysica Acta*, 16, p. 13-18. Reprinted by permission.

Marsh et al, 1955). Dobb et al. (1967) proposed that microfibrils are composed of the crystalline  $\beta$ -structure portion of fibroin such that the pleated sheets lie parallel to the longer, lateral dimension of the microfibril. The amorphous regions of the fibre occupy the space between the microfibrils. Some doubt, however, has been cast on Dobb et al.'s findings, due to possible cellulose contamination (Millward, 1969).

Summary.

In summary, silk fibroin comprises mainly the simple amino acids alanine, glycine, and serine. A primary structure consisting of a multi-chain arrangement of polypeptide chains has been proposed. The fibroin chains form pleated sheets as

a secondary structure, which then stack to produce a  $\beta$ -antiparallel tertiary structure in crystalline regions. The crystalline areas may then combine together to form ribbon-like microfibrils which make up the fibre's fine structure.

### Sericin

When extruded by the *Bombyx mori* larvae, the pairs of fibroin filaments, are cemented together by a second protein present in raw silk, sericin. This protein is significantly different in chemical composition from fibroin, with serine, glycine and aspartic acid residues making up two thirds of its content (Robson, 1985). During the processing of silk for textile usage, the sericin is removed by soaking in a hot dilute soap or alkaline solution, in a process called degumming. The removal of the gum improves the softness and lustre of the silk fibres (Peters, 1963).

## Properties of Silk

### Morphology

Before degumming, the silk cross-section consists of two roughly triangular filaments which together form an elliptical shape. After degumming the triangular filaments, called brins, separate and appear smooth and translucent in the longitudinal direction, with few external markings (Peters, 1963).

Fibre diameter for brins varies from approximately 7  $\mu\text{m}$  to 12  $\mu\text{m}$  depending on spinning conditions and the location within the cocoon (Robson, 1985).

### Physical Properties

The physical properties of silk, using typical values, are summarized in Table 2. Of all the natural fibres, silk is the most similar to synthetic fibres because of its reasonably high strength and breaking extension, which result in a high work of rupture (Robson, 1985). These properties can be explained by examining changes which occur on the molecular level. The silk fibre is made up of oriented crystalline



Table 2  
Properties of Silk Fibres

| Property  | Typical Value                        | Source                           |
|---|--------------------------------------|----------------------------------|
| Density   | 1.33g/cm <sup>3</sup>                | The Textile Institute, 1975, 134 |
| Refractive Index  | n <sub>  </sub> = 1.591              | The Textile Institute, 1975, 133 |
|   | n <sup>⊥</sup> = 1.538               |                                  |
| Birefringence   | n = 0.053                            | The Textile Institute, 1975, 133 |
| Tenacity  | 0.38 N/tex                           | Meredith, 1945, T127             |
| Wet Strength<br>(% of dry strength)                             | 75% to 85%                           | Cook, 1968, 159                  |
| Initial Modulus   | 7.3 N/tex                            | Meredith, 1945, T127             |
| Work of Rupture   | 59.7 mN/tex                          | Meredith, 1945, T127             |
| Breaking Extension  | 23.4%                                | Meredith, 1945, T127             |
| Elastic Recovery<br>(2% extension)                              | 92%                                  | Harris, 1954, 109                |
| Moisture Regain   | 9.9% absorption<br>11.05% desorption | Hutton & Gartside,<br>1949, T167 |
| Swelling in Water<br>(% increase in<br>cross-sectional<br>area) | 30% to 41%                           | Harris, 1954, 201                |

regions, and randomly oriented amorphous areas. The molecules are held together by hydrogen and ionic bonds and Van der Waals forces. A single molecule can pass through both crystalline and amorphous regions (Robson, 1985).

When a load is applied, the amorphous areas are the first to become deformed. Silk has a relatively high resistance to deformation, or initial modulus, because of the strong forces between chains in the amorphous regions, and the strong interaction between amorphous and crystalline regions (Robson,

1985). Elastic recovery is complete if no bonds are broken. If more tension is applied, inter-chain bonds begin to break in the amorphous regions, allowing the molecules to slide past one another and become extended in a process called 'plastic flow'. Permanent deformation occurs when bonds are formed between the newly extended chains. When the chains in the amorphous regions are fully extended, the load is then transferred to the already oriented, extended crystalline regions. When the load can no longer be accommodated, breakage of hydrogen bonds in the crystalline regions occurs, and peptide bonds may also be broken, resulting in fibre rupture (Robson, 1985).

The elastic recovery of silk is affected by both the fineness of the fibre and by moisture content. Moisture also affects other physical properties. Water molecules enter the fibre in the amorphous regions, and compete for the hydrogen-bonding sites between the chains. The result is a general loosening of the structure which allows the amorphous chains to slide past each other more easily, causing greater extensibility and decreased modulus and strength (Denny, 1980; Lucas et al, 1955).

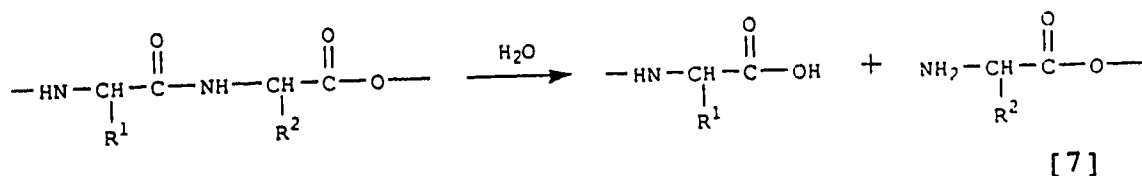
### Chemical Properties

Silk fibroin can undergo several types of chemical reactions including hydrolysis, oxidation, and cross-linking. The mechanisms for these reactions, and how their effects can be measured, are outlined below. The action of specific acids, alkalis and other chemicals, as well as the effect of light and heat will be discussed in the subsequent section on degradation.

#### Hydrolytic effects.

The fibroin protein can undergo hydrolysis, during which a molecule of water is added across the peptide linkage. This

causes breakage of the main protein chain as shown:



Exposure to acids will cause cleavage in a random manner along the polymer, whereas damage from alkalies appears to occur initially at the polymer ends (Otterburn, 1973; Peters 1963).

The extent to which hydrolysis occurs depends upon the pH of the hydrolytic agent, with the least damage generally caused by reagents having a pH between 4 and 8. The damage is most severe when silk is exposed to reagents above pH 11 and below pH 3 (Harris, 1943).

Hydrolytic damage is shown by a decrease in tensile strength as revealed through physical testing, and through several chemical tests. A fluidity measure of a fibroin solution in cupri-ethylene-diamine indicates the degree of degradation. The solution of a more broken-down polymer, consisting of shorter chains, will have a higher fluidity. Another chemical means of assessing hydrolytic damage is to measure the amount of amino nitrogen. As shown in equation 7, when a peptide link is hydrolysed, the chain is broken to form an amino group and a carboxyl group. The increase in amino groups, or amino nitrogen content, can then be used as a measure of hydrolytic degradation. Generally, chemical tests for degradation are believed to be more sensitive than physical, and can detect smaller amounts of damage before they are manifested in physical change (Burgess & Hanlan, 1980).

#### Oxidative effects.

Oxidative reactions introduce oxygen-containing groups along the polymer chain. The oxidation reactions undergone by

silk are very complex, and are thought to affect the polymer in three ways: oxidation of the tyrosine side chains, oxidation of the N-terminal residues, and breakage of the polypeptide links in the polymer backbone (Otterburn, 1973; Peters, 1963; Robson, 1985).

Autoxidation, which occurs through a free radical chain mechanism, can cause great damage to polymers due to the self-perpetuating nature of these reactions (Schnabel, 1981). Autoxidation proceeds through three steps: initiation, propagation and termination.

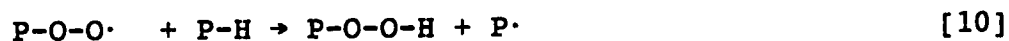
Initiation involves the production of highly reactive free radicals. Heat, light and chemical factors can all initiate autoxidation of a polymer (P):



During the propagation steps, the free radical (P·) reacts with oxygen to form peroxy polymer radicals by addition:



The peroxy radical then abstracts a hydrogen, either from a neighbouring polymer chain or intramolecularly to form a polymer hydroperoxide (POOH):



The new radical produced can then react further to continue the chain reaction until termination is reached. The polymer hydroperoxide, upon exposure to light, can decompose to form highly reactive polymer oxy radicals (PO·) and hydroxy radicals (OH·),

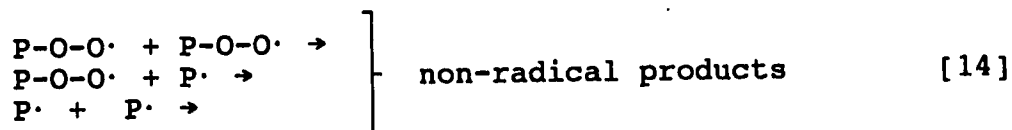


which can then abstract a hydrogen from the same, or neighbouring polymer chains:



Polymer oxy radicals can also participate in other reactions leading to chain scission and the formation of in-chain ketone groups (Rabek, 1990).

According to Rabek (1990), termination most often occurs when two radicals combine to create inactive products:



When silk is oxidized a change in colour varying from yellow, to pink, to brown is observed (Otterburn, 1973; Peters, 1963). Some researchers have proposed that the oxidation of tyrosine residues may produce coloured o-quinones; however, the presence of these products has not actually been detected (Stitch & Smith, 1957). In addition to colour change, oxidation causes a deterioration of physical properties, and a decrease in molecular weight (Kamiya & Niki, 1978).

Oxidative damage can be assessed by the methylene blue absorption test, as was employed by Stitch and Smith (1957). This test measures the degree to which the phenolic tyrosine residue has been oxidized to form an acidic product. The more of the basic blue dye absorbed, the greater the oxidative damage.

When silk is oxidized, ammonia is produced. The amount of ammonia nitrogen present can then be used as a measure of oxidative damage. Fluidity measures as used for hydrolytic detection may also be used to indicate the extent of peptide

breakage through oxidation.

#### Cross-linking effects.

By exposing silk to various cross-linking agents, covalent bonds can be formed between chains. This technique has been employed for structural studies of silk as well as in attempts to alter properties. For example, Oku and Shimizu found cross-linking with formaldehyde caused silk to swell in water, and helped to reduce water-spotting problems (cited in Robson, 1985, p. 687).

### Degradation of Silk

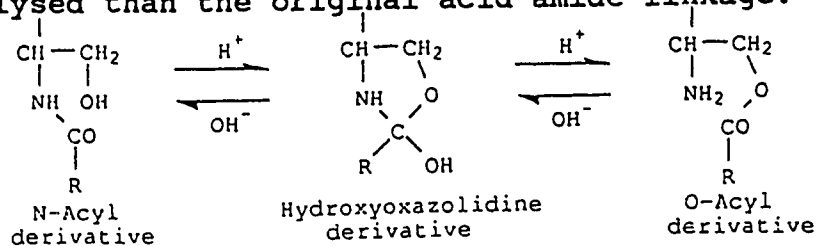
#### Causes of Degradation

Factors which contribute to the breakdown of silk include chemical damage, and damage through exposure to light and heat. Each of these factors will be discussed briefly below.

#### Chemical degradation.

Studies focusing on the chemical reactivity of silk are usually done by industry, and therefore focus on chemical reactions that occur during the processing of silk (Miller, 1986; Otterburn, 1977).

Acids are easily absorbed by silk fibres and once absorbed, are difficult to remove (Cook, 1968). Hydrolysis occurs upon exposure to mineral acids and alkali, with exposure to mineral acids generally being most damaging. Hot concentrated hydrochloric acid will readily dissolve silk and is often used in hydrolytic studies (Peters 1963; Otterburn, 1985). Sulphuric acid can also cause sulphonation of tyrosine residues, and with extended exposure, may cause an N→O peptidyl shift to occur (Iwai & Ando, 1967). The resulting O-acyl product has an ester linkage which is more easily hydrolysed than the original acid amide linkage:



Exposure to sulphuric acid also causes fabrics to shrink, and a loss of lustre is observed (Guoping & Slater, 1990). Nitric acid not only causes degradation through hydrolysis of peptide bonds, but also causes nitration of residues containing benzene rings, resulting in a yellowing of the fibre (Otterburn, 1977; Peters, 1963; Robson, 1985).

Silk shows good resistance to dilute organic acids at room temperature (Howitt, 1946). Low concentrations of tartaric and citric acids are occasionally used in processing to produce a rustling effect called 'scroop', without causing damage. Some concentrated organic acids (98% formic acid) can cause degradation (Robson, 1985). In moderate concentrations, acid causes silk fibres to contract, an effect used in producing crepe fabrics (Cook, 1968).

Silks exposed to alkali become stiff and have a tendency to split into fibrils. This breakdown of physical structure is followed by hydrolysis of peptide bonds (Tweedie, 1938). Whereas acid-induced hydrolysis causes chain scission randomly along the polymer length, alkali attack appears to concentrate at the polymer ends (Lucas, Shaw & Smith, 1958). A treatment with hot alkali also causes a loss of about one third of both the hydroxyamino acids serine and threonine residues and an increase in amide nitrogen (Peters, 1963; Nicolet & Shinn, 1941).

Several studies have also proposed that alkalies can produce cross-linking between residues. Robson and Zaidi (1967) claimed exposure to alkali ( $K_2CO_3$ ) caused cross linkages to form between serine and lysine residues.

Prolonged exposure to boiling water and steam is used in the degumming process can cause hydrolysis, but at a slow rate (Otterburn, 1977; Robson, 1985). Fibrous silk is also highly resistant to enzymic hydrolysis due to its highly crystalline structure. In order to be broken down by enzyme action, the fibre must first be swollen and dissolved in a solvent (Otterburn 1977; Peters, 1963; Robson, 1985).

Hydrogen peroxide and peracids are used to bleach pigmented silks, and are capable of causing damage through oxidation (Robson, 1985). Sitch and Smith (1957) concluded that treatment with hydrogen peroxide or peracid caused cleavage of the tyrosine residue and the tyrosine oxidized to form an acidic product. More acidic groups were formed, and chain breakage was more rapid using peracetic acid than hydrogen peroxide. Oxidation by potassium permanganate was seen by Earland and Stell (1957), and Earland, Stell and Wiseman (1960) to form cross links between tyrosine residues. These linkages were thought to be responsible for the insolubility of fibroin oxidized in this manner.

Silk fibres also have a strong affinity for salts (Cook, 1968) which explains the tendering and staining caused by perspiration on silk clothing. The damaging effect produced by chlorides is thought to be connected to the presence of iron, copper, and other chemicals used to enhance the rustling 'scroop' effect of silk fabrics, and is likely oxidative in nature (Howitt, 1946). Peters (1968) states that chlorine causes oxidative damage through attack on tyrosine residues.

Miller (1986) exposed new silk fibres and fabrics to a variety of chemicals. The effects of acid, alkali, peroxide, and boiling water were all studied. The chemicals chosen were those used in the processing and dyeing of silk. These included sulphuric acid (0.5N), sodium hydroxide (0.5N, 0.75N, 1.0N) and hydrogen peroxide (1N, 10N). She concluded these simulations of silk processing produced a statistically significant ( $p > 0.05$ ) reduction in tenacity, elongation and intrinsic viscosity, and that each treatment caused changes in the amounts of two or more amino acids.

#### Thermal degradation.

Exposure to high temperatures causes irreversible damage to silk fibroin. Magosi and Nakamura (1975) reported silk to have a glass transition temperature of 175 °C, crystallization temperature of 212 °C, and a decomposition temperature of



280 °C. According to the wet heat studies done by Hagiwara and Kato (cited in Miller, 1986, p. 23), at 100 °C  $\text{NH}_3$  is given off, but the fibroin does not visually appear to decompose. Some degradation was seen to occur at 125 °C, and increased at temperatures over 150 °C. The breakage of hydrogen bonds, and subsequent disorientation and hydrolysis of the molecular chains was said to have occurred, as well as an additional competing reaction resulting in increased crystallinity.

The exposure of a polymer to thermal energy causes increased vibration of intramolecular bonds until their bond dissociation energies are exceeded, causing them to break. This type of damage is not common at lower temperatures (150°-300° C), but those breakages that do occur can initiate autoxidation reactions through the formation of a peroxide radical (Schnabel, 1981), as was demonstrated by equations 8 to 13 in the previous section on oxidation. Miller (1986) studied thermal degradation of silk in the presence and absence of air. Some samples were heated in ambient air and others in a vacuum for 8 hours at 125 °C. Those samples heated in a vacuum did not exhibit a statistically significant loss in strength, elongation, or viscosity, while those exposed to air under the same conditions showed a 7% loss in strength.

Hansen and Ginell (1989) exposed silk to dry temperatures of 70°, 80°, 90°, 110° and 150 °C for 158, 109, 118, 45 and 7 days respectively. The rate of deterioration for tensile properties increased with the higher temperatures. The effect of dry heat on silk was also investigated by Hersh, Tucker and Becker (1989). During 96 hours of exposure to a temperature of 150 °C, breaking strength was found to decrease in a linear manner, the overall strength being reduced to 30% of the original.

Hersh, Tucker, and Becker (1989) also observed a dramatic yellowing of the silk; the CIElab\* system of colour

measurement indicated an overall colour change of 39.39 units. A visible yellowing of silk occurred after only 6 hours of exposure. Yellowing was seen to be less pronounced at lower temperatures by Hansen and Ginell (1989). Even after 130 days at 70° C, the total colour change ( $\Delta E$ ) was less than 5 units. Kuruppillai, Hersh and Tucker (1986) noted that dry heat degradation followed first order property kinetics. This allows "the extent of degradation to be calculated for any heating or exposure times on the basis of measurements made after only a few different heating times" (p.125).

The effect of humidity on thermal degradation rate was considered by Hansen and Ginell (1989) using a Hot Pack Temperature-Humidity Chamber. Samples were exposed to relative humidities of <5%, 50%, 70% or 90%  $\pm$  2, at a temperature of 90 °C for 17 days. The degradation rate increased rapidly above a relative humidity of 50%, with very little change in properties evident between 0% and 50%. Setoyama (1982/1983) also found silk samples heated in sealed tubes yellowed more when temperature and moisture content were increased.

Bresee and Goodyear (1986) studied the types of fibre fractures found in historic silk and silk aged by heat and light. By analyzing the frequencies of the types of fractures produced, they concluded laboratory heating (for 6 hours at 60 $\pm$ 2 °C) resulted in increased embrittlement and loss of interfibrillar cohesion.

Researchers have tested the effect of deacidifying agents and antioxidants on the rate of silk degradation. The retardants examined by Kuruppillai et al. (1986) were seen to have little effect on improving breaking strength after exposure to heat, but did appear to retard the formation of amino groups.

#### Photochemical degradation.

Damage to textiles by light is of two types, photolysis and photosensitization. In order for the absorbed light to cause degradation, it must be of the correct wave-length to

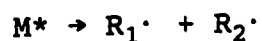
excite or energize the fibre molecules, such that they become chemically reactive. When bonds are directly broken by light energy, photolysis has occurred (Tucker, Kerr, & Hersh, 1980). This type of damage is caused by short-wave UV radiation. Light induced autoxidation can occur when a molecule absorbs a photon of light energy producing an excited state(\*) (Schnabel, 1981).



[16]

The excited molecule can then lose this absorbed energy through fluorescence, phosphorescence, internal conversions (heat), or photochemical reaction. In order for a photochemical reaction to occur, the molecule is usually in an excited triplet state which has a longer lifetime than a singlet state (Zollinger, 1987).

The excited molecule may then dissociate to form free radicals ( $R_1\cdot$  and  $R_2\cdot$ ) which are capable of propagating a free radical chain reaction with oxygen (Schnabel, 1981).



[17]

Most polymers do not absorb radiation having wave-lengths longer than 300 nm (Kamiya & Niki, 1978; Schnabel, 1981). Because radiation with wave-lengths less than 340 nm is filtered out by the atmosphere and by glass, photosensitization is more commonly a problem. For photosensitization to occur, a second substance which is chromophoric and thus is capable of absorbing near UV or visible light, such as a dye, is necessary. Kelly, Mollah and Wilkinson (1990) suggest two or more amino acid side chains may act together as a chromophoric group. They also propose naturally occurring impurities which are not removed by solvent extraction may also be involved.

The energy absorbed by the chromophores is transferred to

the textile (Miller, 1986; Tucker et al, 1980). The following mechanism for this transferal was proposed by Egerton (1948b): The light energy absorbed by the dye is transferred to surrounding air, activating the oxygen which can then combine with water vapour to form hydrogen peroxide. The fibres can be attacked either by the activated oxygen itself, or by the hydrogen peroxide.

To study changes in silk fibroin structure by UV radiation, Tsukada and Hirabayashi (1980) used a 10 watt incandescent ultraviolet bulb with a main wavelength of 253.7 nm. The degummed filaments were placed 20 cm under the bulb and kept at a temperature of 25 °C and 65% humidity for 10 to 45 hours. Using birefringence and X-ray studies, the researchers concluded the degree of orientation for fibroin decreased slightly with exposure to UV light, while the degree of crystallinity remained the same. Strength and elongation sharply decreased within the first 10 hours of exposure. This damage could be due to photolysis due to the purity of the fibres tested, and the low wavelength used to irradiate the samples.

Egerton's study (1948a) on the effects of light on fluidity and tensile strength changes of vat dyed rayon, silk, and nylon was concerned with degradation due to photosensitization. Dyed silk yarns were exposed to sunlight in a south-facing sun gallery for 1000 microwatt-hours/cm<sup>2</sup> /10 Å, and 4000 microwatt-hour/cm<sup>2</sup>/10 Å, measured using a photographic recorder. Results showed the presence of yellow and orange coloured anthroquinone and indigoid dyes greatly accelerated loss in tensile strength of the fabric, and that the effect was enhanced by high humidity.

There is further evidence that the damage done to silk by light is oxidative in nature. Harris (1934) placed silk yarns in a vacuum, and in atmospheres of hydrogen and oxygen, exposing them to north skylight for 4 months. Those in the vacuum and hydrogen atmosphere retained their strength, while

strength loss was apparent in oxygen-exposed samples. Egerton (1948a) irradiated undyed yarns with a 250 watt mercury vapour lamp in the presence of different atmospheres. Virtually no strength loss occurred for those samples exposed to carbon dioxide or nitrogen, whereas those exposed to air or pure oxygen exhibited strength loss of 31% to 55%.

Work by Okamoto (cited in Lucas et al., 1958, p. 189; Robson, 1985, p. 688) showed tyrosine, threonine and leucine as the residues most affected by photodegradation, and that damage was most rapid in the amorphous regions. Nakanishi and Kobayashi, (cited in Lucas et al., 1958, p. 189; Robson, 1985, p. 689) postulated degradation occurs first by the breaking of hydrogen bonds, followed by oxidation of the tyrosine residues, and eventual chain scission at the tyrosine residue. Their results indicated fibroin is oxidized by light, while simultaneously being hydrolysed by water.

The effect of humidity on the photodegradation of silk fibroin has been investigated. Undyed yarns were enclosed in cells containing 0% and 100% relative humidity, and were placed in a south-facing sun gallery for 6 months. The sample exposed to high humidity exhibited a 100% loss in strength, whereas the dry sample showed a 65% loss (Egerton, 1948a).

The effect of pH on photodegradation of fibroin was studied by Harris (1934). Samples treated with 0.1N NaOH and 0.1N H<sub>2</sub>SO<sub>4</sub> were exposed for up to 175 days to sunlight, under glass. Those samples treated with acid had a higher strength loss than the alkaline samples.

In addition to deterioration of tensile properties, silk also yellows during photodegradation, possibly due to degradation of tryptophan residues (Okamoto & Kimura, 1954). The results of Holt, Milligan and Savige (1977) indicated that tryptophan was responsible for some yellowing of bleached or fluorescently whitened wool, but had less support for its effect on unbleached, unwhitened wool. Photodecomposition of histidine or tyrosine residues (Inglis & Lennox, 1963) or the

introduction of double bonds (Hoare, 1974) have also been suggested as contributing to the photoyellowing of wool, so may also play a role in silk (Holt et al., 1977).

#### Weighting agents.

The presence of weighting agents in silk is known to increase the fibre's sensitivity to degradation. By the late 19th century, the addition of these compounds was a standard procedure in the processing of silk.

The weighting process was originally adopted in order to replace the weight lost during degumming, and allowed the weight of the silk to be increased 30% to 300%. By treating the silk with the inorganic salts of aluminum, iron, lead, tin, or zinc, the hand, body, "scroop" and drape of the fabric were improved (Becker, Hersh, & Tucker, 1987).

Tin salts are the most frequently used weighting agent. The fibres are treated with anhydrous stannic chloride which is then hydrolysed to form an insoluble salt within the fibre. This salt is then exposed to sodium phosphate to form high molecular weight complexes. This process is repeated several times to further increase the weight. The silk is then boiled in sodium silicate to produce a high molecular weight, insoluble tin silicophosphate. The appearance of the silk is not noticeably changed because the salts are deposited within the fibre (Robson, 1985).

Weighting agents are often responsible for deterioration of physical properties caused by acid hydrolysis and oxidation during exposure to light, storage, or from the weighting process itself (Robson, 1985). Upon exposure to light, weighted silk may degrade more quickly than nonweighted because most weighting agents are highly acidic (Becker et al., 1987). Harris (1934) showed silk with an acidic pH to be very unstable to light. The effect of humidity on the degradation of weighted silk was found to be small, indicating the photosensitizing reaction occurs through the formation of an activated oxygen intermediate rather than through a

hydrogen peroxide intermediate (Egerton, 1948b).

Weighted silk samples exposed to 4 months of natural sunlight through glass were found to have a higher loss of tensile strength than those stored in the dark (Roberts and Mack, 1936). D'Olier and Mack (1936) also showed strength loss to occur after 6 months, and 23 months of storage in darkness.

In the study by Roberts and Mack (1936), samples were given repeated passes through tin chloride and disodium phosphate baths, and strength per thread was compared to an unweighted control. Results showed a considerable loss of strength occurred due to the weighting process itself, and that strength decreased with increased number of treatments.

#### Summary and Comparison of Degradative Forces

Exposure to chemicals, heat, or light affect silk fibroin in different ways. Miller (1986) found exposure to xenon arc lighting, and sodium hydroxide treatments had the greatest effect on tenacity and elongation. Heat in the presence of air, exposure to light, and chemical treatments all produced statistically significant ( $p < 0.05$ ) changes in the proportions of at least two amino acids. In general, the amino acids with bulky side chains were most affected. Because these residues are most likely found in noncrystalline regions of the fibre, Miller's results suggest the attack occurred primarily in the amorphous areas.

Bresee and Goodyear (1986) used SEM to discover differences in the type of fibre fracture most frequently found in silks aged by different means. Brittle fractures were frequent in samples aged by heat, whereas surface-flaw fractures were dominant for light aged fibres. They also discovered a greater variety of fracture types in naturally aged silks, perhaps indicating these fibres had been aged through a combination of processes. Miller (1986) noted similar results. Bresee and Goodyear (1986) proposed that loss of interfibrillar cohesion, rather than embrittlement,

best describes what happens to naturally aged silk.

Several differences between thermally and photochemically aged silks were noted by Hersh et al (1989). Thermally aged samples were found to have discoloured 10 times more than light aged samples degraded to the same strength. For both light and heat aged samples, a decrease in strength was accompanied by an increase in amino groups, indicating scission of the main polypeptide chain. However, at any given strength, heat aged samples generated more amino groups than light aged, perhaps indicating that the mechanisms for thermal and photodegradation are different. The amounts of ammonia produced by both types of aging was almost identical.

#### Accelerated Aging of Silk

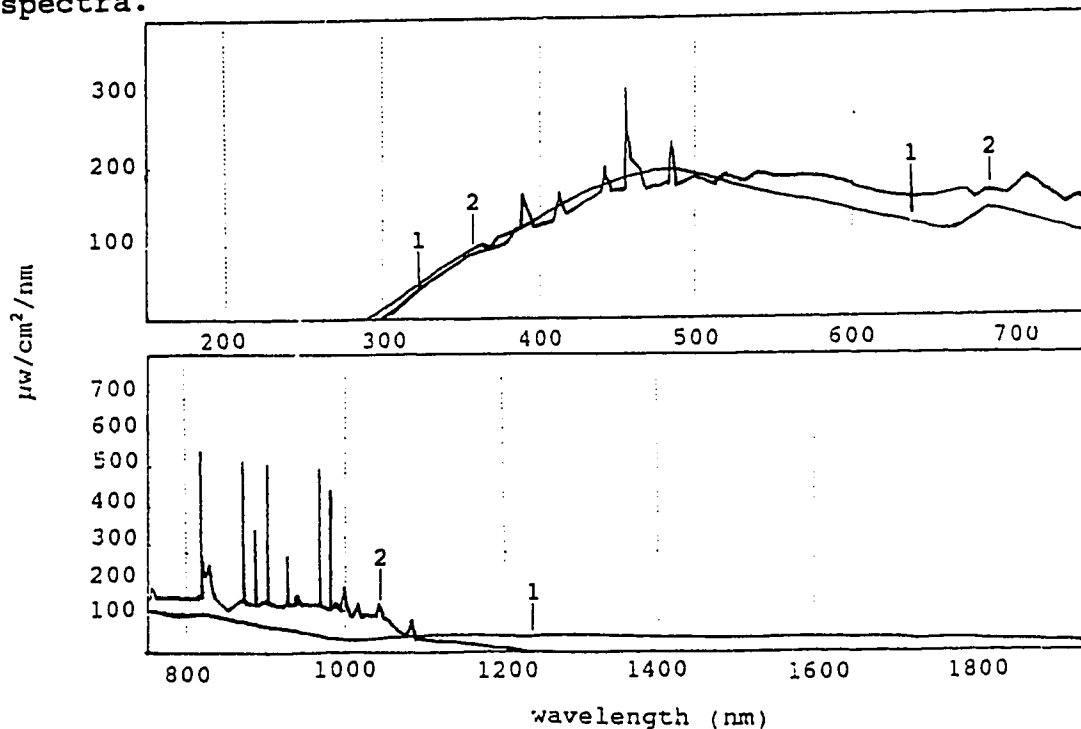
There is no way to accurately simulate naturally aged silk. Nevertheless, artificially aged silk is often used in conservation research because it is easily produced in the lab, thus allowing for a large sample size. Also, variables can be more easily controlled when using artificially aged silk because the way in which it was degraded is known. Historic silk has been exposed to unknown forces and may contain unidentified impurities, both of which will affect results. For these reasons, the use of artificially aged silk yields more reliable results.

Silk can be photochemically aged using either natural sunlight or a simulated solar spectrum. One problem with the use of natural light to artificially age samples is the seasonal fluctuation of UV light reaching the earth's surface which causes difficulty in comparing studies done at different times of the year. Because there are many factors involved in weathering, and because of the length of time needed to chart their effect, lab equipment simulating weathering conditions has been developed. Through controlling relative humidity, temperature and light intensity, the rate of degradation can be accelerated.



Because variables can be carefully controlled using these laboratory instruments, the reliability is better than for the methods using natural light exposure. However, according to Wall and Frank (1971), "Although the xenon arc has been found to compare more closely to sunlight than the carbon arc, laboratory test methods cannot be relied upon to give forecasts of behaviour of textiles in use" (p. 33). Thus in using this equipment, some validity is sacrificed for the sake of reliability.

Carbon arc and xenon arc lamps are most frequently used to simulate daylight. Figure 2 compares the spectra emitted by a xenon arc lamp with borosilicate filters to the daylight spectra.



1. Noon daylight at Chicago, Ill. Sept. 22, 1966.
2. Water cooled xenon lamp 5500 watts, 7740 borosilicate inner and outer filters, lamp age 100hrs.

**Figure 2.** Spectral distributions of daylight and a filtered xenon arc lamp.

**Note.** Adapted from "New Developments in Water-Cooled Xenon Lamps for Lightfastness and Weathering Tests (Part I)" by J. D. Conner, 1969, *Canadian Textile Journal*, May 15, p. 50. Adapted by permission.

A study by Norton, Kiuntke, and Connor (1969) attempted to make the xenon arc spectrum more similar to that of noon sunlight plus skylight through the use of various filters and wattage. Xenon arc equipment is frequently used for accelerated aging studies on silk, most often using AATCC test method 16E-1982 as a guide (Becker, 1988; Hansen & Ginell, 1989; Hersh et al., 1989; Kuruppillai et al., 1986; Miller, 1986; Poffenroth, 1990).

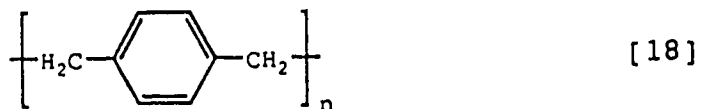
### Parylene

The parylene group of polymers is presently being studied as a new way of dealing with delicate museum artifacts. The nature of this coating will be discussed under three main subject headings. First, the unique deposition process for parylene and the mechanism by which it polymerizes will be explained. Second, the physical and chemical properties of parylene films will be examined. Exploration of these properties reveals many of the polymer's attributes which make it suitable for use in conservation. This information is important also, because according to Fix (1981), "Since polymer degradation is a function of the energy and chemistry of the environment and polymer, a fundamental understanding of its chemistry, physics and mechanics is required to properly evaluate and predict degradation" (p. 483). The last section of this review will discuss the wide uses of these polymers, focusing on studies for use in artifact conservation.

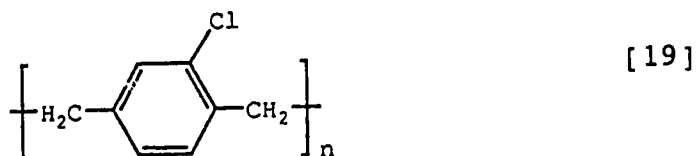
### Parylene Structure and Nomenclature

Parylene is the generic name for the poly-paraxylylene series of polymers (Baker, Fix, and Judge, 1980). The term is also used, when capitalized, as the trade name for these polymers (Reed, Schramm, & Clark, 1973). Poly-paraxylylene's molecular structure consists of alternating benzene rings and

methylene groups in a straight linear chain:



The unsubstituted variety is frequently referred to as parylene N. The other most frequently studied type is polychloro-*p*-xylylene, or parylene C, for which one hydrogen on the benzene ring has been replaced by a chlorine atom (Nova Tran, 1990):



Less common varieties include parylene D with two chlorine substitutions (Reed et al., 1973). and parylene M which has a methyl group added to the ring (Spivack, 1972). Many other substituted varieties have also been studied (Gorham, 1966).

### Polymerization and Deposition of Parylene

#### History

Poly-paraxylylene was first polymerized by Szwarc by flash pyrolysis of *p*-xylylene. Even at the high temperature of 1150 °C, this method only produced a 25% yield of the polymer and other side products were formed (Iwatsuki, 1984). The polymer has also been formed with varying degrees of success through chemical syntheses which are summarized in Iwatsuki's review article (1984). Gorham (1966) reported the polymer constituted by these techniques was usually in the form of a white powder, not a film.

In 1966, Gorham introduced a new vapour-coating technique for polymerization, which offered several advantages over previous methods. The lower pyrolysis temperature allowed the technique to be used on halogenated poly-paraxylylenes. It

produced a higher yield free of by-products. Also, the polymer produced was linear and free of cross-linkages (Gorham, 1966; Iwatsuki, 1984).

### Gas Phase Polymerization

Explanations of Gorham's vacuum deposition process are found in numerous sources (Gorham, 1966; Humphrey, 1984; Iwatsuki, 1984; Szwarc, 1976) and are best illustrated by Figure 3.

First, the cyclic dimer di-para-xylylene is placed into the vaporizer and heated to approximately 150° C, causing this white powder to sublime into a gas. The gas then travels to

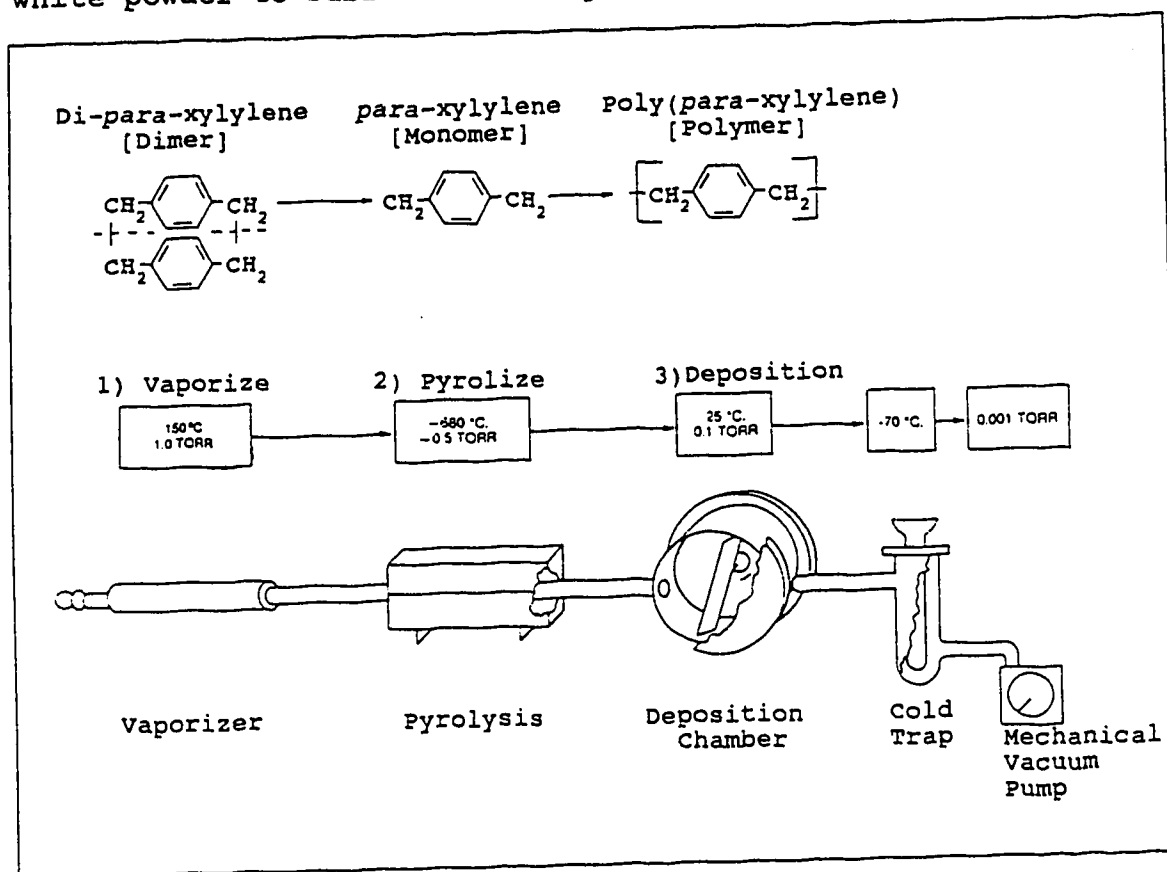
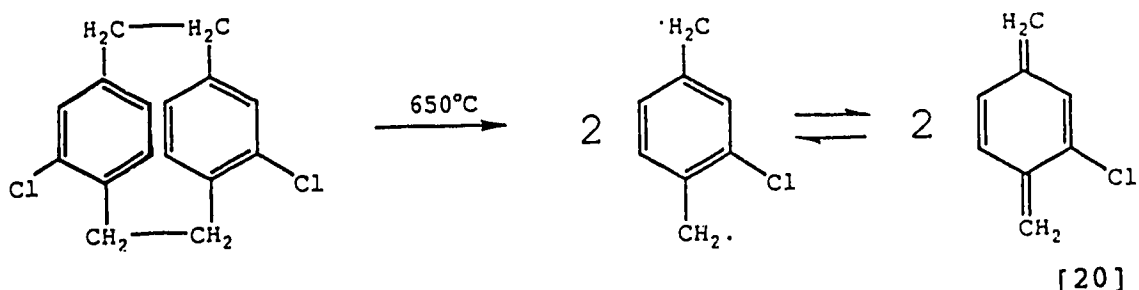


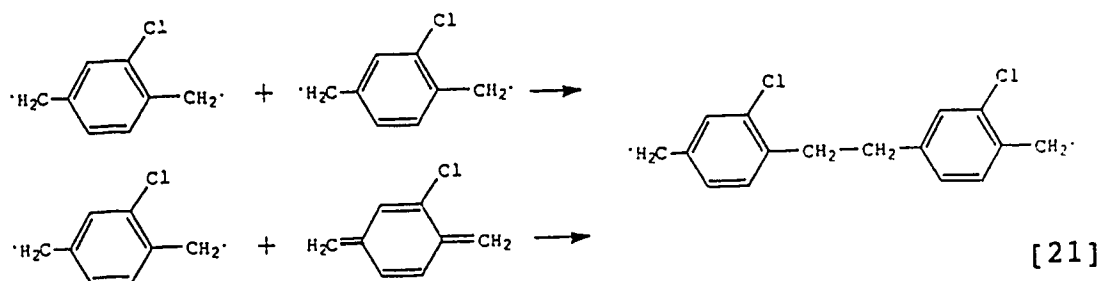
Figure 3. The parylene deposition process.

**Note.** From *Parylene Conformal Coatings Specification and Properties* (p.3) by Nova Tran Corporation, 1990, Clear Lake WI: Author. Copyright 1990 by Nova Tran. Reprinted by permission.

the furnace, where at 650 °C to 690 °C pyrolysis occurs, splitting the dimer into two very active monomers:



The monomers may be in either the quinoid or diradical form (Gazicki, Surendran, & Yasuda, 1985). The monomers then flow into a chamber where the item to be coated has been placed. The chamber is at room temperature and is under vacuum of approximately 0.1 torr. The high energy monomers bounce around the chamber until they have lost sufficient energy to adsorb onto the cool surfaces within the chamber. Then the monomers initiate polymerization by combining to form a diradical dimer (Gazicki et al., 1985):



The incoming monomers react with the radical at either end of the chain to increase its length by one unit. The polymer chains continue to propagate the reaction from both ends with no cross-linking. The ends of existing chains do not often react with each other because their movement is limited due to entanglement with neighbouring chains. Most monomers react with the polymer chains rather than with other monomers (Beach, Bassett, & Austin, 1989).

The polymer reacts only with itself, not with the substrate, causing the coating to be mechanically, but not chemically bonded to the surface (Loeb, Bak, Salcman, & Schmidt, 1977). If the surface is porous the monomers have sufficient energy to penetrate deeply. Starting from these centres the polymer continues to grow outward, thus providing a strong mechanical bond to the substrate (Humphrey, 1990).

Polymerization proceeds in this manner both on and beneath the surface of the growing film (Humphrey, 1990). Theoretically, the process continues indefinitely because termination due to reaction with active mono-radicals, or through the formation of ring-structures is not favorable (Szwarc, 1976). However, as polymerization continues, the growing chains become buried in the thickening film. Because incoming monomers react with centres close to the film surface, older growth centres eventually become buried and 'starved', ceasing to grow (Szwarc, 1976). Clearly, polymerization also ceases when the supply of incoming monomers is stopped (Humphrey, 1990). After deposition is complete, the free radical ends are converted by reactions to oxygen (Beach et al., 1989). No liquid phase between the gaseous monomer and the solid polymer has yet been isolated (Humphrey, 1984, 1988).

The thickness of the coating is determined by the amount of the original dimer used. When calculating the amount needed, the microscopic surface area of porous materials, like paper and textiles, must be taken into account (Humphrey, 1984). The material, shape, and morphology of the substrate have also been observed to affect coating thickness (Sharma, Hahn & Nichols, 1988). These researchers concluded that more dimer alone does not yield thicker coatings of high quality. Increased dimer elevates the system pressure and higher pressure was shown to produce electronically weak, opaque, nonuniform films. A more uniform coating can be achieved by lowering the pressure in the system either by reducing the

sublimation temperature or modifying the sublimation tube geometry. Emphasis has also been placed on the need to balance vacuum pressure with pyrolysis temperature to produce high quality coatings (Williams & Rowen, 1987).

Sometimes an exact measurement of the coating thickness is essential. Kim, Powers and Mason (1982) developed the use of optical reflectometry to monitor thickness during the coating process.

Numerous studies have been conducted on various aspects of the vapour-deposition process. In their investigation of paraxylylene coatings, Baker, Bagdasarian, Fix and Judge (1977) altered vaporization/pyrolysis temperatures and deposition load, and studied the films produced. Chamber pressure and deposition rate were also studied. Among their conclusions they stated that "electrical, mechanical and physical properties of the film are essentially unchanged with minor variations in the deposition conditions" (Baker et al., 1977, p. 900). The same conclusion was also drawn by Loeb (1971).

The penetration of monomers into narrow channels was the subject of a study by Broer and Luijks (1981). By decreasing the monomer pressure, and thereby decreasing the deposition rate, penetration was increased. In addition, polychloro-*p*-xylylene was seen to have less favourable penetration than the unsubstituted variety. This difference was likely due to the high reactivity of the parylene C monomers.

The vacuum deposition coating method has a number of favourable attributes. The parylene coating can "replicate surface irregularities down to 2400 lines/mm" (Loeb, 1971, p. 48), allowing irregular surfaces, and concealed areas to be evenly coated. Parylene is truly conformal and of uniform thickness because it thickens from all areas of the substrate outward simultaneously. The coating produced is colourless, transparent, and pinhole free down to a thickness of 0.001" (Szwarc, 1976). In addition, the process also bypasses the

need for the drying and curing steps necessary in conventional technologies and does not require the use of environmentally harmful solvents (Szwarc, 1976). Because the coating takes place in a vacuum, "even highly reactive substances which are destroyed or spoiled by exposure to air or moisture can be safely coated" (Szwarc, 1976, p. 478).

### The Structure of Parylene Coatings

Extensive research has been done on the molecular structure of parylene films. Beach et al. (1989) stated

In a manner typical of crystalline polymers, the crystallinity of parylenes is normally limited to small submicrometer domains that are randomly and uniformly dispersed through a continuous amorphous phase. Adjacent polymer chains, in order to acquire greater overall system stability, would prefer to be close to one another, but the extent to which they can is limited by the tangles already present (p. 1013).

Each chain is long enough to pass through several crystallites thus providing a strengthening matrix for the bulk polymer (Beach et al., 1989).

Wunderlich (1968) indicated that at temperatures below 30 °C, crystallization occurs after polymerization begins, but before the chain growth is complete. Polymerization and crystallization occur in successive stages during the overall deposition process. Two different structures for the crystalline regions of parylene N have been observed, and are temperature dependent. At ambient temperatures, crystals are of a monoclinic  $\alpha$  form only, which is modified to a  $\beta$  form above 220 °C (Iwamoto & Wunderlich, 1973; Kubo & Wunderlich, 1972). The dimensions of the  $\alpha$  form are:  $a = 5.92 \text{ \AA}$ ,  $b = 10.64 \text{ \AA}$ ,  $c(\text{chain axis}) = 6.55 \text{ \AA}$ ,  $\beta = 134.7^\circ$ , with two monomer repeat units per cell (Iwamoto & Wunderlich, 1973). The  $\beta$  form has the following configuration:  $a = b = 20.52 \text{ \AA}$ ,  $c(\text{chain axis}) = 6.58 \pm 0.02 \text{ \AA}$ , and  $\tau = 120^\circ$ , for 16 monomer units per cell (Niegisch, 1966). The parylene C polymer has only one crystal structure, which is very similar to the  $\alpha$  form of parylene N.



The crystal dimensions have been defined as follows:  $a = 5.96 \text{ \AA}$ ,  $b = 12.69 \text{ \AA}$ ,  $c$  (chain axis)  $= 6.66 \text{ \AA}$ ,  $\alpha = \gamma = 90^\circ$ ,  $\beta = 135.2^\circ$ . The  $b$  axis for parylene C is slightly longer than for parylene N due to the chlorine atoms protruding from the benzene rings (Isoda, Ichida, Kawaguchi, & Katayama, 1983).

Within the  $\alpha$  crystals, the benzene rings are parallel to each other and are oriented in the same direction. The rings are parallel to the  $b$  axis of the crystal. Greatest stability occurs when this  $b$  axis is oriented perpendicular to the substrate surface (Iwamoto & Wunderlich, 1973). Within the crystalline regions, the polymer chains with their constituent benzene rings have a preferred orientation; however, in the rest of the bulk polymer, the chains are completely random showing no preferred orientation (Beach et al, 1989).

### Properties of Parylene

The physical properties of parylene are affected by the presence of different substituents on the benzene rings. Table 3 summarizes the properties of the unsubstituted and chlorinated types, parylene N and parylene C.

#### Mechanical Properties

Parylene C has the highest tensile strength and tensile modulus of the parylene family (Gorham, 1966). Parylene C also has an impressive elongation at break of 220%. The elongation at break for parylene N is highly variable, ranging from 10% to 15% (Gorham, 1966) to up to 250% (Nova Tran, 1990).

Spivack (1972) tested both the uniaxial and biaxial mechanical properties of very thin films ( $0.12 \mu\text{m}$  to  $0.28 \mu\text{m}$ ). He calculated the rupture constant as an indication of biaxial or burst strength, taking pressure to rupture, film thickness and diameter of the unsupported film into account. In keeping with Gorham (1966), he found parylene C to have superior mechanical properties to parylene N and concluded that the thickness of film appeared to have very little effect on

**Table 3**  
**Properties of Parylene**

| Properties <sup>a</sup>                                 | Parylene C | Parylene N <sup>b</sup> | Method  |
|---|------------|-------------------------|---|
| <b>Mechanical and physical properties</b>               |            |                         |   |
| Density (gm/cc)   | 1.289      | 1.10-1.12               | ASTM D1505-57T  |
| Index of refraction ( $N_u^{23}$ )                      | 1.639      | 1.661                   | Abbe refractometer                                    |
| Tensile strength (psi)                                  | 10 000     | 6000-11 000             | ASTM D882-56T<br>10% strain/min                       |
| Young's modulus (psi)                                   | 400 000    | 350 000                 | ASTM D882-56T<br>1% strain                            |
| Elongation to break (%)                                 | 200        | 20-250                  | ASTM D882-56T<br>10% strain/min                       |
| Water % absorption (24hr)                               | <0.1       | <0.1                    | ASTM D570-57T   |
| <b>Thermal properties</b>                               |            |                         |   |
| Melting point (°C)                                      | 280        | 405                     | Secant modulus-temp. curve (1)                        |
| Glass transition temperature (°C)                       | 80-100     | 60-70                   | Secant modulus-temp. curve (1)                        |
| <b>Electrical properties</b>                            |            |                         |   |
| Dielectric strength (volts/mil, short time, 1 mil film) | 5600       | 7000                    | ASTM D149-64  |
| Dielectric constant 60 Hz                               | 3.15       | 2.65                    | ASTM D150 65T<br>1-in <sup>2</sup> mercury electrodes |

Continued

Table 3 (continued)  
Properties of Parylene

| Properties <sup>a</sup>  | Parylene C | Parylene N <sup>b</sup> | Method         |
|--|------------|-------------------------|----------------|
| <b>Barrier properties</b>  |            |                         |                |
| Gas permeability<br>cc-mil/100 in <sup>2</sup> -<br>24hr               |            |                         | ASTM D1434-63T |
| N <sub>2</sub>   | 0.6        | 15                      |                |
| O <sub>2</sub>   | 5          | 55                      |                |
| CO <sub>2</sub>  | 14         | 420                     |                |
| H <sub>2</sub>   | 110        | 540                     |                |
| Moisture vapour<br>transmission<br>gm-mil/100 in <sup>2</sup><br>-24hr | 0.21       | 1.6                     | ASTM E96-63T   |

Note. From *Parylene Conformal Coatings Specifications and Properties* (pp. 4-7) by Nova Tran Corporation, 1990, Clear Lake WI: Author. Copyright 1990 by Nova Tran. Adapted by permission.

<sup>a</sup>Properties measured on films 0.001 to 0.003 inches thick, except where specified

<sup>b</sup>Properties depend somewhat on deposition conditions

uniaxial tensile properties. The exception was ultimate elongation of parylene C, which varied from 65% to 345% with increasing film thickness. From his results, Spivack rated parylene C as tougher than parylene N, implying more work was required to rupture the film. Data published by Loeb (1971) show similar trends to Gorham (1966) and Spivack (1972).

Beach et al. (1989) note mechanical properties can change considerably with age. When the crystallinity of the coating increases with age, the extension decreases while the modulus and tensile strength increase.

### Electrical Properties

Parylenes, in general, are good insulators (Loeb, 1971). Parylene N, because of its nonpolar and highly symmetrical nature, is an extremely good insulator making it useful in the electronics industry. Electronically continuous films can be prepared as thin as  $0.5 \mu\text{m}$  (Gorham, 1966).

### Barrier Properties

Research has shown parylene to be highly impermeable to water vapour. Both Loeb (1971) and Gorham (1966) found parylene C to be substantially less permeable than parylene N to water vapour and all other gases tested on 1 mil thick films (see Table 3). Parylene C has better moisture barrier properties than almost all other plastics (Nova Tran, 1990)

Water vapour transmission was also studied by Kale (1978). Standard porosity fixtures were coated and sealed with a 0.36 mil coating of parylene C. After 72 hours in a desiccator with 100% relative humidity at  $25^\circ\text{C}$ , the fixtures were weighed, and the mass compared with the initial mass. The mass of moisture which had been transmitted (28.6 mg), is equivalent to a water vapour transmissibility of  $23.2 \times 10^{-10}$  cc(STP)  $\text{cm}/\text{cm}^2 \cdot \text{sec} \cdot \text{cm Hg}$ .

### Optical Properties

The parylenes absorb only the shorter wave lengths in the high energy ultraviolet portion of the spectrum, absorbing strongly in the region below  $280 \mu\text{m}$  (Nova Tran, 1990). They are transparent and colourless to visible light (Beach et al., 1989). Unstretched parylene N films have a negative birefringence of  $-0.075 \pm 0.001$  (Corley, Haas, Kane & Livingston, 1954).

### Solubility

Parylene N and parylene C are insoluble under most conditions. Solvents are capable of entering the amorphous phase of the polymer which causes some swelling; however, the solvent cannot penetrate the crystalline areas, provided the temperature is below the melting point of the crystallites.

The crystalline regions are therefore responsible for the high solvent resistance of the coating (Beach et al, 1989). Parylene N will only dissolve in high boiling solvents like benzyl benzoate, above 200 °C. Parylene C is slightly more soluble in these solvents (Gorham, 1966).

### Degradation of Parylene

#### Hydrolytic Degradation

Hydrolytic degradation of parylene is chemically impossible because the coating does not react in any way with water (Beach et al., 1989).

#### Oxidative Degradation

There is one significant undesirable factor related to the basic properties of these polymers: "Poly-p-xylylene is sensitive to degradative attack by oxygen, which can detrimentally affect their useful lifetimes at temperatures in excess of 100° C in air" (Szwarc, 1976, p. 479). A study by Modica, Di Renzo, Tempesti, and Mazzocchia (1988) concluded that chlorinated parylene had a slower degradation rate than the unsubstituted type (1988).

The chapter on oxidative degradation (pp. 79-148) in *Aspects of Degradation and Stabilization of Polymers*, by Kamiya and Niki (1978) gives an excellent introduction to this complex process. The free radical reaction involved in oxidation must be initiated by thermal, photochemical, mechanical or other energy sources.

Various oxygen-containing groups are introduced along the polymer chain or at its ends by oxidation, and some low molecular weight products are also formed. The oxidation of polymers also causes deterioration in physical properties. As the oxidation proceeds, decrease in molecular weight and discoloration of the polymers are observed. (p. 81)

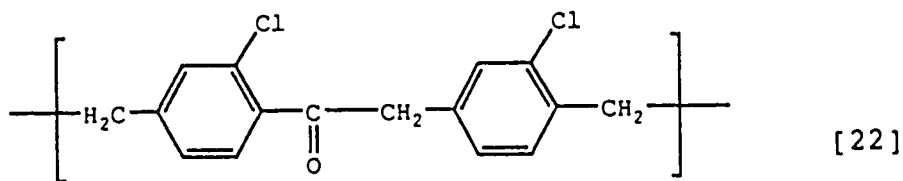
Oxidative chain scission is the primary mode of degradation for the parylenes (Beach et al., 1989).

### Exposure to Heat

Parylene is able to retain its strength at high temperatures because the fortifying structure provided by interconnected crystalline regions remains strong even above the polymer's glass transition temperature (Beach et al., 1989). However, these researchers also reported elongation at break decreased dramatically from 45% to 0% after 100 hours at 150 °C in air. They state that annealing through heat exposure produced an increase in the polymer's crystallinity, which resulted in a lower elongation.

Oxidative degradation of parylene is a problem at temperatures over 100 °C when air is present. A study on the thermal degradation of parylene was conducted by Nowlin, Smith and Cieloszyk (1980). Using neutron activation oxygen analysis, they found the oxygen content of parylene C films increased with thermal aging time, but that the rate of uptake decreased with time. The decrease in rate may be due to a decrease in the amount of polymer accessible to oxidation. The release of volatile, oxygen-containing degradation products during aging may also be a factor ( Nowlin et al., 1980). Change in mechanical properties was only evident after 3500 ppm of oxygen, or 1 oxygen atom per 38 monomer repeat units, had been incorporated into the film. Degradation of mechanical properties occurs when main chain scission or cross-linking occurs. Because a large amount of oxygen was present in the film before loss of strength occurred, the researchers concluded the reactions leading to chain cleavage were less frequent than those leading to the introduction of carbonyl groups (Nowlin et al., 1980)

IR characterization of the oxidated films showed the intensity of the carbonyl absorbance band ( $1695\text{ cm}^{-1}$ ) increased with aging time, indicating an increase in this functional group. Interpretation of the IR readings also suggested one oxidation product to have the following structure (Nowlin et al, 1980):



An IR absorption peak at  $1700\text{ cm}^{-1}$  in oxidated films was attributed to the presence of organic acid functional groups (COOH) by other researchers (Baker, Fix & Judge, 1980; Fix, 1981). This peak increased in intensity as a function of time and temperature.

The problem due to oxidation was addressed by Baker et al. (1980) who tested parylene C films to which an antioxidant had been added. The  $18\text{ }\mu\text{m}$  films, both treated and untreated, were subjected to temperatures of  $140\text{ }^{\circ}\text{C}$  to  $200\text{ }^{\circ}\text{C}$  for up to 500 hours in a forced air oven, and the amount of oxidative degradation was measured. Fourier transform infrared spectroscopy was used to detect the presence of by-products from the oxidative process. A  $180^{\circ}$  bend test was also conducted to measure the amount of embrittlement. The study found the addition of the antioxidant increased the service life of the film by greater than five times. Lower temperature lifetimes were extrapolated from the results. According to this study the untreated film would last 11 years at  $80\text{ }^{\circ}\text{C}$ , the modified one, 58 years.

In research which expanded on the studies by Nowlin et al. (1980) and Baker et al. (1980), Grattan and Bilz (1991) investigated thermal stability as it related to artifact conservation. They exposed  $10\text{ }\mu\text{m}$  to  $20\text{ }\mu\text{m}$  films of parylene C and parylene N to temperatures ranging from  $150\text{ }^{\circ}\text{C}$  to  $201\text{ }^{\circ}\text{C}$ . Some of the films contained an antioxidant. Results demonstrated that as the films oxidized, yellowing and embrittlement occurred. Yellowing was not visually perceptible until the films were too fragile for instrumental colour readings to be taken. Interpretation of IR spectra revealed the rate of carbonyl formation was faster at higher temperatures. Parylene C was also seen to be more stable than

parylene N and the rate of carbonyl formation decreased with time, thus confirming findings by Nowlin et al. (1980).

Grattan and Bilz (1991) also extrapolated their results to predict the films' lifetimes at 25 °C. Even though such extrapolation was acknowledged to be imprecise, results showed both parylene C and N to be extremely stable materials; for example, parylene C was predicted to have a lifetime of approximately 132,000 years in darkness at 25 °C. With this inherent stability, the Grattan and Bilz study questioned the need for adding an antioxidant for conservation purposes. Grattan (1990) has also reported when parylene with a phenolic antioxidant was used to coat books, a bright yellow discolouration appeared in highly degraded areas. The colour change was thought to be caused by a reaction between the antioxidant and the paper degradation products.

#### Exposure to Light

The heat-induced oxidative degradation of parylene is accelerated by exposure to ultraviolet light (Beach et al., 1989). In an internal report obtained from the Nova Tran Corporation, free parylene C films were exposed to a high intensity UV light source in air for intervals up to 300 hours after which the films were yellowed and embrittled. An infrared spectrum of the samples exposed for 72 hours showed a peak at 5.9  $\mu\text{m}$  indicating the formation of carbonyl groups which are an indication of oxidative activity.

As part of the study on parylene-coated silk, Hansen and Ginell (1989) exposed 12.5  $\mu\text{m}$  films to a xenon-arc lamp filtered to simulate sunlight for 500 hours. An IR filter, and a water-cooled support plate were used to reduce the heating of the samples. UV filters with cut-off points at 305 nm, 345 nm, 385 nm and 400 nm were tested to determine the wavelength threshold for yellowing. UV light sensitivity was measured through colour difference. The research revealed significant yellowing did not occur at wavelengths greater than 385 nm. Other properties, such as change in flexibility



or strength, were not tested.

#### Exposure to Chemicals

Parylene C and parylene N are highly unreactive compounds. According to Reed et al. (1973), their chemical resistance is "very good".

#### Uses of Parylene

The unique properties and method of deposition of parylene have made it useful in many areas. The polymer can be used both as a coating and as an unsupported film. Parylene C is used more frequently than parylene N (Humphrey, 1986). This may be due to its superior performance in the various tests cited previously.

#### General Uses

As a conformal coating, parylene's primary application has been in the electronics industry where it is used to protect delicate microcircuitry from chemical and particulate contamination; its mechanical, electrical, and conformal properties make it well suited to this purpose (Kinser, 1980; Szwarc, 1976).

The coating also has potential in medicine as it is compatible with the human biosystem (Szwarc, 1976). Because the polymer is resistant to hydrolytic attack, it does not degrade while inside the body (Beach et al., 1989). The polymer has been used successfully for insulating microelectrodes in neurophysiological research. The coated electrodes are capable of monitoring nervous tissue over extended time periods (Loeb et al., 1977). It has also been used as a protective coating for pacemakers (Olson, 1980).

The coating is also being tried as a replacement for highly polluting chromium plating as a means of protecting low quality steel from corrosion. Its barrier properties have also made it subject for study by the American military as protection against chemical warfare agents (CCI Minutes, 1989).

Unsupported films have found uses for such optical devices as beam splitters and windows for soft x-ray spectrometers. Parylene films are unique because they can be cast more thinly than other substances, and have no inherent stresses due to stretching (Szwarc, 1976).

#### Uses in Artifact Conservation

In recent years, studies have been carried out investigating the possibility of using the parylene coating technology to consolidate fragile museum artifacts. Thicknesses in the range of 2 to 25  $\mu\text{m}$  are generally used depending on the substrate (Humphrey, 1988). Studies have been conducted at institutions including the Royal British Columbia Museum, Library of Congress, The American Museum of Natural History, John Hopkins University, The Getty Conservation Institute, and the Canadian Conservation Institute (Humphrey, 1988, 1990).

#### Miscellaneous artifacts.

The Canadian Conservation Institute has conducted tests on a wide variety of substrates, a brief summary of which appeared in the *CCI Newsletter* (Grattan, 1989). This article focused on the success of the coating in consolidating very fragile cones and leaf mats from the Arctic Fossil Forest. A conference paper presented by Grattan (1990) discussed these applications in more detail.

In addition to its highly successful use on the cones and leaf mats, the coating has also been beneficial in strengthening crustacea and marine specimens which become dry and brittle with age. Results were generally satisfactory when parylene was used to prepare natural history artifacts for exhibit; fragile specimens could be handled more safely. Fossilized material is susceptible to cracking with changes in relative humidity. Parylene showed limited success in inhibiting the humidity-induced dimensional changes which causes this damage (Grattan, 1990).

Many ethnographic artifacts cannot be consolidated with

parylene because they cannot withstand the moisture loss which occurs when the coating chamber is evacuated. The moisture loss in fur pieces resulted in contraction and irreversible distortion of the artifact. Powdery pigments were successfully stabilized with 4  $\mu\text{m}$  or 8  $\mu\text{m}$  coatings, but the leather, parchment, bark and cedar substrates became warped (Grattan, 1990).

#### Paper and books.

The coating causes a minimal change in the appearance of paper. A very slight colour change may be perceptible on some papers, and those with a shiny surface may become slightly more shiny (Humphrey, 1990). Sometimes rainbow-like interference bands occur on smooth papers like coloured plates. These are apparent on areas of the substrate which have a slightly thinner coating, due to "extreme challenges to gas penetration" (Humphrey, 1990, p.58). Parylene causes a change in texture of the paper, imparting a slippery feeling.

A series of tests were conducted by Humphrey (1984, 1986, 1990) on the effect of the coating on books and papers. Treated and untreated paper from a 20 year-old paperback book were subjected to a number of tests, including a flex stress test and water immersion tests. Untreated paper failed the flex test after 85 complete flexures, whereas the coated page showed little sign of breakage after 1000 flexures. Microscopic examination revealed most of the paper fibres were broken in the flex region, but that the paper was being held together by a web of polymer bridges.

After six months of immersion in water, the coated paper showed no sign of damage, whereas untreated samples were limp and easily damaged. The coating was also tested for weathering resistance. Again, the coated papers showed very little sign of deterioration. Some shrinkage was noted, but there was no mention of any yellowing as was observed in the light-aging study by Hansen and Ginell (1989).

Tests conducted at CCI found coated newsprint to have a

42% increase in tear strength (Grattan, 1990). Parylene acts to strengthen paper in two ways. It provides a tough coating for each individual fibre thus increasing the overall strength of each fibre. Interfibre bonding also serves to increase the overall paper strength; the film produces a bond wherever the fibres cross. The strengthening effect of the polymer is determined in part by the type of paper, and its state of degradation. Weak papers exhibit a greater percent increase in strength than do strong papers with the same coating thickness (Humphrey, 1990).

Gas-polymerization is well suited for the coating of entire books. The book is held upright in a special frame and when evacuation occurs, the pages fan-out allowing the gas to coat each individual page (Humphrey, 1986, 1988, 1990). Due to the penetration properties studied by Broer and Luijks (1981), the parylene monomers have sufficient energy to travel down the tiny spaces between the pages of a fanned book. Parylene N is preferred over parylene C in the coating of books because of its superior penetration properties. Humphrey (1990) noted that the outermost edges of the pages receive a thicker coating than areas closer to the spine.

CCI found a 2  $\mu\text{m}$  coating of parylene C was effective in stabilizing red-rotted leather bindings (Grattan 1990). The coating has also been used to strengthen the fragile, charred pages of an airplane log-book so that forensic scientists could use it in their investigation of a major plane crash (Brown, 1990). The treatment has been considered for some of the volumes damaged in the 1988 fire at the Academy of Sciences Library in Leningrad.

Because book embrittlement is such a large-scale problem in libraries and archives, research is being conducted to develop coating systems capable of coating 100 or more books per cycle. Current technology can accommodate only eight books per cycle (Humphrey, 1990).

### Textiles.

Parylene coating technology has been used for the treatment of archaeological textiles, including those from the Windover Bog Site (Humphrey, 1990) and the Red Bay burial textiles. The Red Bay textiles were treated with a 4.4  $\mu\text{m}$  coating of parylene C which was successful in preventing further shedding of wool fibres. It was suggested that the accompanying surface bloom and slight change in hand could be prevented by the application of the polymer in repeated thin layers (CCI Minutes, 1989; Grattan, 1990).

Peatified textile remains were among the items recovered from the Windover Bog Site in Florida from 1986 to 1987. These finds represent the oldest known textile specimens in the New World, having been dated to the 6th millennium BC. After an initial consolidation treatment and freeze drying, the artifacts were still in a friable and extremely delicate state. As a preliminary test, one fragment was coated with 10.6  $\mu\text{m}$  of parylene N; the coating produced no observable change in appearance, yet greatly enhanced the strength of the artifact. This consolidation allowed the fragment to be handled more securely, even allowing it to be turned over to examine the other side (Humphrey, Gardner, Andrews, Adovasio, & Strong, 1990)

Preliminary investigations have been conducted on the use of parylene to stabilize New Zealand Maori textiles (Barton & Weik, 1988). The decorative black-coloured portions of these textiles have deteriorated severely due to the low pH and high iron content of the mud used in the traditional colouring process. These areas are now in an extremely fragile and powdery state, and in many cases have been lost entirely. A coating of 5.4  $\mu\text{m}$  and 8.6  $\mu\text{m}$  of parylene produced a substantial increase in strength. Although some change in appearance was noted, the results were still described as impressive.

Among the many materials coated at the Canadian

Conservation Institute were some degraded silk samples which were treated with 1 to 5  $\mu\text{m}$  of parylene C. Interference bands were apparent on shiny fabrics which had been given coatings from 1 to 3  $\mu\text{m}$ , but were not evident with the 5  $\mu\text{m}$  coating. Weave structure was also seen to play an important role in flexibility change. Those fabrics with open weaves remained more flexible with thicker coatings, whereas those with more compact weave structures became stiff with even a thin coating (Grattan, 1990). Overall, those textiles with a coating of 1  $\mu\text{m}$  were most acceptable and further testing of coatings from 0.1 to 1.0  $\mu\text{m}$  was suggested, as was the use of SEM to examine the textiles (CCI Minutes, 1989).

The most extensive study to date on the use of parylene in textile conservation was conducted at the Getty Conservation Institute by Hansen and Ginell (1989). Tests were conducted on modern and naturally aged silk, with some variation in coating thickness. 12  $\mu\text{m}$  thick films were also used in the previously cited UV light study.

Increased coating thickness (uncoated to 1.5  $\mu\text{m}$ ) on modern silk was seen to increase its tensile strength initially. Coated modern silk samples were then aged in a convection oven. Results from this test indicated that parylene C had no effect on the heat thermal degradation rate of silk's tensile properties; however, the researchers noted the coating may suppress degradation at room temperature because at this lower temperature the coating is a superior barrier to gases and water vapour. In addition, the researchers found untreated silk deteriorated faster above 50% relative humidity, and the addition of parylene C did not alter that rate (Hansen & Ginell, 1989).

The pliability of brittle historic silk was not found to increase with the addition of the coating (Hansen & Ginell, 1989). These results contrast with those of Humphrey (1984) who found the polymer aided paper in resisting breakage through flexing. The initial modulus and breaking load of

historic silk were improved with the coating (Hansen & Ginell, 1989).

Coated modern and coated historic fabrics were also exposed to a xenon arc Weather-Ometer simulating unfiltered sunlight. Both coated and uncoated samples yellowed upon exposure to light; however, the coated fabrics continued to yellow, whereas the uncoated stopped after 50 kJ of exposure. The strength of both coated and uncoated samples continued to decline up to 242 KJ exposure. Although coated samples were initially stronger, after 242 kJ (340 nm) the strength of coated and uncoated samples was similar.

From their research, Hansen and Ginell (1989) concluded that the coating could be considered for treatment of very degraded silk where an increase in tensile strength was of prime importance such as for static display. They strongly advocated the use of filters or special lamps to eliminate wavelengths below 400 nm because the coating was most sensitive to ultraviolet portion of the spectrum.

The use of coating technology on textiles is feared to reduce the drape of coated fabrics. Drape is determined by the ability of the fabric yarns to move and slip past one another at cross-over points. Whether a parylene coating would cause these yarns to weld together, and hence inhibit drape, is thought to be determined by coating thickness and yarn dimension (CCI Minutes, 1989).

#### Reversibility.

Ideally, conservation treatments performed on objects should be able to be removed or reversed without a detrimental effect on the artifact. In this way, if the treatment is unsuccessful, retreatment is possible (Grattan, 1990). In actual practice very few treatments, if any, are strictly reversible. For example, cleaning causes irreversible removal of dirt and other substances from the artifact. The removal of stitching often leaves holes in textile artifacts. Nevertheless, the concept of reversibility is important in

conservation ethics, and needs to be addressed concerning parylene coating treatments.

Because these polymers are highly crystalline, they have great resistance to solvents (Pascoe, 1985). Olson (1986) suggested several methods for selected removal of the coating from high performance printed wiring boards. Unfortunately, none of these techniques, which include exposure to high temperature, and use of wire brushes and abrasive powders can be applied to coated artifacts. For these reasons, such a treatment is irreversible; however, in the case of highly deteriorated objects where immediate consolidation is essential for the survival of the artifact, reversibility may not be of paramount importance (Pascoe, 1985). The coating may be the only treatment option for some artifacts, or may give superior results compared to more traditional treatment methods. Also, the coating does not prevent further consolidation and treatment from being performed (Grattan, 1990).



## CHAPTER 3 MATERIALS AND METHODS

## Fabrics

Both artificially and naturally aged silk fabrics were used in conducting this research. Bresee & Goodyear (1986) and Hersh et al. (1986) also used a combination of artificially and naturally aged samples in their research on silk degradation. Artificially aged silk can be produced in the laboratory and allows for a large number of specimens. Because artificial aging does not replicate natural aging, naturally aged silk fabrics were also used in order for the results to be valid regarding historic artifacts. Modern silk was not coated and tested because it was studied in depth by Hansen and Ginell (1989).

Historic silk fabrics were donated for study by the Clothing and Textiles Collection at the University of Alberta. A variety of fabrics was selected based on size, weight, weave, presence of dye and weighting agents, and degree of degradation. An undyed, unweighted degummed silk fabric with a twill weave (#609 from Testfabrics)<sup>1</sup> was used for the artificially aged samples. A description of each fabric appears in Table 4.

All fabrics were carefully wet-cleaned using a 0.2% solution of Shurgain® anionic detergent in distilled water to remove dirt and other impurities. A standard cleaning method for historic textiles was followed (Appendix A-1). After washing, the new silk twill fabric (fabric 8) was artificially aged using a 300 kJ exposure in a xenon-arc Weather-Ometer. A detailed description of this procedure is found in Appendix A-1.

---

<sup>1</sup>TestFabrics Inc., P.O. Drawer 0, 200 Blackford Ave., Middlesex NJ, 08846

Table 4  
Descriptions of Naturally and Artificially Aged Silk Samples

| #                               | Size (cm) <sup>a</sup> | Weave              | Colour    | Weighted | Condition            |
|---------------------------------|------------------------|--------------------|-----------|----------|----------------------|
| <b>Naturally aged fabrics</b>   |                        |                    |           |          |                      |
| 1                               | 11 x 668               | plain              | plum      | yes      | splitting            |
| 2                               | 15 x 940               | satin              | black     | yes      | stable               |
| 3                               | 51 x 559               | plain              | turquoise | yes      | brittle<br>splitting |
| 4                               | 49 x 280               | plain              | maroon    | yes      | brittle<br>breaking  |
| 5                               | 44 x 103               | plain<br>crepe     | undyed    | yes      | stable               |
| 6                               | 84 x 142               | plain<br>crepeline | undyed    | no       | stable               |
| 7                               | 192 x 40               | plain              | undyed    | no       | stable               |
| <b>Artificially aged fabric</b> |                        |                    |           |          |                      |
| 8                               | 100 x 200              | twill              | undyed    | no       | stable               |

<sup>a</sup>Filling x Warp

#### Sampling Procedure

Warp specimens measuring 14 x 7 cm (LxW) were cut from the new washed fabric 8 prior to artificial aging. Specimens were cut in a staggered fashion, and visible flaws in the fabric were avoided as shown in the cutting diagram in Appendix A-2. No specimens were taken from within 50 mm of each selvedge.

The naturally aged fabrics were cut into panels measuring approximately 17 x 48 cm (LxW). Eight panels were cut from fabric 4, 6 and 7, and sixteen panels were cut from fabrics 2 and 3 to provide extra sets of samples to use if necessary.

The eight panels cut from fabric 5 were smaller (17 x 24 cm) due to the limited amount of this fabric. Fabric 1, a narrow ribbon-like fabric was cut into 49 x 11 cm strips. In all cases, obvious holes, splits and discolourations were avoided as much as possible, in order to minimize differences among samples.

The panels of naturally aged silk were then randomly assigned to coating treatment groups; four of the eight panels from each fabric were assigned to group 1 which remained uncoated, the other four to group 2 which were coated with the parylene C polymer. The artificially aged specimens were also randomly assigned to these two treatment groups.

#### Application of the Parylene-C Coating

The specimens in group 2 were transported to the Nova Tran Laboratory in Clear Lake, WI for coating in a Parylene Deposition System model 1050. To fit into the vacuum chamber conveniently, the 17 x 48 cm panels were cut in half to produce 17 x 24 cm (LxW) specimens. Each of these specimens was placed on a wire mesh rack and twenty-five racks were stacked into a holder for coating. Glass reference slides were placed with the specimens on the top, middle and bottom racks, and were used to measure the coating thickness on the fabric. The specimens were coated in four batches as shown in Table 5.

The holder containing the stacked specimens was placed in the vacuum chamber and the chamber pressure was reduced to 20 mTorr. For each batch, a conservative estimate was made to determine the amount of Parylene-C dimer needed to produce a coating approximately 0.8  $\mu\text{m}$  thick. After deposition was complete, a profilometer was used to measure the coating thickness on the glass reference slides. It was assumed the coating thickness deposited on the slide was the same as the coating thickness on the specimens. If the coating was too thin, the polymerization process was repeated again until the

Table 5  
Parylene-C Coating of Silk Fabric Specimens

| Batch # | Fabric # | Rack # <sup>a</sup> | Dimer <sup>b</sup><br>amount | Coating <sup>c</sup><br>thickness |
|---------|----------|---------------------|------------------------------|-----------------------------------|
| 1       | 6        | 1 to 8              | 9                            | 0.88                              |
|         | 5        | 9 to 16             |                              | 0.70                              |
|         | 7        | 17 to 20            |                              | 0.60                              |
| 2       | 3        | 1 to 16             | 18                           | 1.00                              |
|         | 4        | 17 to 24            |                              | 1.00                              |
| 3       | 1        | 1 to 6              | 12                           | 0.74                              |
|         | 2        | 7 to 22             |                              | 0.74                              |
| 4       | 8        | 1 to 24             | 7                            | 0.85                              |

<sup>a</sup>racks in specimen holder numbered from top to bottom

<sup>b</sup>mass (g) of dimer placed in vaporizer

<sup>c</sup>in micrometers

desired thickness was reached. The three reference slides in batch 1 showed a slight gradation in coating thickness from the top to bottom of the chamber which was corrected for subsequent batches. A summary of the dimer amounts used and the coating thickness produced is given in Table 5. The amount of dimer used varied because the overall surface area for each batch of specimens was different due to variation in fabric weight and the number of specimens included. The specimens were coated with a  $0.8 \pm 0.2 \mu\text{m}$  layer of the parylene C polymer.

#### Accelerated Aging

The coated and uncoated panels were cut into 14 x 7 cm (LxW) warp specimens. The artificially aged fabric specimens had already been cut to this size before coating. These specimens were then randomly assigned to the treatment groups outlined in Table 6. For fabrics 2, 3, 4, 6, 7, and 8, six

Table 6  
Light Exposure Conditions Assigned to Treatment Groups

| Treatment group #       | Light <sup>a</sup> exposure conditions                                       |
|-------------------------|--|
| <b>Uncoated samples</b> |  |
| 1A                      | control- not put in Weather-Ometer   |
| 1B                      | fully masked from light in Weather-Ometer                                    |
| 1C                      | exposed to light in Weather-Ometer with the ultraviolet wave lengths removed |
| 1D                      | fully exposed to all wave lengths of light in Weather-Ometer                 |
| <b>Coated samples</b>   |  |
| 2A                      | control- not put in the Weather-Ometer                                       |
| 2B                      | fully masked from the light in the Weather-Ometer                            |
| 2C                      | exposed to light in Weather-Ometer with the ultraviolet wave lengths removed |
| 2D                      | fully exposed to all wave lengths of light in Weather-Ometer                 |

Note. Weather-Ometer conditions were 250 kJ/m<sup>2</sup> (420nm) exposure at 65 % relative humidity and a black panel temperature of 50 °C.

<sup>a</sup>A xenon-arc lamp filtered to simulate the solar spectrum

specimens were assigned to each treatment group. Due to the limited availability of fabrics 1 and 5, three specimens were placed in each treatment group. Groups 1A and 2A were not put in the Weather-Ometer and acted as the controls for the experiment. Specimens in groups 1B and 2B acted as a second set of controls. They were exposed to the 65% relative humidity and 50 °C black panel temperature within the Weather-Ometer but were shielded from the xenon arc rays by standard test masks. UV filtering film was placed over those

specimens in groups 1C and 2C during irradiation. This transparent polyester film, supplied by University Products<sup>2</sup>, filtered out the ultraviolet portion of the spectrum with wave lengths below 400 nm. Such a film would be readily available to the museum community through University Products' mail-order catalogue. The remaining specimens in groups 1D and 2D were exposed to all wave-lengths produced by the xenon arc lamp.

The specimens were aged in an Atlas Weather-Ometer model Ci35W using a procedure based on AATCC test method 16E-1987. The xenon arc lamp was fitted with borosilicate inner and outer filters to simulate the daylight spectrum. The specimens were inserted into standard test holders and were backed with acid-free mat board. Specimens from the same fabric underwent photochemical aging together. They were given an exposure of 250 kJ/m<sup>2</sup> with a lamp irradiance of 0.75 w/m<sup>2</sup> measured at 420 nm, which took approximately four days. The relative humidity was 65 ± 5% and black panel temperature was 50 ± 2 °C, the same conditions applied by Hansen and Ginell (1989).

### Measurement of Physical Properties

#### Rationale

Measuring changes in physical properties is one way to monitor the degradation of silk. Hansen and Ginell (1989) tested breaking load of textile fabrics, but yarn breaking tests have also been used (Becker, 1988; Hersh et al., 1989; Kuruppillai et al., 1986; Miller, 1986; Poffenroth, 1990). For this study, fabric strength tests were chosen over yarn tests because the fabric strength test is a better indicator of the coating's overall effect on fabric structure. Also, fabric tests allowed for comparison with the results from Hansen and

---

<sup>2</sup>University Products c/o Bury Media and Supplies Ltd.  
B5-4255 Arbutus Street, Vancouver, BC Canada V6J4R1

Ginell (1989).

Colour change has been measured by Becker (1988), Hersh et al.(1989), Kuruppillai et al.(1986) and Poffenroth (1990), all of whom used the CIElab\* system described below and reported  $\Delta E^*$  values for overall colour change. The CIElab\* system was used for this research as well.

At present, no study has been located addressing the effect of the parylene C coating on the flexibility and moisture regain properties of textiles. These properties are of interest to textile conservators and therefore were measured in addition to strength and colour change.

Scanning electron microscope techniques have been used to study fibre damage due to mechanical stress, or heat and light exposure. SEM analyses of fibre fractures have been used by Bresee and Goodyear (1986) and Zeronian, Alger, Ellison and Al-Khayatt (1986) to draw conclusions about fibre degradation mechanisms. The technique may provide information on how the coating affects the fibre surfaces and fabric structure. Such observations would help clarify some of the coating's effects on flexibility and drape. The Minutes of the Parylene Review (1989) at the Canadian Conservation Institute (CCI) suggest SEM observation of coated specimens would be useful. Such analysis was not undertaken by CCI or the Getty Institute.

#### Colour Change

The Hunterlab D25M-9 Tristimulus colorimeter was used to measure change in colour between treated and control samples following the guidelines outlined in the AATCC Test Method 153-1985 "Color Measurement of Textiles-Instrumental". The colorimeter had a 45° circumferential incidence/0° viewing instrument geometry, which measured the specimen at the angle of least specular reflectance. The instrument utilized the 1931 2° observer, and Standard Illuminant C which is similar to the visible light portion of the daylight spectrum. Measurements were taken with a 5.1 cm specimen port.

Using the CIE 1976 L\*a\*b\*<sup>3</sup> system for colour measurement, L\*, a\* and b\* coordinates were generated to describe lightness/darkness, red/green and yellow/blue respectively. The change in colour between treated and control samples was measured in terms of change in these three colour coordinates, or  $\Delta L^*$ ,  $\Delta a^*$ ,  $\Delta b^*$ . A measure of overall colour change,  $\Delta E$ , is related to  $\Delta L^*$ ,  $\Delta a^*$ ,  $\Delta b^*$  as follows:

$$\Delta E^* = [(\Delta L^*)^2 + (\Delta a^*)^2 + (\Delta b^*)^2]^{1/2} \quad [23]$$

where

$$\begin{aligned} L^* &= 116(Y/Y_n)^{1/3} - 16 \\ a^* &= 500[(X/X_n)^{1/3} - (Y/Y_n)^{1/3}] \\ b^* &= 200[(Y/Y_n)^{1/3} - (Z/Z_n)^{1/3}] \end{aligned}$$

and X, Y and Z are the colour response readings as taken by the instrument (Billmeyer & Saltzman, 1981).  $X_n$ ,  $Y_n$  and  $Z_n$  are the tristimulus values of the white reference tile (Billmeyer & Saltzman, 1981).

The  $\Delta L^*$ ,  $\Delta a^*$ ,  $\Delta b^*$ , and  $\Delta E^*$  values of the uncoated specimens were taken by comparing the L\* a\* b\* for each of the masked, filtered and fully exposed specimens (groups 1B, 1C, and 1D) to the average reading of the uncoated control group (1A). Two sets of delta values for the coated specimens were calculated, using both the coated control (2A), and the uncoated control (1A) as the standards for comparison with the Weather-Ometer exposed coated specimens (groups 2B, 2C, and 2D).

In addition to  $\Delta E$ , a yellowness index (YI) reading was also taken on the undyed specimens (fabrics 5, 6, 7, and 8). This index was developed specifically to study yellowing due to degradation or weathering (ASTM E313-73), so is preferable to  $\Delta E$ , which is a more general measure. YI is defined as

---

<sup>3</sup>The more recent CIE 1976 L\*a\*b\* scale is recommended over the Hunter L,a,b scale



follows in ASTM E313-73 "Standard Test Method for Indexes of Whiteness and Yellowness of Near-White, Opaque Materials":

$$YI = \frac{100 (Y - 0.847Z)}{Y} \quad [24]$$

The colour of each 14 x 7 cm (LxW) specimen was measured on the side which faced the xenon arc lamp. Four readings were taken on each specimen, two in the warp and two in the weft direction; these readings were averaged to give the overall colour reading for the specimen. A stack of the six specimens from each treatment group was presented to the colorimeter specimen port, thus imparting opacity to the specimen being read, and preventing the white tile backing from showing through.

#### Flexibility

Following colour measurement, each 7 x 14 cm specimen was cut in half lengthwise to produce twelve 12 x 2.5 cm (LxW) warp test specimens. The edges which had been protected from exposure by the Weather-Ometer test frame were trimmed off. These strips were then conditioned to 65 ± 2% relative humidity and 20 ± 2 °C.

ASTM test method D1388-64 "Standard Test Method for Stiffness of Fabrics" was followed using the Cantilever Test. The strip was placed on a level platform, and a small rectangular weight placed on top of it. By moving the weight, the specimen was then slowly pushed in the longitudinal direction over the edge of the platform until the free end bent down in an arc under its own weight and touched a centimeter scale which made a 41.5° angle with the horizontal platform. The overhang distance (the distance in centimeters from the contact point on the scale to the level platform) for each strip was read four times: face up, face down, first one end and then the other. These measurements were averaged for each strip, and bending length and flexural rigidity

calculated as follows:

$$\text{Bending Length} = O/2 \quad [25]$$

where O is the length of overhang in cm,

$$\text{Flexural Rigidity (mg-cm)} = W \times (O/2)^3 \quad [26]$$

where W is the weight per unit area in mg/cm<sup>2</sup> (ASTM D1388-64).

Prior to aging, the mass per unit area for each fabric was determined. Two cleanly cut 14 x 7 cm specimens were conditioned and weighed to the nearest 0.1 mg and the mass per unit area for each calculated. These two results were then averaged.

#### Tensile Properties

The same specimens used for the flexibility test were also used to determine the breaking load, extension at break and energy at break according to CAN/CGSB 4.2 no. 9.1-M90, "Breaking Strength of Fabrics--Strip Method--Constant time-to-break Principle". Tests were conducted using the ravel-strip method for fabrics 2, 5, 6, 7, and 8. The warp strips were produced by ravelling away yarns on each side, forming a 2.0 cm strip with a 2.5 mm fringe down each side. It was necessary to use the cut strip method for fabrics 1, 3, and 4, because some specimens were too degraded to unravel. For these fabrics, 2.5 mm were trimmed off each side to produce a test strip measuring 12 x 2.0 cm (LxW).

The testing was done under standard conditions of 65 ± 2% relative humidity and 20 ± 2 °C with an Instron Universal Testing Instrument Model 4202. Pneumatic grips with a width of 25 mm and rubber grip faces were used, and the gauge length was set to 75 mm. The cross-head speed was adjusted so the average time-to-break was 20 ± 3 seconds. Ten strips were measured for each treatment group, except for fabrics 1 and 5, where five strips were measured.

In addition to breaking strength, the Instron machine also measured energy to break and elongation. Energy to break, or work of rupture is calculated as the area under the load-elongation curve, and is a measure of overall toughness of a material. Elongation is the change in length undergone by the fabric at its breaking point. Extension at *break* expresses this change in length ( $\Delta L$ ) as a percentage of the original length ( $L_0$ ) as follows:

$$\text{extension (\%)} = \frac{\Delta L}{L_0} \times 100 \quad [27]$$

#### Moisture Regain

The moisture regain for the treatment groups of each fabric was determined using the procedure outlined in CAN/CGSB 4.2 no. 3-M88 "Determination of Moisture in Textiles", Procedure B. The test strips used previously for flexibility and tensile property measurements were unravelled and the yarns cut in 1 cm lengths. Those fabrics which could not be unravelled (1, 3 and 4) were cut into tiny 4 mm<sup>2</sup> pieces. The unravelled material for each treatment group was divided into three samples and the moisture regain measured for each of these samples. Two strips from each group were reserved for SEM analysis.

The unravelled fabric was allowed to equilibrate to standard testing conditions (65 ± 2% relative humidity and 20 ± 2 °C) for a minimum of two days. The conditioned mass was then determined on a Mettler analytical balance. Empty weighing vessels were dried to a constant mass by placing in a laboratory convection oven at 105 °C overnight. Then the vessels were removed from the oven and allowed to cool over Drierite® desiccant for one hour in glass desiccators before weighing. They were replaced in the oven for a minimum of one hour between weighings. A constant weight was achieved when successive weighings differed by less than ±0.0005 g. The

specimens of known conditioned mass were then transferred to the dried containers and placed in the oven to dry at 105 °C over night. Using the procedure described above, the specimens were weighed and dried repeatedly until a constant weight had been obtained.

From these measurements, moisture regain was calculated as follows:

$$\text{Moisture regain(\%)} = \frac{\text{conditioned mass} - \text{dry mass}}{\text{dry mass}} \times 100 \quad [28]$$

### SEM Analysis

The fabrics and corresponding treatment groups selected for viewing under SEM are listed in Table 7. Because the properties of the masked samples (groups 1B and 2B) did not differ from the overall controls (groups 1A and 2A), specimens in groups 1B and 2B were excluded from SEM analysis. The fabrics chosen represent examples of dyed and weighted, undyed and weighted, naturally aged and artificially aged undyed and unweighted fabrics with a variety of weaves.

Table 7  
Samples Analyzed With SEM

| Fabric # | Description                                      | Treatment groups     |
|----------|--|----------------------|
| 2        | naturally aged weighted<br>black satin           | 1A 1C 1D<br>2A 2C 2D |
| 5        | naturally aged weighted<br>undyed crepe          | 1A 1C 1D<br>2A 2C 2D |
| 7        | naturally aged unweighted,<br>undyed plain weave | 1A 1C 1D<br>2A 2C 2D |
| 8        | artificially aged<br>unweighted, undyed twill    | 1A 1C 1D<br>2A 2C 2D |

A specimen 0.5 cm<sup>2</sup> was mounted on a stub with double-sided adhesive tape. Conductive carbon glue was applied to the edge of the specimen to increase its conductivity through the stub. The specimen was then sputter-coated with 15 nm of gold to provide a conductive surface, and viewed under various magnifications using a Cambridge Stereoscan 250 scanning electron microscope. Photographs were taken at magnifications of 1500x, 3900x and 8000x.

Energy Dispersive X-Ray Analysis (EDXA) was also performed on several specimens to determine what elements were present in the specimen. Only elements in sufficient amounts with molecular weights higher than sodium were able to be detected.

#### Statistical Analysis

The inter-relationship of three independent variables (type of fabric, light exposure, and presence of coating) was evaluated for each of the dependent variables. The dependent variables were: total colour difference ( $\Delta E$ ), yellowness index, flexural rigidity, tensile strength, extension, energy to break, and moisture regain. Guidelines given by Milliken and Johnson (1984) for analyzing studies with three-way treatment structures were followed. First, a three-way analysis of variance was performed on the data for each dependent variable to determine which main effects and interactions were statistically significant. The UANOVA procedure, available through the Spss<sup>x</sup> statistics package on the University of Alberta mainframe computer, was used. Tables summarizing which main effects and interactions were statistically significant are given in Appendix A-4. For those dependent variables in which the coating-by-light-by-fabric three-way interaction was significant, the Duncan's Multiple Range Test was performed for a two-way treatment structure (between coating and exposure) at each level of the

third independent variable (fabric). In this way, the statistically significant differences among the treatment groups for each fabric were determined.

For dependant variables in which the three-way interaction was not statistically significant, the Duncan's Multiple Range Test was performed on pairs of factors that interacted in a statistically significant way. When the three-way interaction is not statistically significant, this indicates two of the independent variables, coating and exposure for example, have the same effect on the dependent variable at all levels of the third independent variable (fabric). Analysis of their effect on each individual fabric is not necessary, therefore, as the effect is the same for each fabric.

The effects of fabric structure, weighting agents, dye, and whether the fabric was naturally or artificially aged were also considered. Each fabric was assigned a binary code to indicate if it was dyed, weighted, and/or naturally or artificially aged. The raw data obtained by the physical property tests were converted to normalized data by dividing the raw data points in each treatment group by the mean of their corresponding unexposed control group. Normalized data effectively describes the change in a specific property, thus allowing the diverse fabrics to be compared to each other. The following three-way ANOVAs were performed on the normalized data set for each dependent variable: coating-by-exposure-by-age, coating by-exposure-by-dye, and coating-by-exposure-by-weight. Summary tables of the main effects and interactions are included in Appendix A-4. Duncan's Multiple Range Tests were then performed to determine where there were statistically significant differences between groups. The effect of fabric structure was not analyzed using statistics.

## CHAPTER 4 RESULTS AND DISCUSSION

In order to evaluate the long term effect of the parylene C coating on degraded silk fabric, measurements of physical properties were taken before and after accelerated photochemical aging. The exposure of the samples to accelerated light aging was conducted using two sets of controls. Control group A (unexposed) was not placed in the Weather-Ometer, and group B was placed in the Weather-Ometer but masked from the light. Group B differed from group A because it was exposed to 65% relative humidity and a black panel temperature of 50 °C for a 4 day period in the aging chamber. There was no statistically significant difference between group A and B for the properties measured, suggesting exposure to these conditions alone did not cause sufficient degradation to affect physical properties. Henceforth, all comparisons of the light exposed samples were made with control group A. Changes in colour, flexibility, tensile properties, and moisture regain were monitored. Scanning electron microscopy was also employed to detect surface changes.

## Colour Change

$\Delta E$  is a measure of overall colour change, which mathematically combines the  $L^*$ ,  $a^*$  and  $b^*$  numerical colour coordinates. Without reference to these coordinate values,  $\Delta E$  has limited meaning, therefore the  $L^*$ ,  $a^*$  and  $b^*$  values for each treatment group are given in Appendix A-3. The  $\Delta E$  values for the uncoated treatment groups were calculated using the unexposed uncoated fabric as the standard. The coated fabrics in each treatment group were compared to the unexposed coated fabric. The changes in colour apparent immediately after application of the parylene C coating are summarized in Table 8. Six of the eight fabrics exhibited a statistically significant change in colour. Light coloured, or undyed

Table 8  
Initial Effect of Parylene C Coating on the Colour of Silk Fabrics

| Fabric description |   |                     | Change in colour after coating |      |
|--------------------|---|---------------------|--------------------------------|------|
| #                  | n | Finish <sup>a</sup> | $\Delta E$                     | SD   |
| 1                  | 3 | W D                 | 1.1*                           | 0.26 |
| 2                  | 6 | W D                 | 3.0*                           | 0.52 |
| 3                  | 6 | W D                 | 2.7*                           | 0.96 |
| 4                  | 6 | W D                 | 5.1*                           | 0.95 |
| 5                  | 3 | W UD                | 0.7                            | 0.17 |
| 6                  | 6 | UW UD               | 0.7                            | 0.08 |
| 7                  | 6 | UW UD               | 1.4*                           | 0.26 |
| 8                  | 6 | UW UD               | 1.4*                           | 0.19 |

<sup>a</sup>W=weighted D=dyed UW=unweighted UD=undyed  
 \*statistically significant change determined by Duncan's Multiple Range Test ( $\alpha=0.05$ )

specimens exhibited a negligible change in colour; for example, the colour changes for fabrics 1, 7, and 8, although statistically significant were barely perceptible, if at all. Billmeyer and Saltzman (1981) state that colour differences below 1  $\Delta E$  unit of change are not visible. The visible colour change which occurred for fabrics 2, 3 and 4 was in the form of an iridescent sheen. These fabrics were black, turquoise and maroon in colour, all dark or intense hues. All three also had compact weaves, and smooth or shiny surfaces. The change in appearance was due to interference bands which are caused by a slight variation in coating thickness on surfaces which are difficult for the gaseous monomer to penetrate (Humphrey, 1990). This effect has been observed by Grattan (1990) on silk textiles with shiny surfaces, and by Humphrey

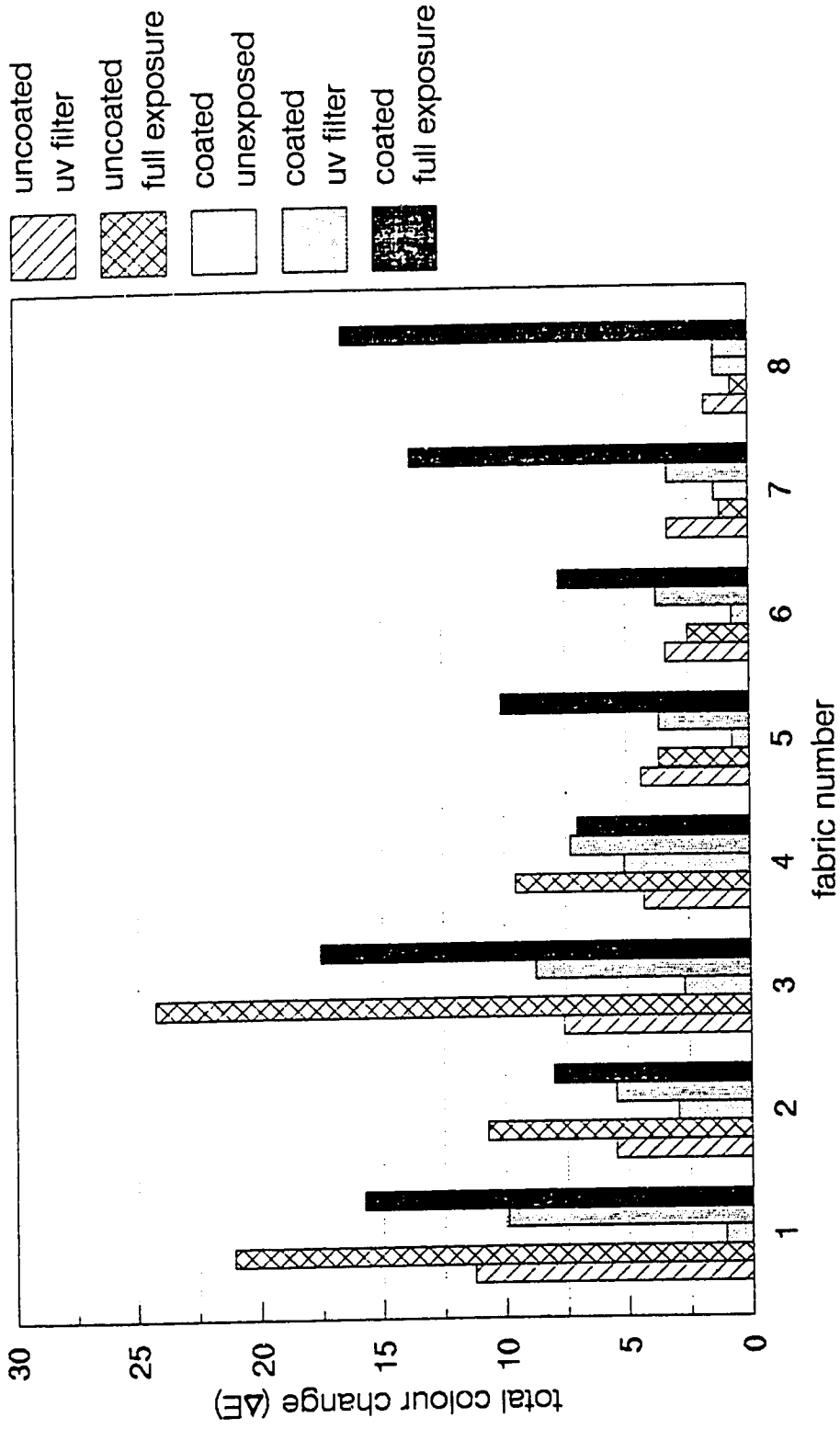


(1990) on coloured plates in books, which are often printed on smooth glossy paper. The appearance of interference bands is an inherent property for all types of thin transparent films, so is not unique to parylene. They disappear when the thickness of the coating is increased (Grattan, 1990; Humphrey, 1990).

As revealed in Figure 4 and Table 9, the dyed and undyed fabrics reacted differently when exposed to the xenon-arc lamp. The dyed fabrics exhibited distinct fading even when the UV component of the light had been filtered out; irradiation with wave-lengths in the visible region of the spectrum had sufficient energy to fade the dyes considerably. The colour change for coated and uncoated dyed fabrics was essentially the same. When samples were exposed to the xenon arc spectrum without a UV filter, however, the colour of the coated specimens changed less than the uncoated specimens if the fabric was dyed. For example, the uncoated fabric 3 faded from a brilliant turquoise to grey, a total change of 24.3 Colour Difference Units (CDU). Coated specimens of the same fabric also faded noticeably, but the overall colour difference was less (15.7 CDU). In contrast, the coated white specimens exhibited a larger change in colour than uncoated white specimens, as is illustrated by fabric 7: the coated specimens exhibited a visible colour change of 13.8 CDU due to yellowing, whereas the uncoated specimens exhibited a negligible change of 1.2 CDU.

In the CIElab\* colour measurement system, the  $b^*$  coordinate defines the yellowness ( $+b^*$ ) or blueness ( $-b^*$ ) of a material. Evaluation of the changes in the  $b^*$  coordinate of the fabrics revealed that after full exposure, the  $b^*$  values of the coated coloured specimens increased less than the  $b^*$  values for the coated white specimens. Surprisingly, these values for two of the four coated dyed specimens showed they actually yellowed less than their uncoated counterparts. Upon visual inspection however, the faded coated specimens appeared

**Figure 4**  
**Total Colour Change ( $\Delta E$ ) of Parylene C-Coated Silk Fabric After Exposure to Simulated Daylight**



Note. Samples were compared to the uncoated unexposed control sample, which had a  $\Delta E = 0$ .

Table 9  
Change in Colour ( $\Delta E^a$  and  $YI^b$ ) of Silk Fabrics After Exposure to Simulated Daylight

| Fabric # | $f^e$ | Uncoated               |       |                   |       | Coated     |       |            |       |
|----------|-------|------------------------|-------|-------------------|-------|------------|-------|------------|-------|
|          |       | UV filter <sup>c</sup> |       | Full <sup>d</sup> |       | UV filter  |       | Full       |       |
|          |       | $\Delta E$             | YI    | $\Delta E$        | YI    | $\Delta E$ | YI    | $\Delta E$ | YI    |
| 1        | W D   | 11.3*                  | -     | 21.1*             | -     | 9.6*       | -     | 16.0*      | -     |
| 2        | W D   | 5.5*                   | -     | 10.7*             | -     | 5.8*       | -     | 6.9*       | -     |
| 3        | W D   | 7.6*                   | -     | 24.3*             | -     | 7.1*       | -     | 15.7*      | -     |
| 4        | W D   | 4.3*                   | -     | 9.5*              | -     | 3.1*       | -     | 4.6*       | -     |
| 5        | W UD  | 4.4*                   | 0.73* | 3.7*              | 1.24* | 3.9*       | 0.78* | 10.0*      | 1.76* |
| 6        | UW UD | 3.4*                   | 0.74* | 2.5*              | 0.86* | 3.3*       | 0.71* | 7.3*       | 1.75* |
| 7        | UW UD | 3.3*                   | 0.64* | 1.2*              | 1.07* | 3.1*       | 0.64* | 13.8*      | 2.54* |
| 8        | UW UD | 1.8*                   | 0.72* | 0.7*              | 0.93* | 2.7*       | 0.73* | 15.3*      | 2.35* |

Note. n= 6 except for fabrics 1 and 5 where n=3  
<sup>a</sup>total colour difference (unexposed control has  $\Delta E=0$ )  
<sup>b</sup>yellowness index: normalized data (unexposed control=1)  
<sup>c</sup>wave-lengths below 400 nm excluded  
<sup>d</sup>exposed to full simulated daylight spectrum (xenon arc lamp)  
<sup>e</sup>fabric finish: W=weighted D=dyed UW=unweighted UD=undyed  
 \* statistically significant change from control as determined by Duncan's Multiple Range Test ( $\alpha=0.05$ )

darker than their uncoated counterparts, but were not necessarily less yellow.

The uncoated white specimens showed minimal total colour change ( $\Delta E$ ) upon full exposure, whereas the coated specimens visibly yellowed, suggesting the parylene C polymer coating had undergone degradation. Fabric 5, a weighted crepe fabric exhibited the largest colour change (3.7 CDU) by a fully exposed uncoated white specimen. This change was far lower than the colour differences for the white specimens with the parylene C coating, which ranged from 8 to 15 CDU. These results correspond to the general trends observed by Hansen

and Ginell (1989) on new undyed silk fabric, but were less extreme. For their research, uncoated specimens exhibited a colour change of 5 CDU and coated specimens 22 CDU due to yellowing after a 242 kJ/m<sup>2</sup> exposure. The same Weather-Ometer temperature and relative humidity parameters (50 °C and 65% RH) were used for both studies.

Free parylene C films (12 µm thick) have been shown to yellow upon exposure to light but only when ultraviolet light was present. Films protected by a UV filter which excluded wave-lengths below 400 nm did not change in colour (Hansen & Ginell, 1989). Similarly, the UV filtered, coated silk samples in the present study did not yellow. Grattan (1990) has hypothesized that with the use of very thin coatings, any yellowing which occurs might be undetectable. The thinly coated fabrics in the present study challenge this concept, as they showed considerable yellowing upon exposure to the full spectrum. The colour change due to yellowing of the undyed coated fabrics, ranging from 8 to 15 CDU, was readily seen.

For the undyed fabrics, a measurement of yellowness index (YI) was taken in addition to the measure of total colour difference,  $\Delta E$ . This index quantifies the nature of the light-induced colour change for neutral coloured fabrics better than  $\Delta E$  because it specifically measures yellowness/whiteness, but is not suitable for use on dyed fabrics. The YI values for fabrics 5 to 8 are summarized in Table 9. The table shows that normalized YI values for specimens exposed to UV filtered light range from 0.64 to 0.74 for uncoated fabrics and from 0.64 to 0.78 for coated fabrics. This drop in YI of approximately 30% indicates that both the coated and uncoated specimens were bleached when exposure was limited to the visible spectrum. All the undyed fabrics were visually whiter after exposure to the UV filtered xenon arc light. Visible light is known to have a bleaching effect on wool, whereas ultraviolet light (below 365 nm) induces yellowing (Bendak, 1973; Launer, 1965a, b). The same

behaviour was displayed by the undyed silk used in the present study. In research on the effect of visible light (wave lengths above 398 nm) on a variety of organic materials, Launer (1968) also demonstrated silk fabric to exhibit visible bleaching. In the present study, the uncoated, white specimens exposed to the full spectrum, which includes both ultraviolet and visible light, showed a negligible visual change in colour, possibly because bleaching and yellowing occurred in competition, simultaneously.

In general, the oxidation of polymers results in discolouration, or yellowing (Kamiya & Niki, 1978). The chemical mechanism by which silk yellows is uncertain. Researchers have postulated that the oxidation of specific amino acid residues, including tryptophan (Okamoto & Kimura, 1954), histidine and tyrosine (Inglis & Lennox, 1963) is responsible for the photoyellowing of wool and silk (Holt et al., 1977).

According to Maclaren and Milligan (1981) "Neither the chromophores responsible for the initial color of natural wool nor those produced by irradiation are known. Consequently little is known of the chemical changes responsible for photobleaching" (p. 227). Visible light does not have sufficient energy to break bonds, yet coloured structures are somehow removed, and the chromophores formed upon exposure to shorter more energetic wave-lengths are not produced (Bendak, 1978).

#### Flexural Rigidity

Flexural rigidity is a measure of fabric stiffness, calculated from the bending length and mass per unit area of the fabric. A 10% change in flexibility represents a just perceptible change in fabric hand (ASTM method: D1388-64). The parylene C coating produced a statistically significant ( $\alpha=.05$ ) initial increase in stiffness of all fabrics, as determined by the Duncan's Multiple Range Test (Table 10).

Table 10  
Initial Effect of Parylene C Coating on the Flexural Rigidity  
of Silk Fabrics

| Fabric #<br>& finish <sup>a</sup> | Uncoated<br>stiffness<br>(mg-cm) SD |      | Coated<br>stiffness<br>(mg-cm) SD |       | Change in<br>stiffness<br>(%) |
|-----------------------------------|-------------------------------------|------|-----------------------------------|-------|-------------------------------|
|                                   |                                     |      |                                   |       |                               |
| 1 W D                             | 10.3                                | 1.53 | 48.3                              | 5.1   | 368*                          |
| 2 W D                             | 13.4                                | 3.62 | 42.9                              | 19.2  | 220*                          |
| 3 W D                             | 14.8                                | 1.72 | 83.1                              | 6.15  | 460*                          |
| 4 W D                             | 29.7                                | 1.99 | 185.8                             | 28.89 | 524*                          |
| 5 W UD                            | 12.7                                | 0.78 | 55.3                              | 6.22  | 336*                          |
| 6 UW UD                           | 16.6                                | 2.63 | 32.0                              | 1.28  | 93*                           |
| 7 UW UD                           | 24.2                                | 3.64 | 64.7                              | 5.27  | 167*                          |
| 8 UW UD                           | 34.1                                | 7.92 | 233.7                             | 15.89 | 585*                          |

Note. n= 10 except for fabrics 1 and 5 where n= 6  
<sup>a</sup>W=weighted D=dyed UW=unweighted UD=undyed  
\* statistically significant change determined by Duncan's  
Multiple Range Test ( $\alpha=0.05$ )

Those fabrics with compact weave structures showed the largest increase in flexural rigidity. Fabric 4, a tightly constructed plain weave increased in stiffness by 524%, while fabric 8, a compact twill weave increased 584%. Fabric 6 had a loose open construction and was least affected by the coating, showing an initial change of 92.9%. These results were in agreement with Grattan (1990) who noted the degree of change in flexibility was dependent on the weave structure.

In paper, the parylene coating forms contact bonds at the points where cellulose fibres cross one another, thus creating an overall strengthening effect (Humphrey, 1990). Plates 2, 4, and 5 in the subsequent section on Scanning Electron Microscopy illustrate that the coating performs the same

function when applied to textiles. This action on textiles, however, prevents movement of fibres or yarns past one another, which reduces the ability of a fabric to drape. Because the yarns in tightly woven fabrics are packed closely together, there is an increased possibility of adjacent fibres becoming bonded together by the coating, thereby increasing stiffness.

The flexural rigidity measurements in mg-cm are listed in Appendix A-3 and illustrated by Figure 5. The changes in flexural rigidity for those specimens placed in the Weather-Ometer are summarized by the normalized data in Table 11. In all cases the flexibility did not change significantly

Table 11  
Fraction of Flexural Rigidity Retained by Parylene C-Coated Silk Fabrics After Exposure to Simulated Daylight: Normalized Data<sup>a</sup>

| Fabric #<br>& finish <sup>b</sup> | Uncoated               |                   | Coated    |      |
|-----------------------------------|------------------------|-------------------|-----------|------|
|                                   | UV filter <sup>c</sup> | Full <sup>d</sup> | UV filter | Full |
| 1 W D                             | 1.31                   | 2.34*             | 1.03      | 1.18 |
| 2 W D                             | 1.59                   | 2.13*             | 1.17      | 1.09 |
| 3 W D                             | 0.07                   | 2.28*             | 1.07      | 1.08 |
| 4 W D                             | 0.97                   | 1.98*             | 1.04      | 0.98 |
| 5 W UD                            | 1.05                   | 3.28*             | 0.97      | 1.24 |
| 6 UW UD                           | 1.13                   | 1.36*             | 1.00      | 1.01 |
| 7 UW UD                           | 1.18                   | 1.68*             | 1.14      | 1.14 |
| 8 UW UD                           | 0.89                   | 1.40*             | 0.91      | 0.98 |

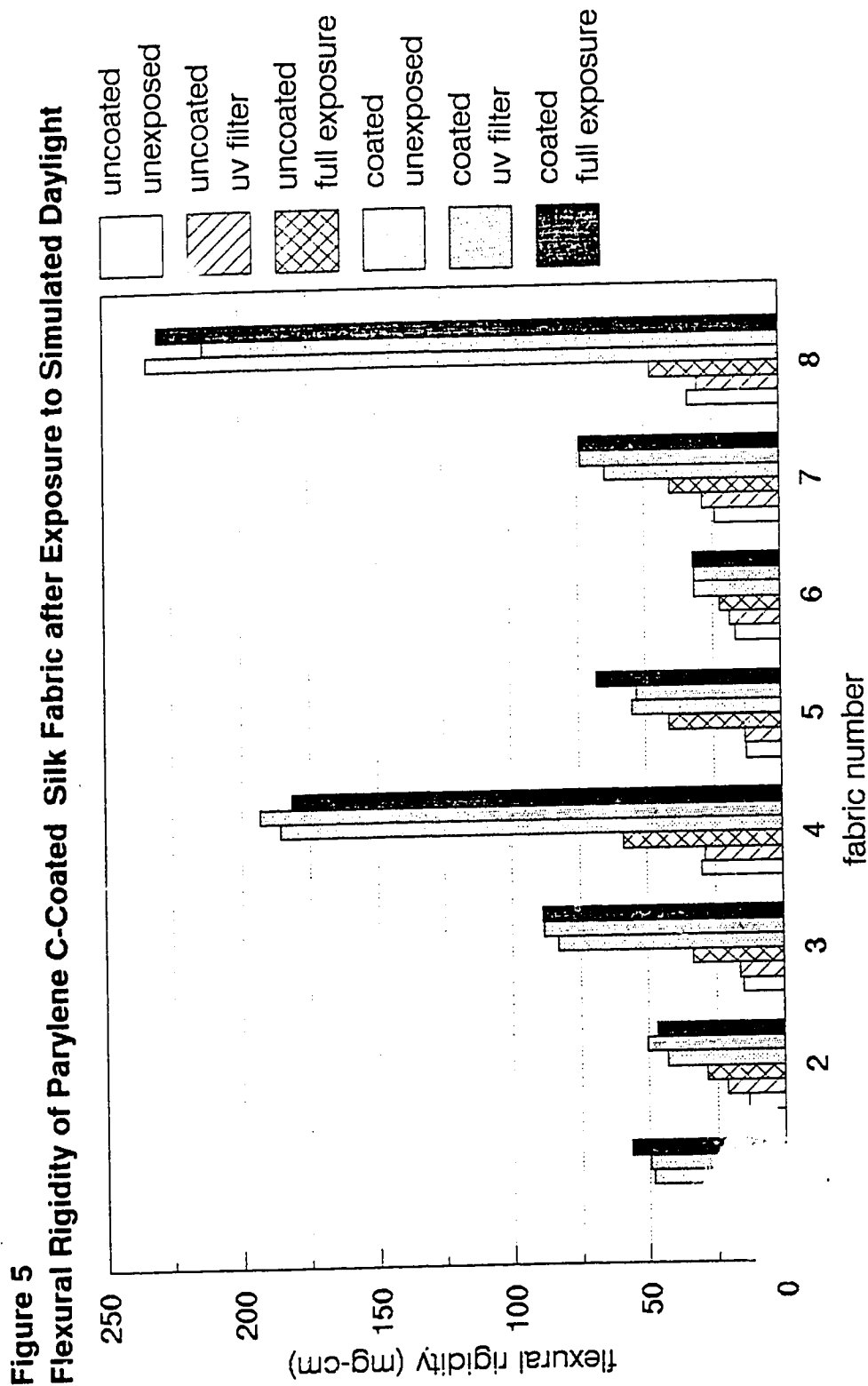
<sup>a</sup>uncoated unexposed control= 1 and coated unexposed control=1

<sup>b</sup>W=weighted D=dyed UW=unweighted UD=undyed

<sup>c</sup>wave-lengths below 400 nm excluded

<sup>d</sup>exposed to full simulated daylight spectrum (xenon arc lamp)

\* statistically significant change from control as determined by Duncan's Multiple Range Test ( $\alpha=0.05$ )



Note. Samples were given 250 kJ of exposure in a xenon arc Weather-Ometer with 65% relative humidity and a black panel temperature of 50 °C



provided the specimens were protected from full irradiation by a UV filter. The uncoated specimens which were exposed to the full xenon-arc spectrum showed a statistically significant increase in flexural rigidity, with the weighted fabrics exhibiting more change than nonweighted. The most pronounced light-induced change in flexibility occurred with fabric 5, an undyed weighted crepe fabric, which became stiffer by 328% upon exposure. The chemical changes leading to increased embrittlement and stiffness are discussed in the section on extension.

The fabrics coated with parylene C were already more rigid than their uncoated counterparts before irradiation, but unlike the uncoated specimens, they did not exhibit a statistically significant change in flexibility upon full exposure to simulated daylight. Apparently, the exposure of 250 kJ/m<sup>2</sup> (420 nm) was not sufficient to reduce the flexibility of the parylene coating. Exposure to heat has been shown to cause embrittlement of free parylene films, as determined by failure to sustain a 180° bend test (Baker et al., 1980). Interestingly, the coating also appeared to keep the underlying silk from stiffening, because the parylene C-coated silk did not stiffen with exposure to light, whereas the uncoated silk did.

In summary, the results showed the coating initially caused a large increase in flexural rigidity; however, the uncoated specimens became stiffer with exposure to the full simulated daylight spectrum, while the coated specimens did not.

## Tensile Properties

### Tensile Strength

The effect of the coating on tensile strength for all fabrics is illustrated in Figure 6; further data from the strength tests is found in Appendix A-3. Although the parylene C coating produced an initial increase in tensile

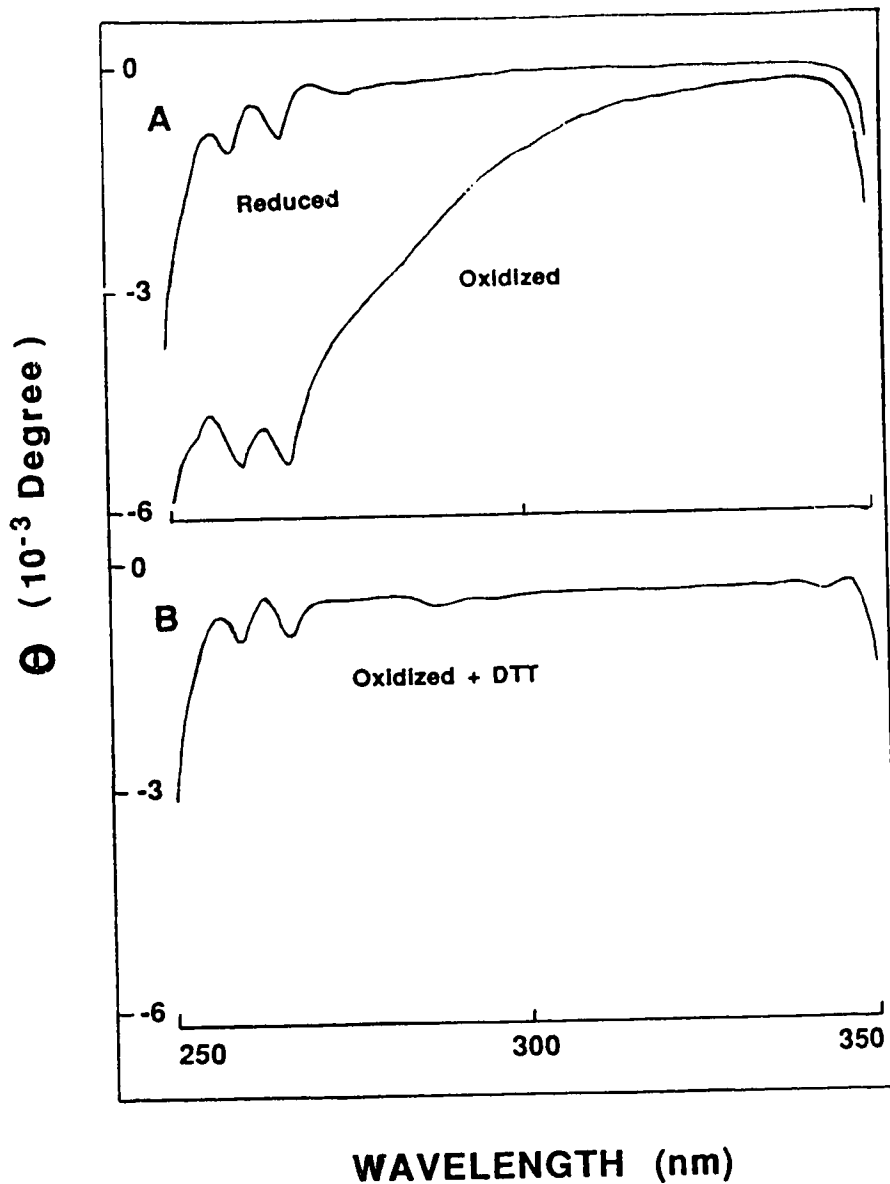


Figure III.4. The circular dichroism spectra of reduced and oxidized AcPAK 128-144. A: a 1.0 mg/ml solution of the peptide was used in each case and the buffer used contained 50 mM phosphate, pH 7.0. The relative ellipticity values ( $\Theta$ ) are expressed in millidegrees. B: spectrum of the oxidized peptide after addition of a 1.0 mM dithiothreitol solution.

TABLE III.1 Retention times of reduced and intrachain disulfide-bridged peptides on RPC.

| Peptide No. | Amino acid sequence <sup>a</sup>  | No. of residues within disulfide loop | Retention time (min) <sup>b</sup> |                          |
|-------------|---|---------------------------------------|-----------------------------------|--------------------------|
|             |   |                                       | (-SH)                             | (-S-S-) ( $\Delta R_t$ ) |
| 1           | NH <sub>2</sub> -GIVECSTSI <sup>∇</sup> C <sup>∇</sup> SLY-NH <sub>2</sub>                | 4                                     | 31.22                             | 31.34 1.88               |
| 2           | desamino-CYFQNC <sup>∇</sup> PRG-NH <sub>2</sub>  | 4                                     | 26.82                             | 26.82 0.00               |
| 3           | NH <sub>2</sub> -AGCKNFFWKTFTS <sup>∇</sup> C-OH  | 10                                    | 35.44                             | 34.44 1.00               |
| 4           | Ac-KCTSDQDEQFIPKGC <sup>∇</sup> SK-OH   | 12                                    | 23.23                             | 21.24 1.99               |
| 5           | Ac-ACAAADQDEQFIPKGC <sup>∇</sup> SK-OH  | 12                                    | 25.84                             | 24.09 1.75               |
| 6           | Ac-ACAAAADQDEQFIPKGC <sup>∇</sup> SK-OH   | 12                                    | 27.56                             | 25.19 2.37               |
| 7           | Ac-ACAAAAAQFIPKGC <sup>∇</sup> SK-OH  | 12                                    | 31.54                             | 28.29 3.25               |
| 8           | Ac-ITLRTAADGLWK <sup>∇</sup> CTSDQDEQFIPKGC <sup>∇</sup> SK-OH                            | 12                                    | 34.89                             | 33.02 1.87               |
| 9           | Ac-ACKSTQDPMFTPKGC <sup>∇</sup> DN-OH   | 12                                    | 24.67                             | 24.67 0.00               |
| 10          | Ac-CFGRMDRIGAQSG <sup>∇</sup> LG <sup>∇</sup> C-NH <sub>2</sub>                           | 15                                    | 29.80                             | 29.17 0.63               |
| 11          | Ac-CFGRMDRIGAQSG <sup>∇</sup> LG <sup>∇</sup> CNSFRY-OH                                   | 15                                    | 32.87                             | 32.07 0.80               |
| 12          | NH <sub>2</sub> -SSCFGRID <sup>∇</sup> RIGAQSG <sup>∇</sup> LG <sup>∇</sup> CNSFRY-OH     | 15                                    | 28.82                             | 28.07 0.75               |
| 13          | NH <sub>2</sub> -SLRRSC <sup>∇</sup> FGGRMDRIGAQSG <sup>∇</sup> LG <sup>∇</sup> CNSFRY-OH | 15                                    | 29.36                             | 28.73 0.63               |
| 14          | NH <sub>2</sub> -SLRRSC <sup>∇</sup> FGGRMDRIGAQSG <sup>∇</sup> LG <sup>∇</sup> CNSFRY-OH | 15                                    | 29.45                             | 28.07 1.38               |

<sup>a</sup> The symbols,  $\Delta$  and  $\circ$  denote single amino acid sequence changes between peptides,  $\nabla$  denotes position of cysteine residues; Ac-, acetyl; -OH C-terminal carboxyl group; NH<sub>2</sub>, N-terminal amino group  
<sup>b</sup>  $\Delta R_t$  denotes the difference in retention time between reduced (-SH) and (-S-S-) oxidized peptides.

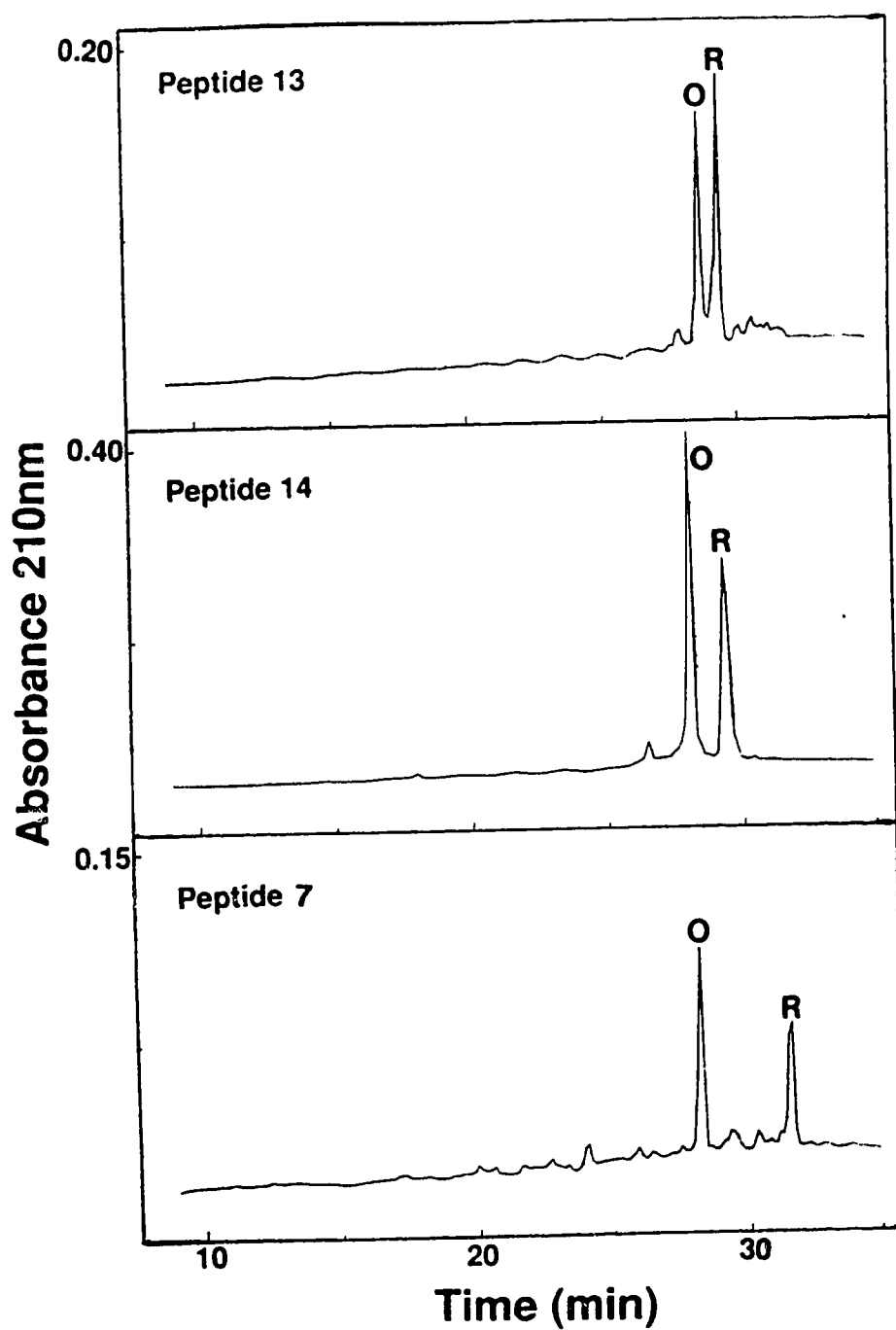


Figure III.5. The separation of three peptides in their reduced and oxidized forms using RPC. Column: Aquapore RP-300 C-8 (220 x 4.6 mm i.d.). The chromatographic conditions have been described in the legend in Figure III.2. The oxidized peptide is denoted by O and the reduced peptide by R.

Representative chromatograms of the separation of the reduced and oxidized forms of three peptides are shown in Figure III.5. The difference in retention time between reduced and oxidized forms of Peptides 7, 13 and 14 was 3.3, 0.6 and 1.4 minute, respectively. In fact, as summarized in Table III.1, the separation of the reduced and oxidized forms of most of these peptides was possible with the exception of Peptides 2 and 9. These two peptides showed no clear separation between the conformers. In addition, no dimeric interchain peptides were observed when a low concentration (0.1 mg/ml) of peptides was used in the air oxidation. Whenever a difference in retention time was observed between the two forms of a peptide, the reduced conformer was always eluted later than the disulfide-bridged peptide. This result suggested that, on formation of the disulfide loop, some residues in the peptide were not as accessible to interact with the stationary phase as they were in the reduced peptide. In other words, the loop formation resulted in a decrease of the hydrophobicity of the peptide binding domain.

##### *5. RPC of the NEM-modified and oxidized peptides*

Peptides 2 and 9 used in these studies did not show any noticeable separation between the reduced and oxidized forms, and were eluted from the column as a single peak. In order to improve the resolution between the reduced and oxidized conformers, a thiol-specific reagent, N-ethylmaleimide (NEM), was used to modify the reduced peptide. This modification resulted in the formation of a stable covalent linkage between the thiol and NEM, since the thiolate anion attacks one of the double bonded carbon atoms to form N-ethyl succinimidyl cysteine as depicted in Figure III.6. The covalently modified reduced peptide becomes more hydrophobic and is eluted from the column later. Baseline resolution of these two conformers would give us another option for monitoring an oxidation process. The disappearance of the reduced peptide peak with time and the concomitant appearance of the peak corresponding to the oxidized peptide would be

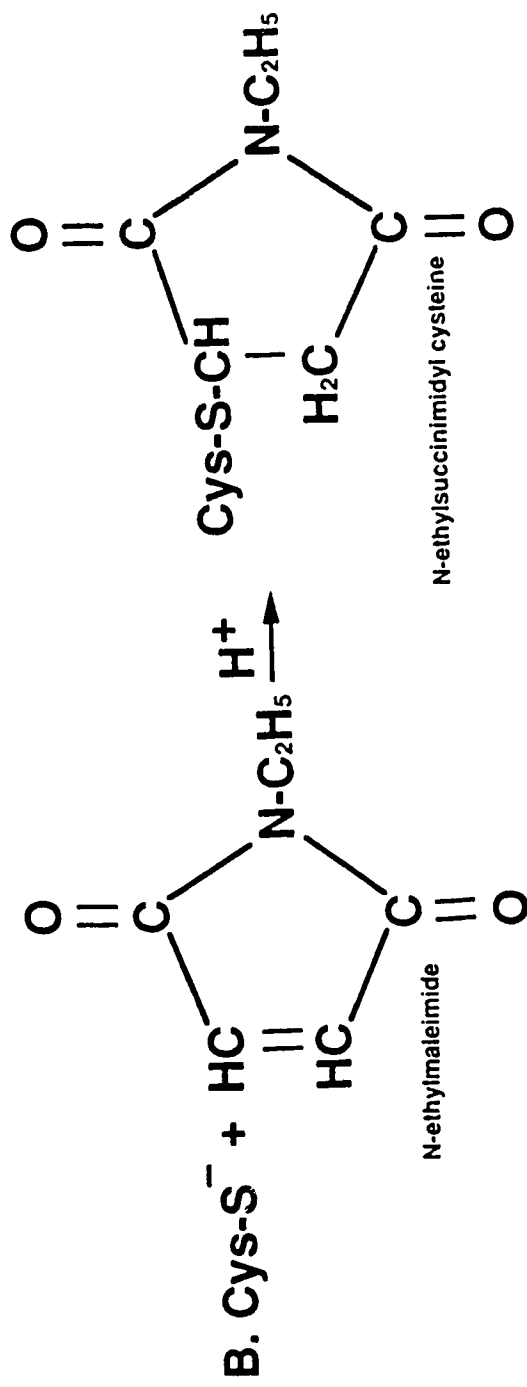


Figure III.6. The air-oxidation reaction of the sulfhydryl groups (A) and the modification reaction of the sulfhydryl groups (B) with N-ethylmaleimide (NEM) as described by Creighton (1983).

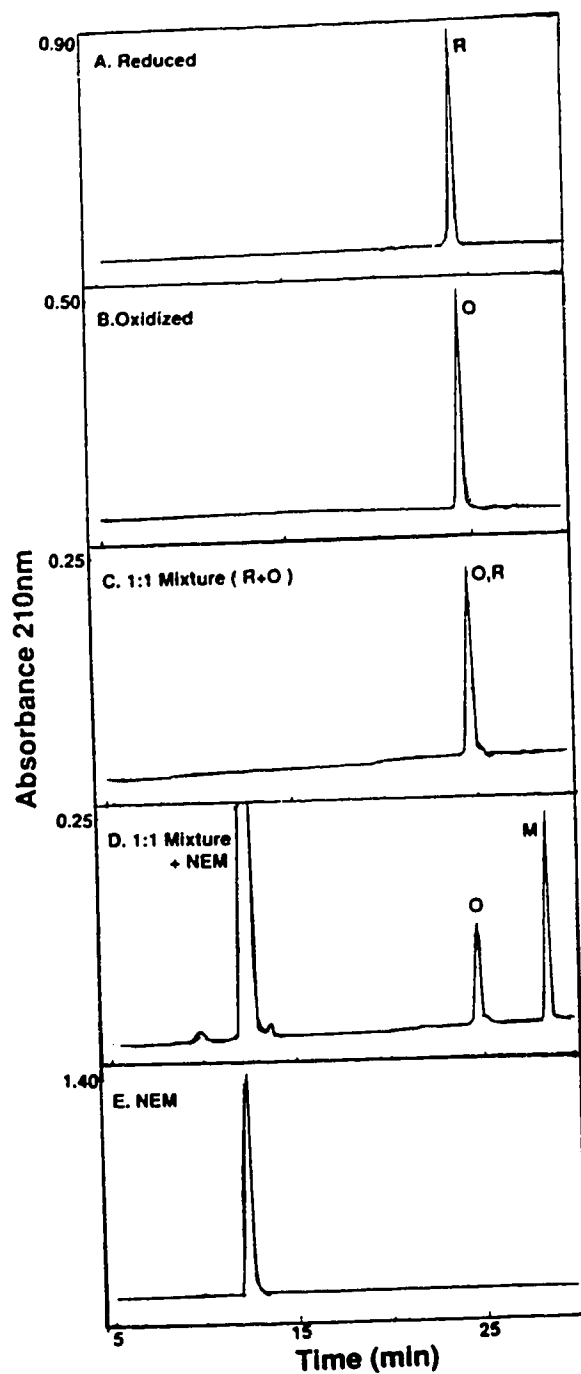


Figure III.7. The separation of reduced and oxidized forms of Peptide 9 following the modification of the reduced peptide with NEM. The NEM-modified peptide is denoted by M. The conditions of chromatography have been described in the legend of Figure III.2.

indicative of the oxidation process. As shown in Figure III.7C, reduced and oxidized Peptide 9 were eluted from the column at 24.8 min and a 1:1 mixture injection resulted in a single peak. When the same mixture was reacted with NEM, it was found that the modified reduced peptide was eluted off the column at 28.6 min. The reagent itself is quite hydrophilic, being eluted from the RPC column after only 12 min. The best resolution of peptides by RPC is usually achieved between 15 - 40% of the organic modifier in the gradient (Hermodson and Mahoney, 1983). Thus, the presence of the excess NEM reagent would not interfere or coincide with most peptides which are eluted off the column later than 15 min.

A more hydrophobic thiol-modifying reagent, N-phenylmaleimide, was also used (data not shown). This particular reagent produced a bigger separation (8 min) between modified and unmodified peptides, compared with NEM. However, the more hydrophobic phenyl rings resulted in the reagent being eluted from the column at around 22 min. This reagent might be coeluted with some peptides and thus, was not the reagent of choice.

The results shown in Figures III.8 and III.9 illustrated the use of RPC to monitor the oxidation of peptides that show no separation between their two conformers. Such a monitoring procedure could be used for any peptides, whether or not they show good separation. At various time points, samples were removed and reacted with the NEM reagent, thus stopping any further oxidation by covalently modifying the free -SH groups of the reduced peptide, denoted by M in Figure III.8. Monitoring the intrachain disulfide bridge formation by RPC allowed simultaneous quantitation of the two conformers, unlike the Ellman titration of free sulfhydryls of the reduced peptides. Although these modified peptides could not be retrieved, only a small amount of peptides are required because of the high sensitivity of UV detection. The modified peptide was also shown to have an enhancement of absorption at 210 nm due to the NEM reagent. The peak height of the modified peptide at the beginning of the oxidation process was 89 mm and the completely oxidized peptide was only 54.5 mm. The injection volumes were 100  $\mu$ l in both cases.



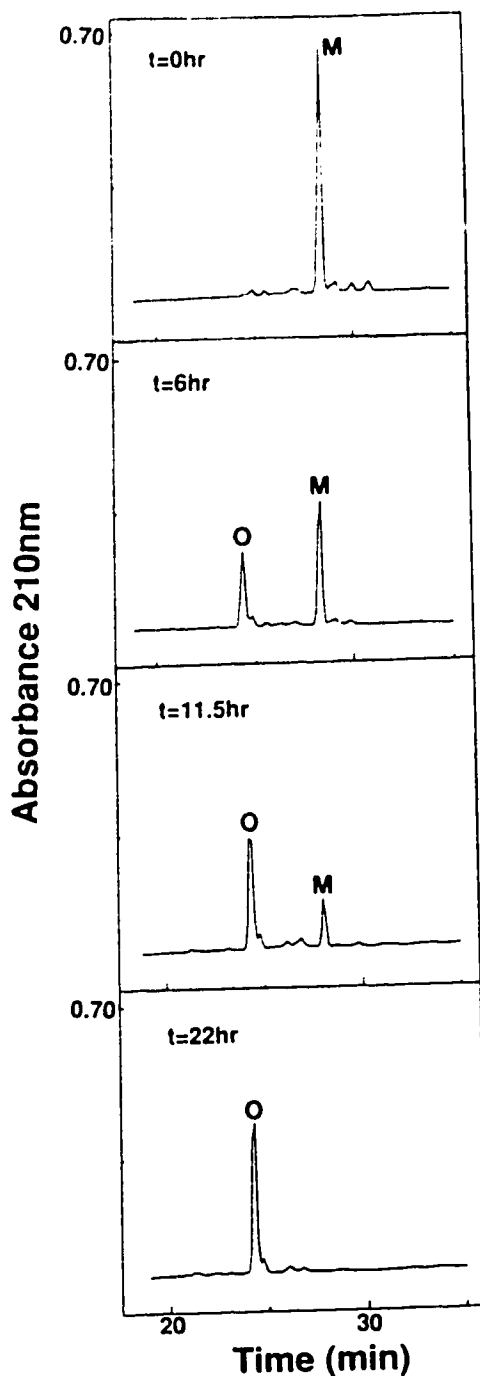


Figure III.8. Monitoring the formation of the intrachain disulfide bridge with time during air-oxidation of Peptide 9 by RPC. The reduced peptide was modified with NEM prior to injection onto the column to increase the separation between oxidized and reduced conformers. The modified peptide is denoted by M and the oxidized peptide by O. The chromatographic conditions have been described in the legend of Figure III.2. Conditions for air-oxidation and chemical modification with NEM are given in the Materials and Methods section.

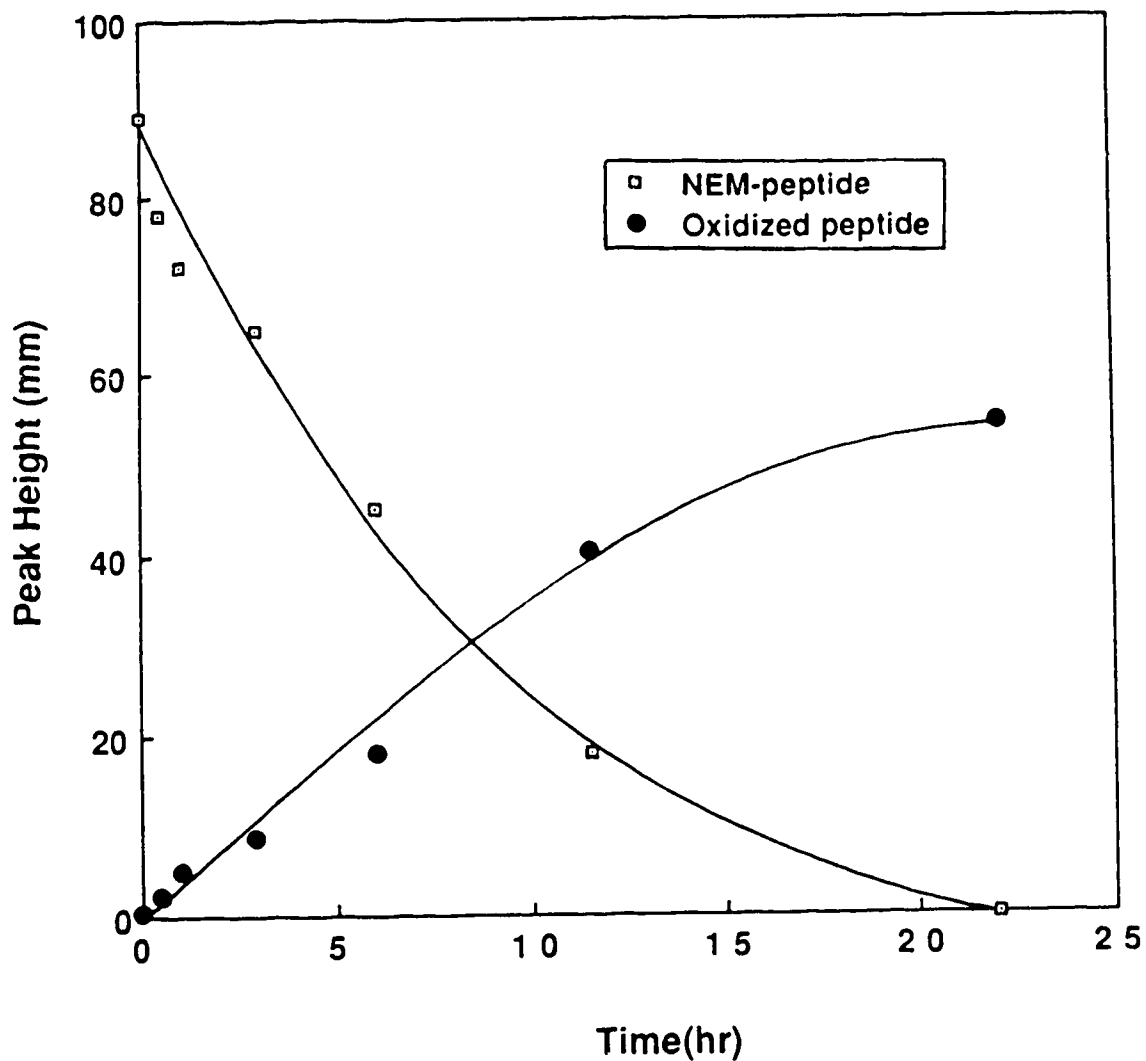


Figure III.9. Quantitative measurements of the reduced and oxidized Peptide 9 during an air-oxidation process. The peak heights of the two conformers obtained from RPC chromatograms (Figure III.8) were used.

This enhancement of absorbance at 210nm would help in detecting any small quantity of reduced peptide left in the air oxidation mixture.

### C. Discussion

In these studies, peptides were purified by RPC with a shallow gradient (0.2% B/min) on an analytical column. Purifications on a semi-preparative column (10 mm I.D.) using a gradient of 1% B/min were also carried out. In these instances, multiple runs were made and the peaks of interest were collected as they were eluted off the column. Although these were the only procedures used, there are other methods of purification which have been developed including the novel sample displacement chromatography approach (Hodges *et al.*, 1988; Burke *et al.*, 1988). Different modes of chromatography such as ion-exchange chromatography can also be applied if peptides possess charged amino acid residues. More detailed aspects of the application of HPLC to peptide separation have been reviewed by Mant and Hodges (1990).

A study on the retention behaviour of 14 peptides in their reduced and oxidized forms was carried out. The separation of the two conformers could vary from no resolution at all to as much as 3.3 min. In all instances where resolution was obtained, the reduced conformers were eluted from the column after the oxidized peptide. It has been noted by Creighton (1983) that cystine has a lower solubility in water than cysteine, thus making the disulfide group relatively more hydrophobic than the thiol group. The solubility for cystine in water was 0.01g/100mL, less than 1/1000 that of cysteine. An observation made by Schulze-Gahmen *et al.* (1983) showed that the reduced form of a 16-residue peptide (NH<sub>2</sub>-YGCTVGGGGGGVTCTG-OH) was eluted 1-2 min earlier than the oxidized form. The column used by these authors was a Baker C-18 column, 250 x 4.6 mm I.D., 300Å pore-size. The column was run at ambient temperature with a flow rate of 1.0 mL/min and a linear gradient of 2%B/min, where solvent A was 0.1%TFA in water and solvent B was 0.1%TFA in 60% aq. acetonitrile. This observation could be explained

by the increase in hydrophobicity of the peptide due to the presence of cystine versus two cysteine residues. Differences in retention behaviour of the disulfide-bonded peptides, compared to their reduced conformers during RPC, could also be due to differences in conformation of the looped peptides as a result of sequence variability. For example, with the series of peptides (4 to 9), which have 12 amino acid residues between the cysteine residues, the  $\Delta R_t$  between reduced and oxidized conformers ranged from 0 to 3.3 min. Similarly, for peptides with 4 amino acid residues between cysteine residues, the  $\Delta R_t$  for Peptide 1 was 1.9 min while Peptide 2 showed no noticeable difference between the two conformers. In addition, Peptides 13 and 14 differed by only a single amino acid change within the loop (aspartic acid to arginine) and yet the  $\Delta R_t$  between reduced and oxidized conformers varied from 0.6 min for Peptide 13 to 1.4 for Peptide 14. These results suggested that there was no direct correlation between the size of the loop and the differences in  $\Delta R_t$  obtained on RPC.

As we have seen from Table III.1, not all reduced and oxidized peptides were resolved by RPC (Peptides 2 and 9). Some of the peptides tested were only partly resolved (not baseline resolved) even on very good columns, as illustrated by the series of peptides 10 to 13 in Table III.1. Hence, a new method was developed which could resolve the reduced and oxidized peptides. Modification of the free sulfhydryl groups of the cysteine residues with NEM has previously been applied by Lunte and Kissinger (1985) to modify free thiol groups in liver samples for electrochemical detection. These workers were interested in monitoring the presence of free sulfhydryls and cystine groups. In our case, the separation of reduced and oxidized conformers on RPC was the goal. Modification of the reduced peptide resulted in an increase of 3 min in its retention time (i.e.,  $\cong 1.5$  min per -SH). The reagent reacted only with the reduced peptide (data not shown). The modification resulted in the loss of a small sample of the peptide in the analysis. However, small nanomolar quantities are sufficient for these assays because of the high sensitivity of the ultraviolet detection system. This procedure has an added advantage over the Ellman

method (Ellman, 1959) in that both the reduced and oxidized peptides are monitored simultaneously. In the Ellman method, only the free sulfhydryl groups are monitored and the absence of spectroscopic detection at 412 nm would be interpreted as a completion of the oxidation process. Because the use of this RPC approach, with or without NEM (depending on the baseline resolution of the reduced oxidized conformers), allows one to observe both conformers on a given chromatogram, the oxidation process could be followed by removing samples from an oxidation mixture. The peak area or peak height could be quantitated. An example of this is shown in Figures III.8 and III.9, where the oxidation of Peptide 9 was monitored. The increase in peak height corresponding to the oxidized peptide was followed by a concomitant decrease in the reduced peptide as the oxidation progressed over the time period, illustrated the usefulness of this procedure.

This method of monitoring reduced and oxidized peptides is now routinely used in our laboratory. Such a method of verification of free sulfhydryls may have a wider application than that described for this thesis project. The presence of intrachain disulfide bridges in peptides and proteins is a common feature. Some examples of these are found in peptide hormones such as insulin and vasopressin, and in enzymes such as lysozyme, ribonuclease, serine proteases and other small proteases. The functions of these disulfide bridges are to stabilize the protein (Pace, 1990) and to confer active functional domains. With the technological advances in peptide synthesis, many active fragments of proteins and peptides are being made with their native disulfide bonds or with the addition of disulfide bonds to confer to the fragments a structure similar to that which they exhibit in the native proteins (Atassi *et al.*, 1988). The RPC-NEM approach would provide researchers with a new effective method to monitor the reduced and oxidized conformers of the peptides of interest.

## Chapter IV. Immunogenicity and Antigenicity of the C-terminal Disulfide-Bridged Region of *Pseudomonas* Pili

### A. Introduction

At the time when this project began, there was the question of the importance of the disulfide bridge located at the C-terminal end of the pilin molecule and its relevance to the immunogenicity of the pilin protein. The cysteine residues of pilin molecules are found to be conserved in all *P. aeruginosa* strains (Johnson *et al.*, 1986; Paranchych, 1989; Pasloske *et al.*, 1988; Sastry *et al.*, 1985). The location of the cysteines within a region of the pilin molecule that is semiconserved could be important from an immunological standpoint. Regions on bacterial and viral components that are immunodominant are often used as a diversion mechanism against the host immune system. The region that is conserved is important for a particular function in the bacterium and its lack of immunogenicity (immunorecessiveness) enhances the survival of the organism in that antibodies would not bind and block the function of the conserved region.

The gonococcus pilus is also a class of NMePhe pilus that is involved in the adhesion of *N. gonorrhoeae* to host cells (Swanson, 1973). The gonococcal pilin has a molecular weight that varies between 17.5 - 21 kilodalton, depending on the strain (Buchanan, 1977). It has a hydrophobic N-terminal region which is homologous to the *P. aeruginosa* pilin (Schoolnik *et al.*, 1984). The C-terminal end of the gonococcal pilin has a disulfide bridge. Cyanogen bromide cleavage of pilin from gonococcal strain MS11 gave rise to a C-terminal disulfide-bridged fragment, CNBr-3, which contained the immunodominant, type-specific antigenic determinant (Schoolnik *et al.*, 1984). Two strain-specific epitopes in regions 121-134 and 135-151 were located within the disulfide loop (Rothbard *et al.*, 1984). Reduction and subsequent alkylation of the intrachain disulfide bond in the CNBr-3 fragment destroyed the antigenicity of this region (Schoolnik *et al.*, 1984). Watts *et al.* (1983) have reacted enzymatically cleaved *Pseudomonas* pilin

fragments with native PAK anti-pilus antiserum and have found that a fragment corresponding to the C-terminal end (residue 121-144) reacted positively in direct ELISA experiments. However, the C-terminal region of the *Pseudomonas* pilin is not the immunodominant region (Watts *et al.*, 1983; Sastry *et al.*, 1985). In contrast with the gonococcal pilin, modification of the two cysteine residues in the fragment by reduction and carboxymethylation of the disulfide bridge did not abolish the antigenicity of this determinant. It has also been demonstrated in the PAK pilin that the C-terminal region may be part of the pilus-binding domain, and that the C-terminal disulfide bridge is important in maintaining the functionality of this binding domain (Doig *et al.*, 1988; Irvin *et al.*, 1989; Lee *et al.*, 1989; Paranchych *et al.* 1985). We have now investigated the immunogenicity of this region in the synthetic peptides (reduced and oxidized PAK 128-144-OH, PAK(A<sup>129</sup>) (128-144)-OH) to produce anti-peptide antibodies which bind to native PAK pili. The synthesized peptide sequence of the PAK pilin and the corresponding sequence of the disulfide bridge region of PAO pilin are shown in Figure IV.1. The importance of the disulfide bridge to the immunogenicity and antigenicity of this region was further investigated using competition ELISA experiments with both native anti-pilus antiserum and antisera raised against the synthetic peptides. These studies could be important in understanding the role of the disulfide bridge and the significance it might have in developing vaccines against *P. aeruginosa* infections.

## B. Results

### 1. Peptide synthesis.

The peptides used in this study, PAK 128-144 and PAK 116-144, were synthesized by the solid-phase procedure described in the Methods and Material Section (Chapter II). The PAK sequences are shown in Figure IV.1. The corresponding region of PAO 128-144 is also shown for comparison purposes as this study relates to both pilin molecules. As noted earlier, the two cysteines form a disulfide bond in the native

**PAK 116-144** I T L T R T A A D G L W K C T S D Q D E Q F I P K G C S K  
**PAK 128-144** . . . . . K C T S D Q D E Q F I P K G C S K  
**PAO 128-144** . . . . . A C K S T Q D P M F T P K G C D N

Figure IV.1. Amino acid sequence of the C-terminal region of PAK and PAO pilins. The sequence data were derived from Sastry *et al.* (1985)



molecule. Both the reduced (free sulfhydryl groups on the cysteine residues) and the oxidized (disulfide-bonded) forms of the PAK 128-144 and PAK 116-144 peptides were used in the following experiments.

## *2. Determination of the concentration range of BSA-peptide conjugates for ELISA*

The experiments used in this study involved a large number of ELISAs and so a quantitation of the amount of antigens to be coated on the wells of the microplate was first carried out. Four concentrations of the BSA-PAK 116-144 conjugate were tested. Two dilutions of an anti-PAK pilus antiserum, 1:300 and 1:600, were used to perform the quantitation. The results are shown in Figure IV.2. The maximum absorbance was obtained when the wells were coated with an antigen solution of about 10 µg/ml concentration. However, to minimize the amount of antigen to be used while maintaining a high sensitivity in the assays, a solution of 5 µg/ml was used in subsequent experiments. This concentration gave approximately 80-90% of the maximum sensitivity in this assay system.

## *3. Antipeptide antisera reactivities with PAK pili*

The antipeptide antisera raised against reduced or oxidized PAK 128-144-OH peptide bound to native PAK pili in direct ELISA experiments. The antipeptide antiserum raised against the reduced and oxidized peptides were designated as 17-R and 17-O, respectively. The antibody titers are tabulated in Table IV.1. The titers were obtained after a subtraction of the  $A_{405}$  values of the primed rabbit antisera with values from preimmune antisera. High antibody titers in the range of a  $1 \times 10^{-6}$ -fold dilution were engendered by the peptide-KLH immunogens. The antipeptide antibody titers were similar for both the reduced and oxidized peptides when tested against the corresponding BSA-peptide conjugates. The antipeptide antisera were able to bind to native PAK pili, and titers in the range of  $1.5 \times 10^{-5}$  were recorded. One concern that must be addressed is the possibility

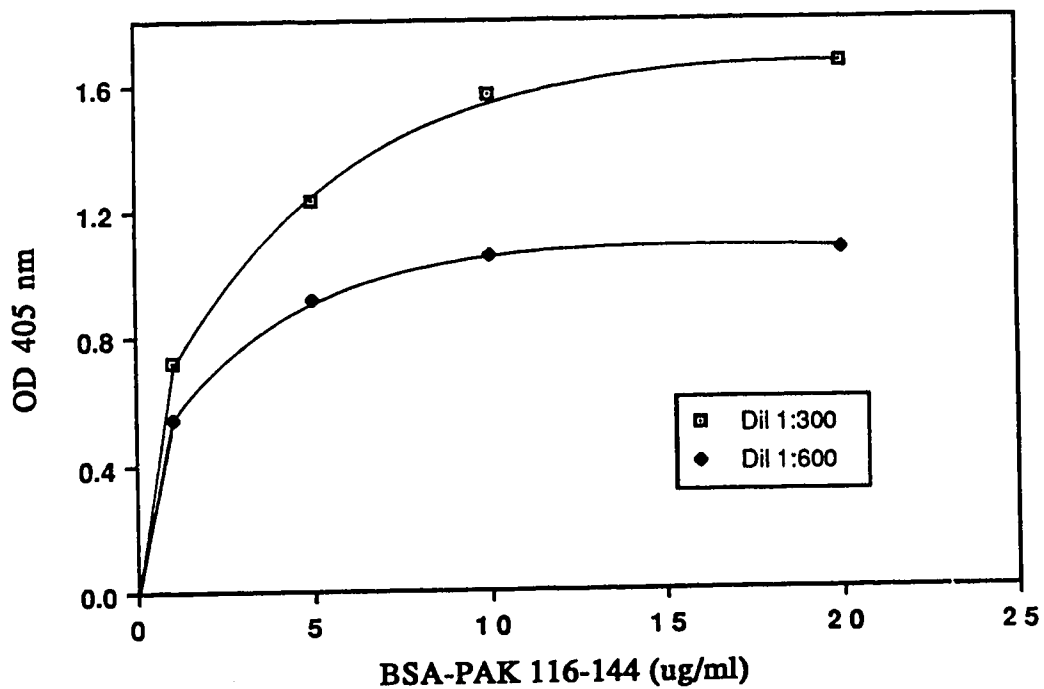


Figure IV.2. Determination of the concentration range of BSA-peptide conjugates to be used for direct ELISA. Two dilutions, 1:300 (□) and 1:600 (◆) of an anti-PAK pilus antiserum were used with varying concentrations of BSA-PAK116-144 conjugates coated on the wells of the microplate. Absorbance readings at 405nm were taken after a 30 min incubation with the enzyme substrate, *p*-nitrophenylphosphate (1 mg/ml).

TABLE IV.1. End-point titers of antisera raised against reduced and oxidized PAK (128-144)-OH and to PAK (A<sup>129</sup>) (128-144)-OH peptides

| Antisera                | Peptide-Conjugate      | End-point Titers <sup>a</sup> |                             |
|-------------------------|------------------------|-------------------------------|-----------------------------|
|                         |                        | PAK pili                      | PAO pili                    |
| 17-R1                   | 3.5 x 10 <sup>-6</sup> | 1.0±1.2 x 10 <sup>-5</sup>    | 4.15±3.7 x 10 <sup>-4</sup> |
| 17-R2                   | 7.1 x 10 <sup>-6</sup> | 1.6±0.4 x 10 <sup>-5</sup>    | 4.50±0.3 x 10 <sup>-4</sup> |
| 17-O1                   | 4.5 x 10 <sup>-6</sup> | 1.5±0.7 x 10 <sup>-5</sup>    | 2.0 ±0.8 x 10 <sup>-5</sup> |
| 17-O2                   | 2.1 x 10 <sup>-6</sup> | 2.0±1.2 x 10 <sup>-5</sup>    | 1.3 ±1.6 x 10 <sup>-4</sup> |
| PAK (A <sup>129</sup> ) | 9.8 x 10 <sup>-6</sup> | --                            | --                          |

<sup>a</sup> The end-point titers ± standard deviation (n = 3) determined by direct ELISA experiments for the antisera from five rabbits are shown. R1 and R2 antisera have been raised against reduced PAK (128-144)-OH peptide; while O1 and O2 antisera have been raised against the oxidized PAK (128-144)-OH peptide; PAK A<sup>129</sup> antiserum has been raised against the cysteine 129-substituted peptide. The end-point was determined as the cut-off at an A<sub>405</sub> reading of 0.05 absorbance unit above the background value of the control after a 30 min incubation with the substrate.

that the reduced peptide, when coupled to the carrier protein, does not remain reduced after immunization. One approach would be to carboxamidomethylate the cysteines which would prevent formation of the disulfide bond. However, the presence of the carboxamidomethyl groups would be expected to generate anti-peptide antibodies that would also recognize these groups in the peptide and, thus, the anti-peptide antibodies would not recognize the native protein. This is strongly supported by the antigen-antibody studies of Hodges *et al.* (1988) which clearly demonstrated that the removal of a single methyl group can result in loss of antibody binding. We felt the only option available was to substitute cysteine-129 with an alanine residue at the N-terminal of the peptide near the site of attachment to the carrier protein. In this way, formation of the disulfide bridge was prevented leaving the C-terminal 15 residues identical to the native protein. Interestingly, the anti-peptide antibodies (PAK-A129, Table IV.1) to this sequence bound poorly to the native PAK and did not crossreact with PAO pili, suggesting the importance of the disulfide bond in generating anti-peptide antibodies that bind the native proteins or the importance of the side-chain of cysteine-129 in antibody binding. The importance of a disulfide-looped peptide in raising anti-peptide antibodies that bind to native protein was illustrated in an early study employing a synthetic peptide corresponding to the looped region (62-84) of lysozyme (Sela *et al.*, 1971). These workers showed that the destruction of the disulfide bridge with performic acid resulted in a loss of binding to native lysozyme.

#### 4. Crossreactivities of anti-PAK 128-144 antisera with PAO pili

When the ELISA plates were coated with PAO pili, it was found that the 17-R and 17-O antisera were able to bind and crossreact with the heterologous pili. However, only antiserum 17-01 (Table IV.1) gave an end-point titer with PAO pili similar to PAK pili. The other three antisera titers with PAO pili were at least 10-fold lower compared to PAK pili. From the sequence data (Figure IV.1), it can be seen that the amino acid residues in the C-terminal end of the PAK and PAO pilin proteins are only semi-conserved. From the

primary amino acid sequences, surface profile predictions based on the combination of hydrophilicity, mobility and accessibility parameters (Parker *et al.*, 1986) were carried out and it was shown that the C-terminal regions of both PAK and PAO pilin are surface exposed regions (Chapter V, Figure V.1). This C-terminal region of PAO pilin also contains two cysteine residues which can form a disulfide bridge in the native molecule. The results of the direct ELISA experiments showed that the anti-peptide antisera raised against the oxidized peptide were able to bind better to PAO pili than those raised against the reduced peptide, PAK (128-144)-OH. This was also shown by the competitive ELISA experiments (see below). This was not the case with PAK pili, where antisera to reduced or oxidized peptide had similar binding activities. These crossreactivities were also observed in immunoblot assays.

### 5. Immunoblot assays

The binding of anti-peptide antibodies to pili was checked using immunoblot assays (Figure IV.3). Purified PAK and PAO pili (lanes 1 and 3, respectively) and also pili from the lysate fractions of whole cell *P. aeruginosa* strains PAK and PAO (lanes 2 and 4, respectively) (see Materials and Methods) were used. A faint band appearing on the lefthand side of lane 1 in each of the panels is a low molecular weight prestained colored marker. As shown in panel *a* (Figure IV.3), anti-PAK pilus antiserum bound to homologous pili and also crossreacted with heterologous PAO pili. The lysate fractions from PAK and PAO contained some other bands which crossreacted with the anti-PAK pilus antiserum. Anti-PAO pilus antiserum bound to homologous pili and also crossreacted with PAK pili (panel *d*, Figure IV.3). The pilin bands from the lysate fractions from PAK and PAO whole cells appeared as doublets and the cause for this is not known. Both anti-peptide antisera raised against reduced (17-R) and oxidized (17-O) peptides reacted with purified pili and pili from the whole cell PAK preparation. It was also seen that the two different antisera, 17-R and 17-O, crossreacted with purified PAO pili (panels *b*, *c*, *e* and

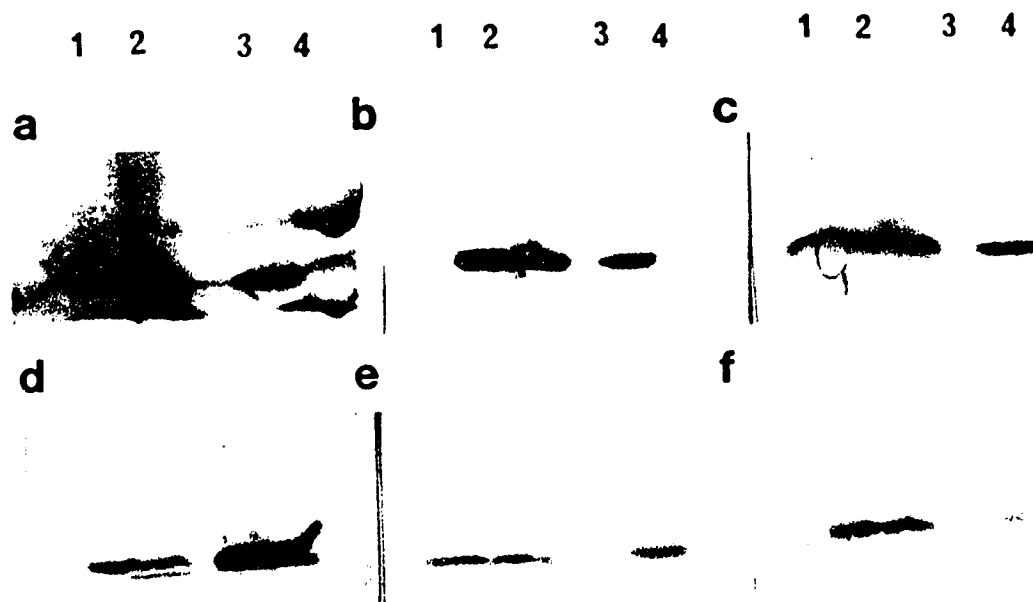


Figure IV.3. Immunoblot assays demonstrating the interaction between purified pili and whole cell pili from PAK and PAO strains with all four anti-peptide antisera 17-R1, 17-R2, 17-O1 and 17-O2 (Panels b, c, e and f, respectively). Lane 1 is purified PAK pili; lane 2 is solubilized membrane of PAK whole cell; lane 3 is purified PAO pili; and lane 4 is solubilized membrane of PAO whole cell. Control experiments using antisera raised against native PAK and PAO pili are shown in panels a and d, respectively.

f). This interaction between anti-PAK 128-144 antibodies and PAO pili was not as strong as that observed with the PAK pili, even though an approximately equal amount of material was loaded onto the gel. However, antisera 17-O1 showed equally intense pilin bands with PAK or PAO pili (panel e), consistent with the ELISA data of Table IV.1. Interaction of the antipeptide antisera with PAO pili from whole cell only gave faint bands. This could be due to smaller quantities of pili produced per PAO cell, or to a combination of a reduced amount of pili and the weaker interactions between antisera and pili. In addition to the interactions with the PAO pilin molecules, some crossreactivities were observed between the antipeptide antisera with a high molecular weight band from the PAO lysate fraction (especially in panels c and e).

#### 6. *The relative affinities of antipeptide antibodies to PAK pili*

The relative affinities of the antibodies raised against reduced and oxidized peptides for the PAK pili were determined using competitive ELISA experiments. Protein-A purified IgG (1.0 nM) from each serum (17-R1, 17-R2, 17-O1 and 17-O2) were incubated with a serially diluted solution of reduced and oxidized AcPAK 128-144-OH peptides. The results are shown in Figures IV.4 and IV.5. In each instance, where either reduced or oxidized peptide was used to compete for binding to IgG, there was no significant difference in the ID<sub>50</sub> (inhibition dose which gave a fifty percent reduction in binding of the peptides for either IgG raised against the reduced or oxidized 17-residue peptide). In the case of reduced peptides, incubations were carried out in the presence of a small concentration of  $\beta$ -mercaptoethanol to keep them in a reduced state. The antibodies that were raised against the oxidized peptide were also able to recognize the reduced peptide and vice-versa. This suggested that the native conformation with the disulfide chain was not critical in the antigenicity of this region. This was illustrated again when native pili were used as the competing antigen with either IgG raised against the reduced or oxidized peptide, as shown in Figure IV.6. When the 17-R or 17-O IgG was preincubated with

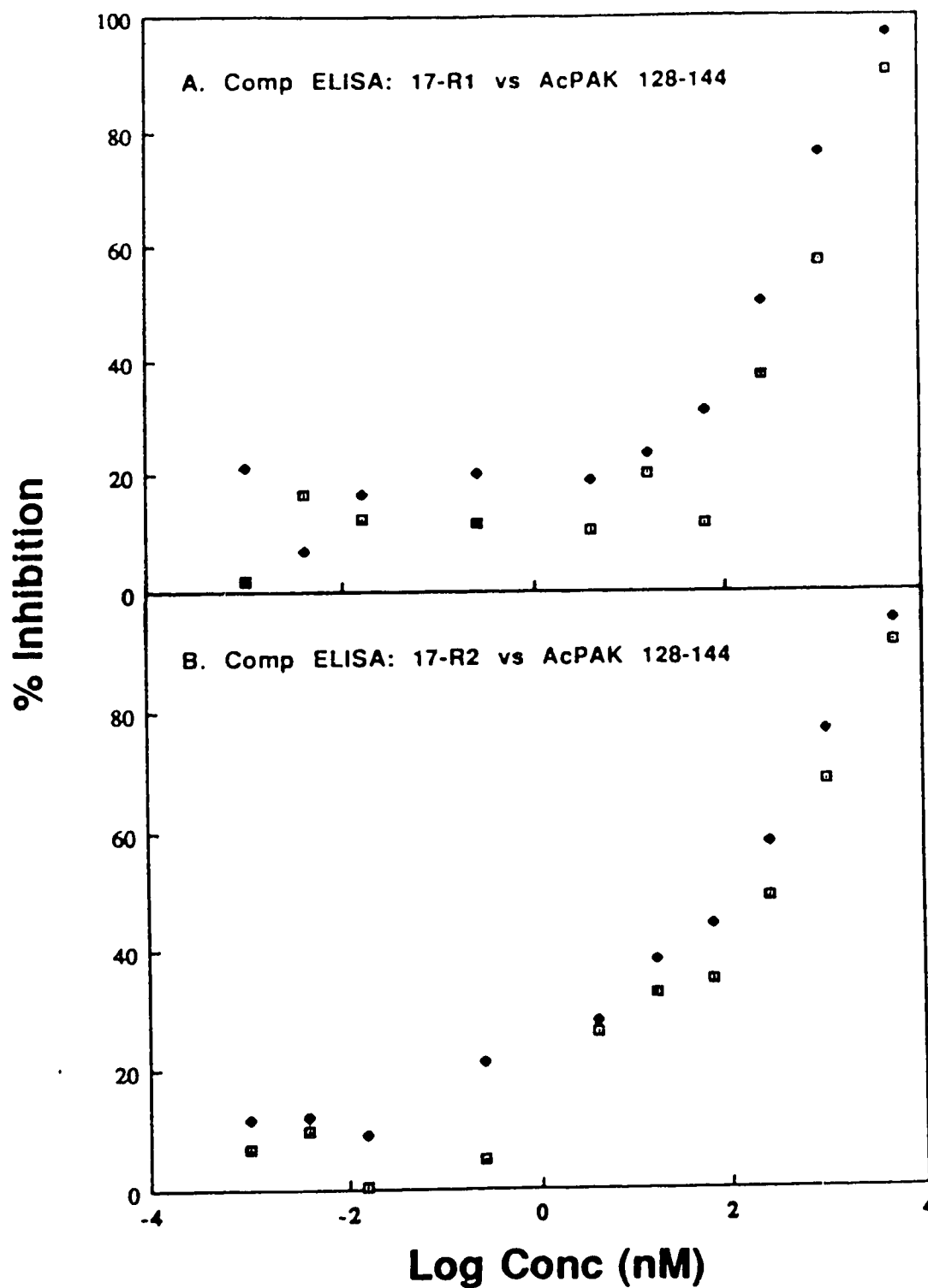


Figure IV.4. Competitive ELISA with IgG (10nM) of 17-R1 and 17-R2. The wells on the microplate were coated with a 5 ug/ml PAK pili solution. The competing antigens used in these assays were AcPAK 128-144 oxidized peptides (▲) and reduced peptides (◻). The abilities of the peptides to bind and compete at a given concentration is represented as a percentage of the absorbance in the absence of competing antigen.



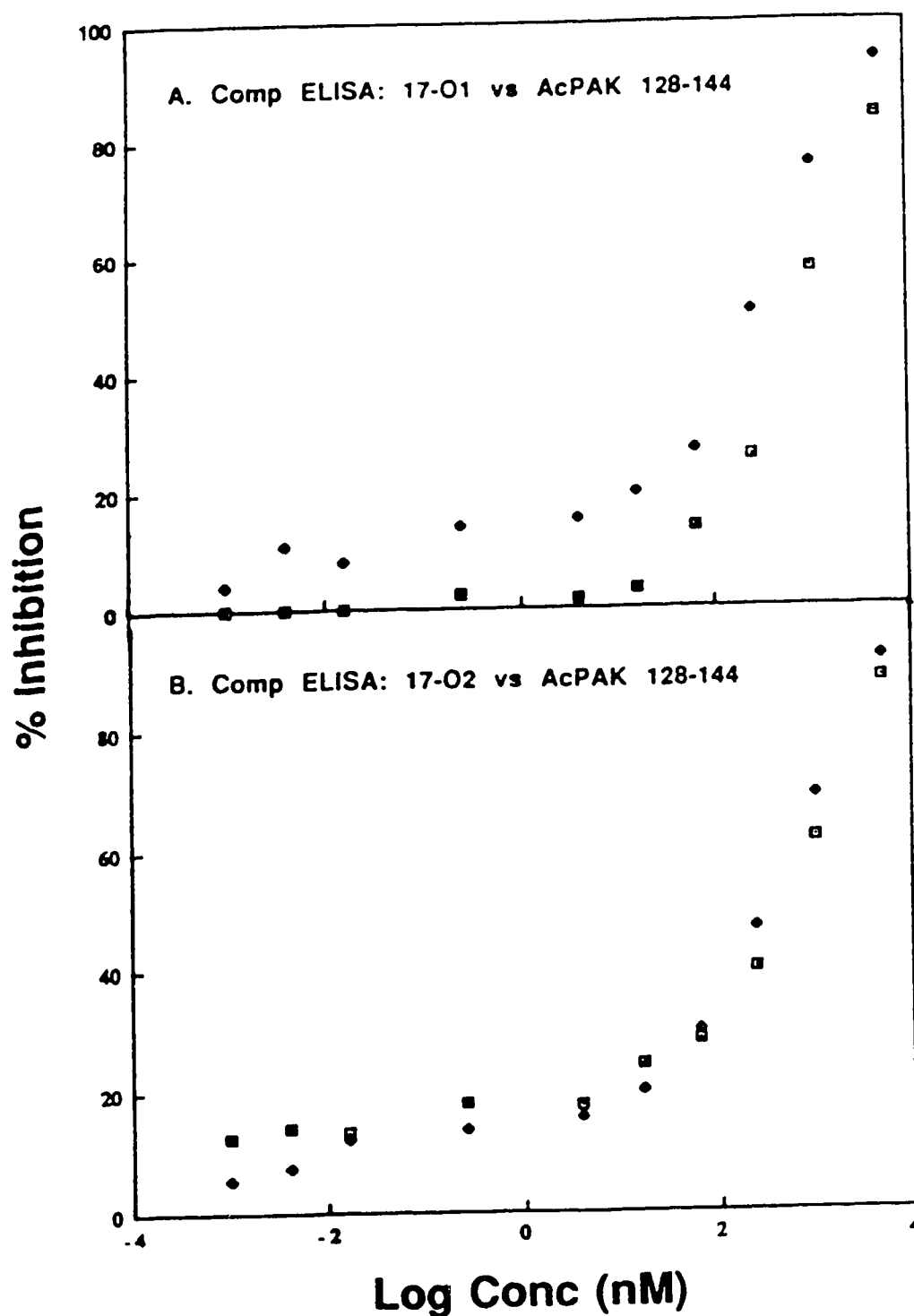


Figure IV.5. Competitive ELISA with IgG (10nM) of 17-O1 and 17-O2. The wells on the microplate were coated with a 5 ug/ml PAK pili solution. The competing antigens used in these assays were AcPAK 128-144 oxidized peptides (▲) and reduced peptides (◻). The abilities of the peptides to bind and compete at a given concentration is represented as a percentage of the absorbance in the absence of competing antigen.

native PAK pili, the competitive ELISA experiments showed that all four sets of data points could be fitted by a single line, illustrating the similarities in the antibody interactions of the two different antibodies with PAK pili. Another set of experiments was carried out with papain-digested IgG, i.e., the Fab fragments, to show that the bivalency of IgG did not affect the results (Figure IV.7A and IV.7B). Although the inhibition patterns using Fab fragments were similar to those obtained with IgG (in that both reduced and oxidized peptides had similar affinities for the antigen binding sites), a much higher concentration (about 26-fold) of the competing peptides were required in the assays with IgG to give rise to a 50% inhibition.

#### *7. The binding of an anti-PAK pilus antiserum to PAK 128-144 and PAK 116-144*

The binding of an anti-PAK pilus antiserum to PAK 128-144 and PAK 116-144 was assayed and the results compared. The results are shown in Figures IV.8 and IV.9. As indicated by the intensities of the absorbance at 405 nm, the antiserum bound better to the oxidized peptides than the reduced peptides under the conditions used in the direct ELISA. The antibodies also bound better to the longer peptide than the shorter one. These results indicated that the C-terminal region is immunogenic.

#### *8. The binding of anti-PAK pilus antiserum to the C-terminal peptide*

The binding of native PAK anti-pilus antiserum to the C-terminal AcPAK 128-144 peptide was also studied using competition ELISA experiments. In this case, the wells of the ELISA plates were coated with the reduced or oxidized peptide-conjugate. The peptide-conjugate was used instead of native PAK pili because the C-terminal region is not the immunodominant region and the percentage of antibodies in the native anti-pilus antiserum which bind to this region is less than 10 percent. Any changes in the absorbance readings due to the inhibition by the peptides would be small and, hence, if pili were used to coat the

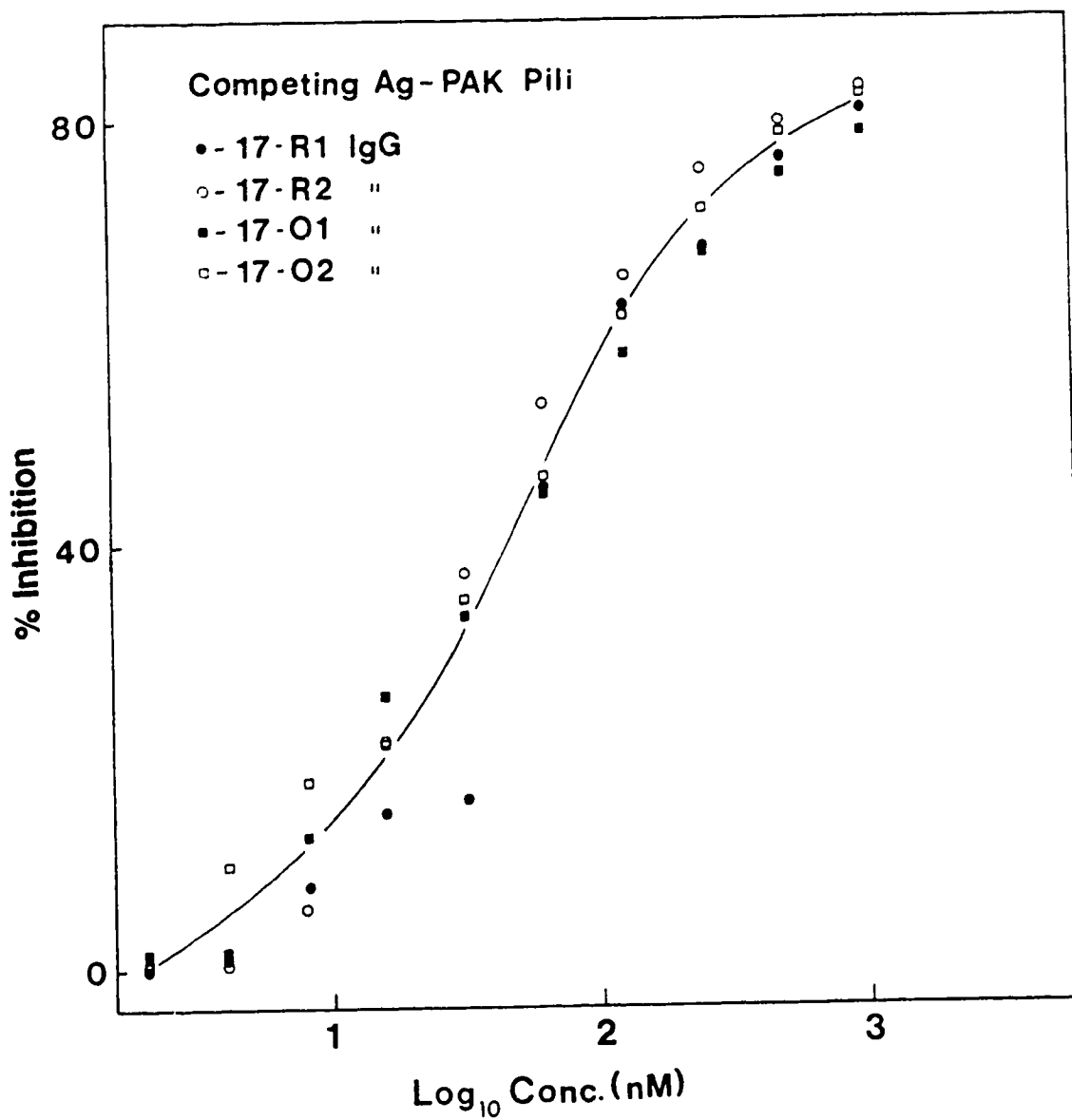


Figure IV.6. Competitive ELISA with native PAK pili. The wells were coated with a 5  $\mu\text{g/ml}$  PAK pili solution and four anti-peptide antibodies (1.0 nM) were assayed; ●, 17-R1; ○, 17-R2; ■, 17-O1; and □, 17-O2. A single line was able to fit all four sets of data points, illustrating the similarities in their interactions with PAK pili.

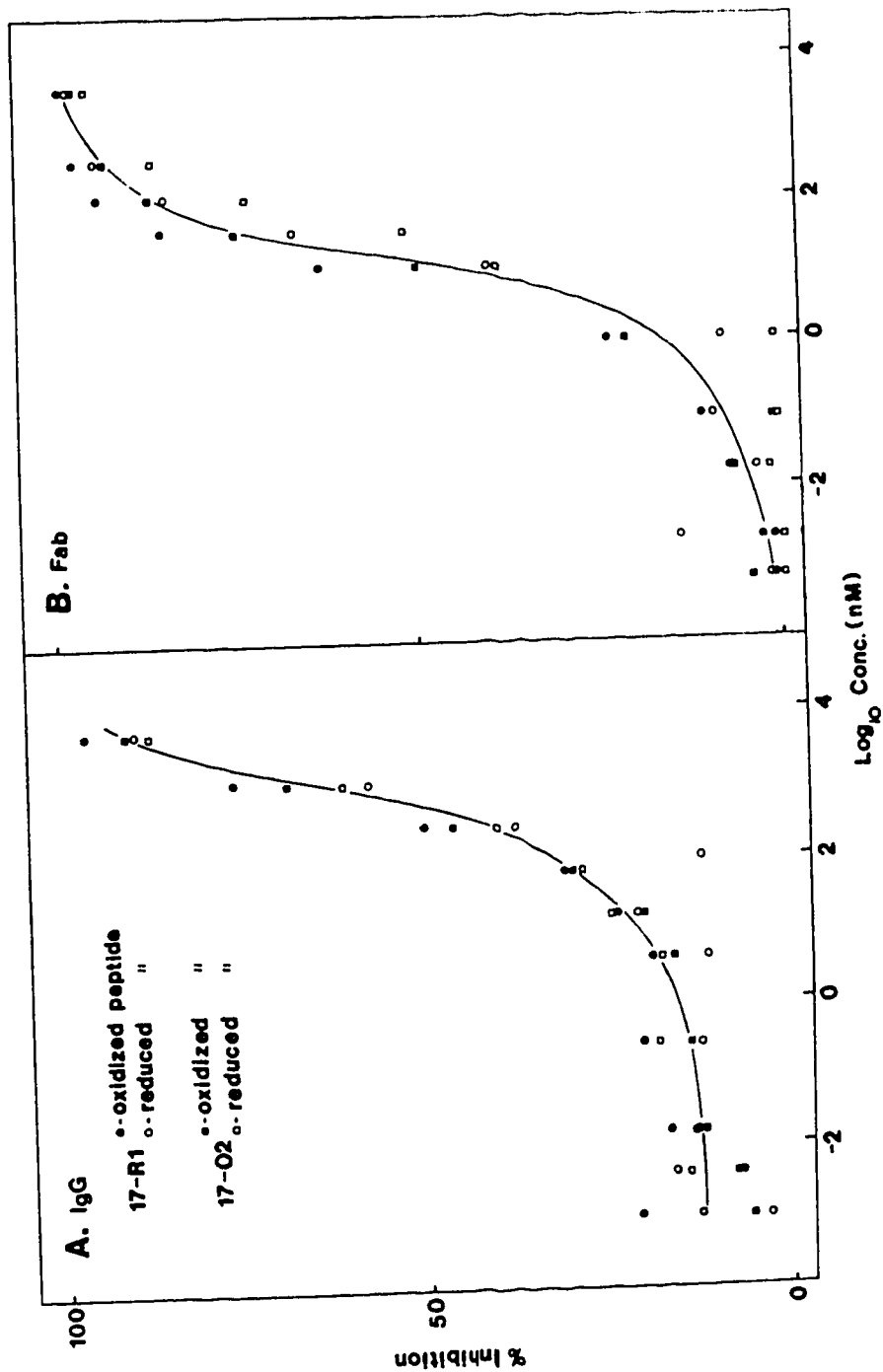


Figure IV.7. Comparison between IgG (panel A) and its Fab fragments (panel B) in competitive ELISA. Two antipeptide antibodies, 17-R1 and 17-O2, and their Fab derivatives are shown. The wells were coated with 5 ug/ml PAK pili and competed with varying concentrations of reduced and oxidized AcPAK 128-144 peptides. The affinities of these peptides are represented by the percent inhibition.

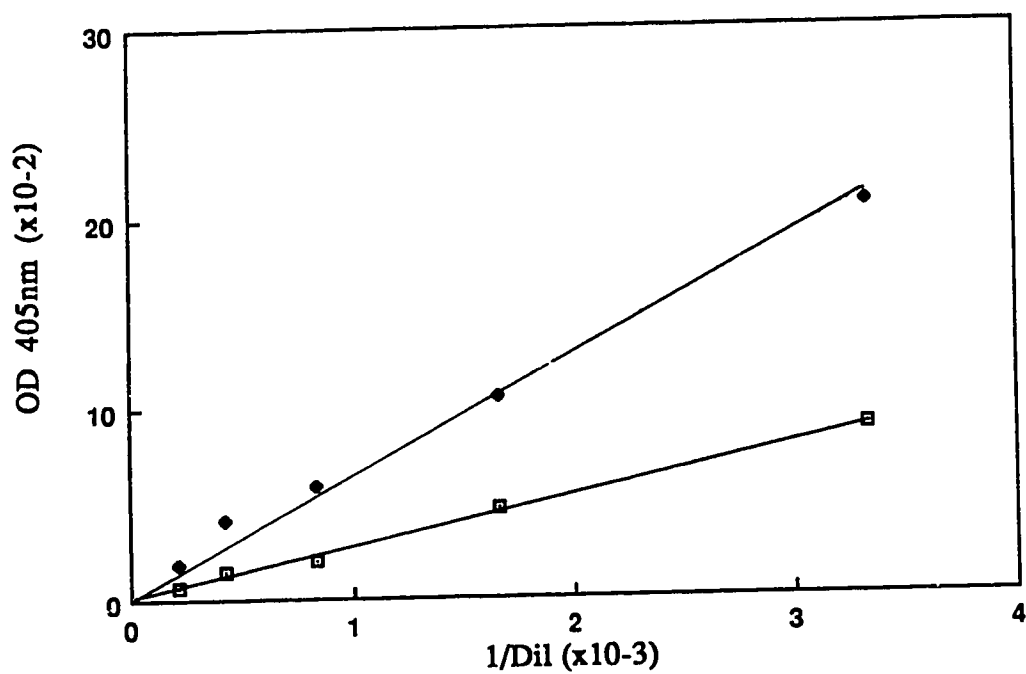


Figure IV.8. The binding of an anti-PAK pilus antiserum to the BSA-peptide conjugates of PAK 128-144. Both the reduced ( $\square$ ) and oxidized ( $\blacktriangle$ ) forms of the AcPAK 128-144 peptide were assayed. The absorbance readings at 405nm were taken after a 30 min incubation with the enzyme substrate.

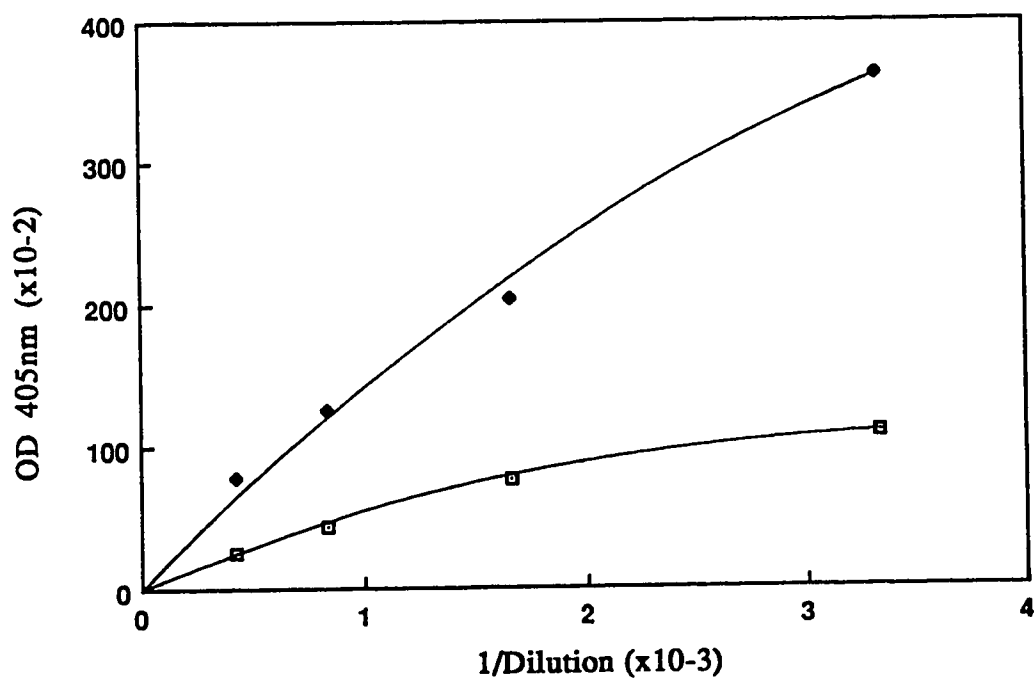


Figure IV.9. The binding of an anti-PAK pilus antiserum to the BSA-peptide conjugates of PAK 116-144. Both the reduced (◻) and oxidized (▲) forms of the AcPAK 116-144 peptide were assayed. The absorbance readings at 405nm were taken after a 30 min incubation with the enzyme substrate.

wells, these small changes would be difficult to detect in the presence of all the other epitopes on the pili which would be bound by other antibodies in the polyclonal serum. Native antiserum (1:8000 final concentration) was pre-incubated with oxidized or reduced peptide before addition to the peptide-conjugates. The incubation with the reduced peptide and coating of the wells with reduced peptide-conjugate were carried out in the presence of  $\beta$ -mercaptoethanol. The results are shown in Figure IV.10A and IV.10B. When the wells were coated with oxidized peptide-conjugate, competition with reduced or oxidized peptide showed similar inhibition patterns with almost identical  $ID_{50}$  values. The converse experiment, with wells coated with reduced peptide-conjugates, gave similar results with reduced and oxidized peptides competing equally well for binding to antibodies from native PAK anti-pilus antiserum.

#### *9. Crossreactivities of anti-PAK peptide antisera with PAO pili*

An interesting result was obtained when PAO pili were used as the competing antigen in these competitive ELISA experiments with IgG molecules and the wells were coated with PAK pili. Earlier results with the direct ELISA and immunoblot experiments have shown that all four of the antipeptide antisera raised against either reduced or oxidized peptide were able to bind to PAO pili. As shown in Figure IV.11, only one of the four antisera (17-O1), was saturated and competed out by the PAO pili. The other three antipeptide antisera showed little or no preference for binding to PAO pili. With the 17-01 IgG, the  $ID_{50}$  when PAO pili was used as the competitor was 4.36 fold less compared with PAK pili. From the amino acid sequence of the disulfide bridge region, both PAK and PAO show some sequence homology (nine out of the seventeen residues). There is a stretch of five out of six residues which are conserved in one region. It is possible that, on binding to the ELISA wells and to the nitrocellulose paper, denaturation of the pilin subunits may enable all four anti-peptide antisera to recognize and

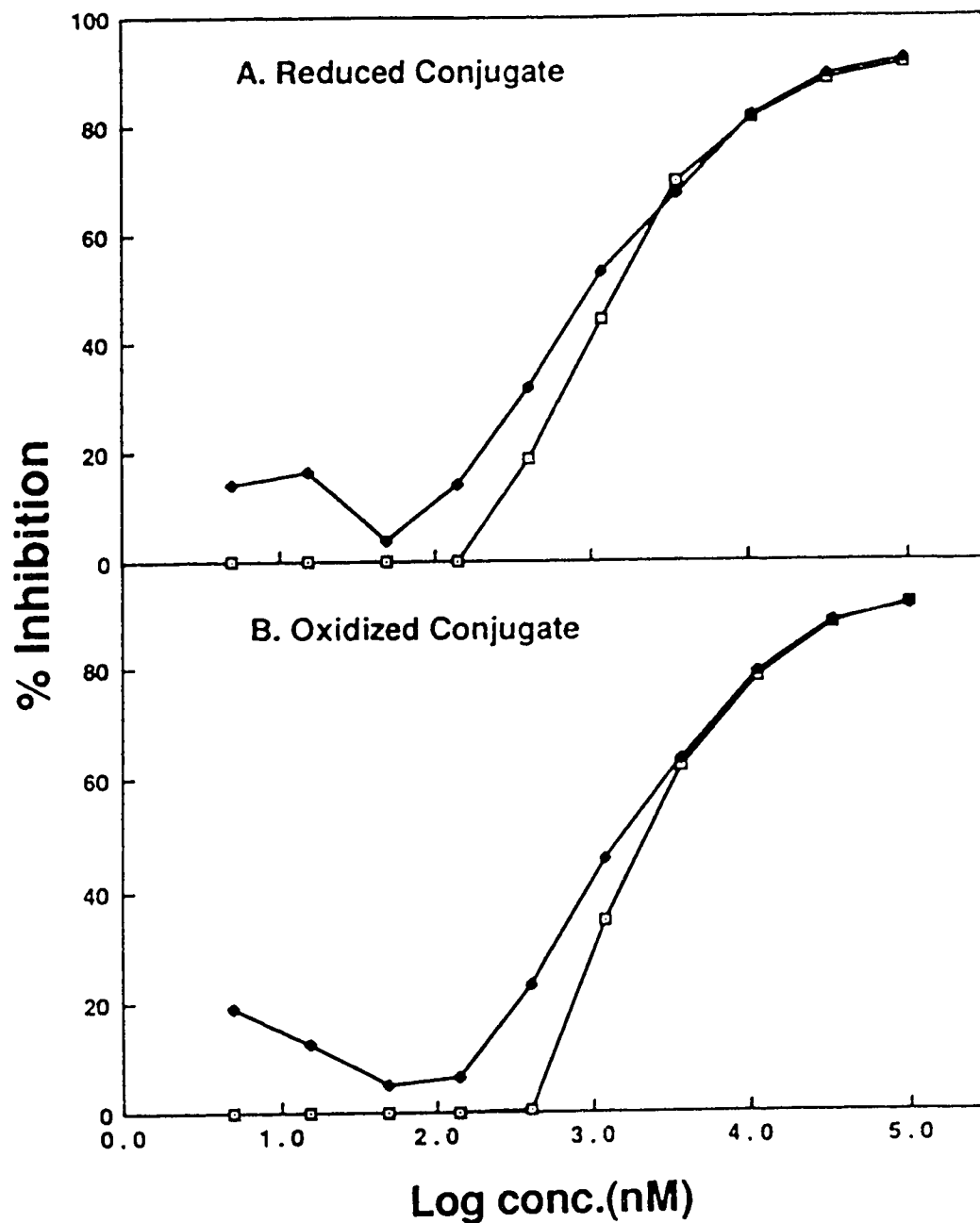


Figure IV.10. Competitive ELISA with anti-PAK pilus antiserum. The wells were coated with a 5  $\mu\text{g}/\text{ml}$  solution of BSA-PAK 128-144 conjugate in either the reduced (A) or oxidized (B) form. The reduced conjugate was incubated with a small amount of reducing reagent to keep it in the reduced state. The concentration of the native antiserum used was a 1:8000 dilution. The conjugates were competed with reduced (□) and oxidized (◆) AcPAK 128-144 peptides.



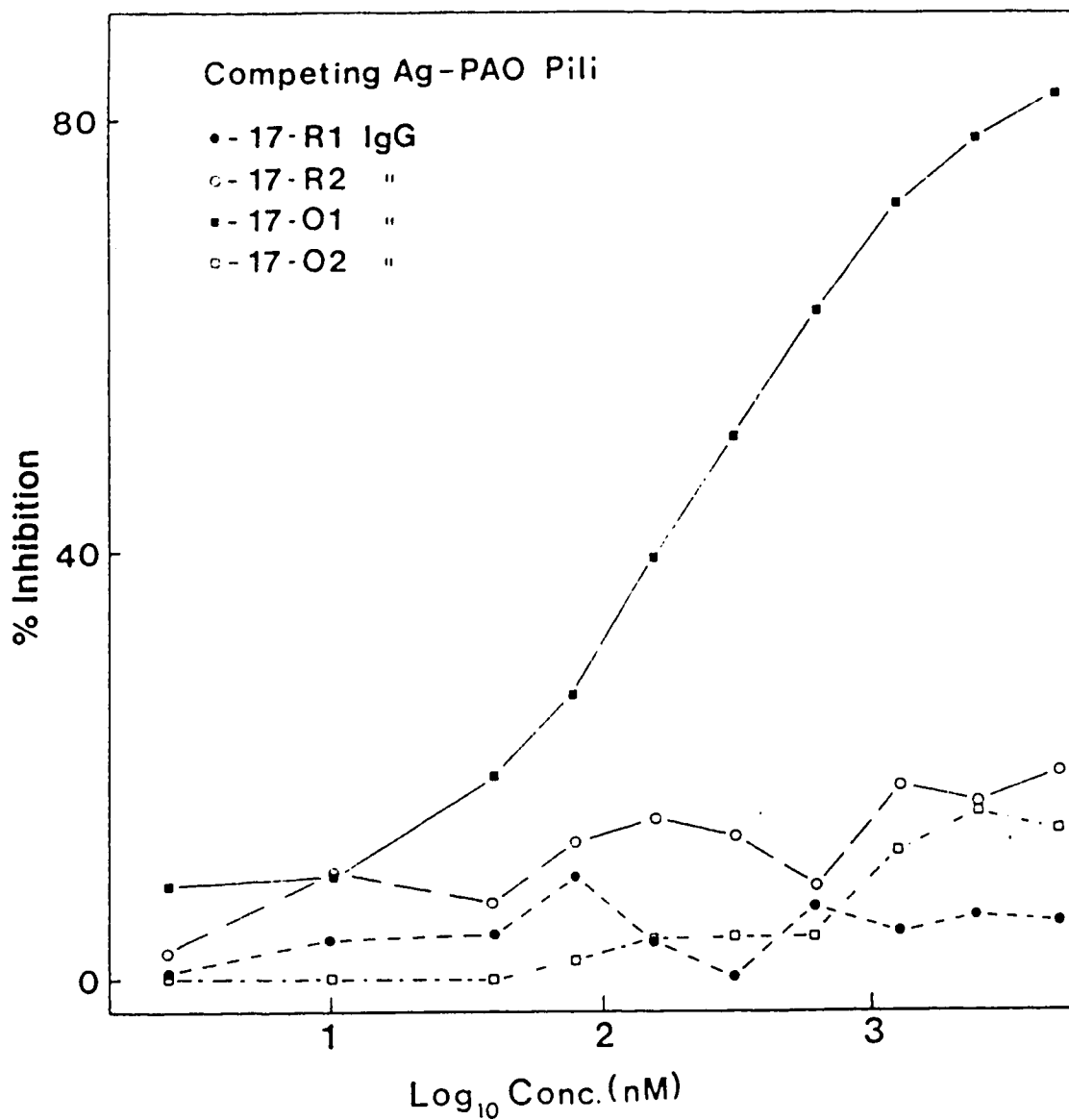


Figure IV.11. Competitive ELISA with native PAO pili. The wells were coated with a 5 ug/ml PAK pili solution and four antipeptide antibodies (1.0 nM) were assayed; ●, 17-R1; ○, 17-R2; ■, 17-O1; and □, 17-O2.

bind to this conserved region with affinities in the ELISA and immunoblot experiments. In a competitive ELISA test, where the PAO pili are in solution, the pili are in their native state and only the 17-01 IgG which recognizes this native conformation would bind to give rise to the inhibition that was observed. The observation that only one of the two antisera raised against oxidized peptide (17-01 and not 17-02) bound to PAO pili could have been attributed to different specificities of those antibodies prepared in different rabbits. Although all four antisera reacted equally well with the PAK pili in the competitive ELISA in Figure IV.6, it was interesting that only the 17-01 IgG bound well enough to PAO pili to give a binding curve. The kinds of interactions observed in the binding to the C-terminal region of the PAK pili were equally strong, as shown by the similarities in the binding curves in the competitive ELISA, but the abilities to bind to PAO pili were different. Even though both the 17-01 and 17-02 antisera were raised against the same oxidized peptide, only one of them recognized and bound PAO pili. As noted earlier in Figure VI.1, there is a stretch of five out of six amino acids which is conserved in both PAK and PAO pilins. The 17-01 IgG may be recognizing this epitope and the 17-02 may recognize a separate epitope.

### C. Discussion

The application of synthetic peptides corresponding to the C-terminal disulfide-bridged region of the *P. aeruginosa* PAK pilin has allowed a better understanding of the immunogenicity and antigenicity of this region. Anti-PAK pilus antiserum was shown to bind synthetic peptides corresponding to residues 128-144 and 116-144 of the PAK pilin (Figure IV.8 and IV.9). This suggested that this region of the PAK pilin is immunogenic. These results were in agreement with the findings of Sastry and Paranchych (1985) and Watts *et al.* (1983). In their studies, a fragment of the PAK pilin (121-144) was found to be weakly immunogenic and reduction and carboxymethylation of the sulfhydryl groups did not affect the antigenicity of the peptide. The anti-PAK pilus antiserum was found to bind better to the 29-mer than its shorter 17-mer version. This may be due to the presence of a fraction of antibodies that could bind to the additional residues prior to the disulfide loop region, or perhaps the longer peptide gave rise to conformational epitopes akin to those found in the native pilin, thus enabling better binding to antibodies in the serum. The data in Figures IV.8 and IV.9 also suggested that the oxidized conformers (PAK 128-144 and 116-144) showed better binding to the anti-PAK pilus antiserum than the corresponding reduced conformers. The formation of the disulfide loop could have resulted in a conformation in the peptide which resembles its conformation in the native pilin. Although the competitive ELISA Figure IV.10 showed that the anti-pilus antibodies bound well to both reduced and oxidized AcPAK 128-144-OH, there may be a slight preference for the oxidized over the reduced conformer. From Figure IV.3, an estimation of the ID<sub>50</sub> revealed that with the reduced PAK 128-144 conjugate immobilized onto the solid phase, the ID<sub>50</sub> for the oxidized AcPAK128-144 peptide was 1.0 nM *versus* an ID<sub>50</sub> of 1.6 nM for the reduced conformer. With the oxidized PAK 128-144 conjugate immobilized on the microplate, the ID<sub>50</sub> for the oxidized AcPAK 128-144 peptide was 1.6 nM *versus* an ID<sub>50</sub> of 2.2 nM for the reduced AcPAK 128-144 peptide. The ability of the reduced peptide to bind to the anti-PAK pilus antibodies, whose epitope has a disulfide

bridge, may be attributed to the ability of the peptide to fold into the pocket of the antigen binding site. It is also possible that the peptide has an inherent ability to fold into a conformation akin to the native protein. The disulfide bond locks the conformation into a stable configuration which could result in a higher binding affinity for the antibodies.

When the synthetic PAK 128-144 peptides were used as immunogens, it was shown that anti-peptide antisera to both reduced (17-R) and oxidized (17-O) conformers bound very well to the PAK pili in direct ELISA and immunoblot assays (Table IV.1 and Figure IV.3). Although this region of the pilin molecule is immunorecessive, the use of synthetic peptides have helped overcome this problem. High antibody titers were obtained and these antibodies bound to this region on the native protein. Furthermore, there is a conserved epitope in this region of the *P. aeruginosa* pilin molecule that allowed crossreactivities between the 17-R and 17-O anti-peptide antisera with the PAO pili. The integrity of the disulfide bridge may be important in the generation of crossreacting anti-PAK 128-144 antibodies since the 17-O1 antibodies were the only ones of the four antisera that could effectively compete for binding to PAO pili in indirect ELISA (Figure IV.11). The titers of these other three antisera (17-R1, 17-R2 and 17-O2) were also 10-fold lower than the 17-O1 when assayed against PAO pili in direct ELISA (Table IV.3). This was also illustrated by the immunoblot assays (Figure IV.3). The PAO pilin band lighted up by the 17-O1 antiserum was as intense as those of the PAK pilin bands. The other three antisera gave rise to a PAO pilin band that was much fainter. Thus, the epitopes that are recognized by the 17-O1 antibodies may be different from the epitopes recognized by the 17-R1, 17-R2 and the 17-O2 antibodies. Although the 17-O2 antiserum was also raised against the oxidized PAK 128-144 peptides, it did not bind to PAO pili as well as the 17-O1 antiserum. Obviously, the epitopes of the 17-O1 and 17-O2 were significantly different to account for the different affinities. Recognition of the oxidized peptides by different populations of B-lymphocytes in the two different rabbits that were used have led to

production of antibodies that have subtle differences in their epitopes; these differences gave rise to strain-specific and crossreactive antibodies.

The fact that the disulfide bridge is not critical to the antigenicity of this C-terminal region of *P. aeruginosa* seems to be in contrast to the results obtained with gonococcal pilin (Schoolnik *et al.*, 1983). The results of the present studies and those of Watts *et al.* (1983) showed that the antigenicity of the disulfide loop region of *Pseudomonas* pilin was not destroyed by the disruption of the disulfide bond. The disulfide loop region in the gonococcal pilin, which has 30 residues within the loop (Schoolnik *et al.*, 1984) is larger than the *Pseudomonas* pilin, which only contains 12 residues within the loop. Schoolnik *et al.* (1983) reported that the reduction and carboxymethylation of the cysteines in the loop region of gonococcal pilin resulted in the destruction of strain-specific immunodominant epitopes. There were no detailed data presented in their report. These workers proposed that this intrachain disulfide bond conferred to the loop region a conformational epitope. However, subsequent studies by these workers (Rothbard *et al.*, 1984) revealed two strain-specific antigenic determinants within this loop region (121-134 and 135-151). Antipeptide antisera against these two regions bound to the gonococcal pili and inhibited adhesion of *N. gonorrhoea* organisms to mammalian cells (Rothbard *et al.*, 1985). In addition, reactivities of monoclonal antibodies to the highly variable region in the disulfide loop of the gonococcal pilin block pilus binding to epithelial cells, suggesting that the loop region may contribute to pilus-host cell adhesion (Nicholson *et al.*, 1987). In a comparative study of the NMePhe pilin from different genera by Dalrymple and Mattick (1987), it was observed that the C-terminal region of pilin from *N. gonorrhoea*, *P. aeruginosa* and *M. bovis* contains two cysteines which form a putative disulfide bond. In *B. nodosus*, the location of the cysteine residues are in the central region of of the pilin molecule. The conservation of cysteine residues and the formation of a putative disulfide loop suggest that this loop region could play an important role in pili function.

The studies here show that antibodies in the polyclonal sera raised against PAK pili are able to recognize and bind to the C-terminal 17-mer peptide in the presence or absence of an intra-chain disulfide bridge. This suggests that the antigenic determinants in this region of the pilin molecule are mostly linear epitopes when native pili is used as the immunogen. Thus, this disulfide bridge is not critical in the antigenicity of this region unlike the case of the gonococcal pilin. Although the presence of an intact disulfide bridge was not important in the antigenicity of the *Pseudomonas* pilin, it was found that only one of the anti-peptide antisera which was raised against the oxidized peptide was able to bind and cross-reacted well enough with PAO pili to give good inhibition curves in an indirect ELISA experiment. Hence, there may be other structural features in the native oxidized state which allowed us to raise antibodies that cross-reacted well with other *Pseudomonas* strains. This cross-reactivity would be important in looking for a suitable vaccine candidate for *Pseudomonas aeruginosa*.

## Chapter V. Mapping the Surface Regions of PAK and PAO Pilins: Crossreactive and Strain-Specific Antibodies

### A. Introduction

Bacterial infections are multistep processes (Smith, 1984). They involve the adherence and colonization of the organisms on the epithelial surfaces of the host, the invasion into the mucosal layer and dissemination of the organisms in the tissues of the host. The prevention of the first step to an infection is the key to producing an effective vaccine. Hence, the understanding of the adherence processes of *P. aeruginosa* to epithelial cells could yield vital information towards the achievement of producing an effective *P. aeruginosa* vaccine. *P. aeruginosa* appears to be capable of employing two adhesins when adhering to epithelial cell surfaces (McEachran and Irvin, 1985; Ramphal and Pier, 1985; Ramphal *et al.*, 1987). The adhesins for nonmucoid *P. aeruginosa* strains are the polar pili, whereas mucoid strains can employ both mucoid exopolysaccharide (also referred to as alginate) and pili as adhesins.

The pilus-mediated adherence of *P. aeruginosa* to epithelial cells was investigated as it is believed that nonmucoid strains are the initial colonizers in *P. aeruginosa* infections (Dogget, 1969; Hoiby, 1974). In order to elucidate the mechanism of adherence, a study was first carried out to determine the surface regions of pilin, and then to determine the part/s of pilin which is/are involved in the attachment process. The pili-mediated attachment process in other organisms has been shown to involve adhesin molecules, which are proteins organized at the tip of the pilus or along the shaft of the pilus, but are not the structural pilin proteins (Hanson and Brinton Jr., 1988; Lindberg *et al.*, 1987; Maurer and Orndorff, 1987). However, in the NMePhe pilus of *P. aeruginosa*, no other minor pilus-associated proteins, besides the structural pilin subunit, have been found. The gonococcal pilin, which is also of the same class of NMePhe pilin, is also believed to be the adhesin in the gonococcal attachment process (Swanson, 1973). The studies of

Schoolnik and coworkers (Schoolnik *et al.*, 1983; Rothbard *et al.*, 1984; Rothbard *et al.*, 1985) and Heckels, Saunders and their coworkers (Nicholson *et al.*, 1987) have revealed that there are two regions in the gonococcal pilin which are involved in the adherence of the gonococcal whole cell to epithelial cells. Recently, there has been speculation that there might be other proteins associated with the gonococcal pilus (Muir *et al.*, 1988; Parge *et al.*, 1990). The proteins have yet to be characterized and their roles have not been determined.

As a first step to elucidating the region(s) of pilin which may have an important role in the adherence of *Pseudomonas* to host cells, the surface regions of the pilin molecule were mapped using anti-peptide antibodies raised against synthetic peptides corresponding to the pilin sequence of *P. aeruginosa* strain K (PAK). The PAK strain was chosen because the biological characteristics and the amino acid sequence of the pilus protein are known (Sastry *et al.*, 1983). In addition, a similar study was carried out with PAO pilin to compare the surface regions of the two pilin molecules. In this way, we could obtain crossreactive and strain-specific anti-peptide antibodies. The selection of peptides to be synthesized was based on prediction algorithms from a computer program, Surfaceplot, which utilized hydrophilicity, accessibility and mobility parameters to determine the surface potential of any region from the primary sequence of the protein (Lee *et al.*, 1989; Parker *et al.*, 1986; Strynadka *et al.*, 1988).

## **B. Results**

### **1. Comparisons between predicted surface regions of PAK and PAO pilins**

The Surfaceplot prediction algorithm of Parker *et al.* (1986) suggested that there are eight potential surface regions in both PAK and PAO pilins (numbered 1-8 on Figure V.1). The heights and lengths of these regions gave indications of the degrees of their surface potential. In the case of the PAK pilin, the regions with the highest surface potential were 3, 5, 6 and 8 (residues 58-70, 89-96, 106-112 and 130-141, respectively), whereas in



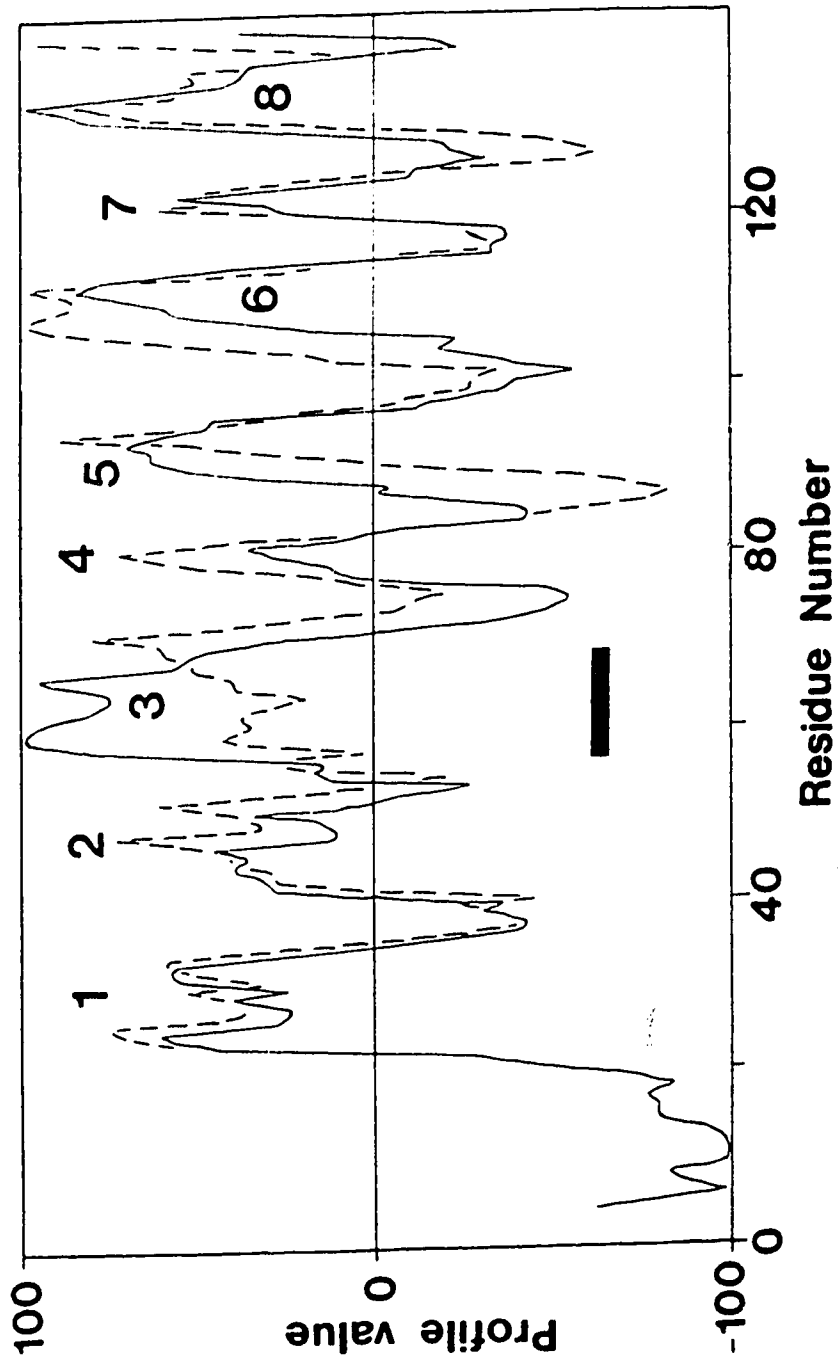


Figure V.1. Plot of the predicted surface regions of PAK (—) and PAO (----) pilins using Surfaceplot program of Parker *et al.* (1986). Profile values above zero represent predicted surface regions and those below represent hydrophobic regions. The solid bar denotes the region 58-70 where the largest difference between the surface profile values of PAK and PAO was observed.

PAO pilin, these were regions 5, 6 and 8 (residues 92-96, 105-112 and 130-140, respectively). The rest of the surface potential regions of PAO pilin were moderately high, with the exception of region 7 (residues 120-122). However, in PAK pilin, regions 2, 4 and 7 (residues 42-47, 77-81, and 120-122, respectively) all have relatively low surface potential. The main difference in the profiles was observed in the central region of the sequences of the PAK and PAO pilin molecules (represented by a solid bar in Figure V.1). The predicted surface region 3 of PAK pilin (residues 58-70) has more surface potential than the corresponding region 3 (residues 55-71) of PAO pilin, while the converse was true for region 4 (residues between 77-81). The regions of the molecule which were predicted to be buried in the interior of the molecule have large negative profile values, as depicted in Figure V.1. The N-terminal regions of both pilins are conserved and, hence, the plots overlapped with each other. It has been proposed that the highly conserved region preserves an important function of maintaining the structural integrity of the NMePhe pilin subunit-subunit interactions by being buried within the subunit (Hermodson *et al.*, 1978; Paranchych *et al.*, 1978). Synthetic peptides encompassing the predicted surface regions of both pilins were made and coupled to protein carriers [keyhole limpet hemocyanin (KLH)] to raise rabbit antipeptide antisera (see Materials and Methods Section). The amino acid sequences of the synthetic peptides are shown in Figure V.2. Two of the eight predicted surface regions have identical sequences in both pilins (regions 22-33 and 41-49). The corresponding antisera were designated anti-PAX 22-33 and anti-PAX 41-49 to indicate the sequence identity between strains. In the case of the PAK pilin, the sequence of an interior region (residues 34-40) was also synthesized to serve as a negative control.

## **2. Reactivities of antipeptide antisera with PAK and PAO pili**

Direct ELISAs were performed with the microplates coated with each of the BSA-peptide conjugates to screen for the presence of its respective antipeptide antiserum (see Methods and Materials Section). Each antipeptide antiserum was subsequently assayed for

| Predicted Surface Regions        | Peptide Region Synthesized | Amino Acid Sequences   |
|----------------------------------|----------------------------|--|
| 23-29, 31-33<br>23-34            | PAX 22-33<br>PAX 22-33     | P-Q-Y-Q-N-Y-V-A-R-S-E-G-NH <sub>2</sub><br>P-Q-Y-Q-N-Y-V-A-R-S-E-G-NH <sub>2</sub>     |
| 42-47<br>42-51                   | PAX 41-49<br>PAX 41-49     | N-P-L-K-T-T-V-E-E-NH <sub>2</sub><br>N-P-L-K-T-T-V-E-E-NH <sub>2</sub>                 |
| 58-70<br>55-71                   | PAK 58-70<br>PAO 58-70     | K-S-G-T-G-T-E-D-A-T-K-K-E-NH <sub>2</sub><br>S-K-I-K-I-G-T-T-A-S-T-A-T-NH <sub>2</sub> |
| 77-78, 80-81<br>78-81            | PAK 74-83<br>PAO 75-84     | G-V-A-A-D-A-N-K-L-G-NH <sub>2</sub><br>G-V-E-P-D-A-N-K-L-G-NH <sub>2</sub>             |
| 89-96<br>92-96                   | PAK 88-97<br>PAO 88-97     | K-P-D-P-A-D-G-T-A-D-NH <sub>2</sub><br>V-A-I-E-D-S-G-A-G-D-NH <sub>2</sub>             |
| 106-113<br>105-112               | PAK 105-114<br>PAO 105-114 | G-G-A-G-P-K-N-K-G-K-NH <sub>2</sub><br>G-T-S-S-P-K-N-A-T-K-NH <sub>2</sub>             |
| 120-122<br>120-122               | PAK 117-125<br>PAO 117-125 | T-L-T-R-T-A-A-D-G-NH <sub>2</sub><br>T-L-N-R-T-A-D-G-V-NH <sub>2</sub>                 |
| 130-137, 141<br>130-137, 139-140 | PAK 128-144<br>PAO 128-144 | K-C-T-S-D-Q-D-E-Q-F-I-P-K-G-C-S-K-OH<br>A-C-K-S-T-Q-D-P-M-F-T-P-K-G-C-D-N-OH           |

Figure V.2. Amino acid sequences of the synthetic peptides which corresponded to the predicted surface regions of PAK and PAO pilins generated from Surfaceplot program. The boxed regions represented nonconserved residues between the two pilin sequences. In addition to the sequences shown, BB-Nle, was added to the N-termini of the peptides, where BB is the photoaffinity probe (benzoylbenzoic acid) used to couple the peptides to the protein carrier and Nle is the norleucine residue. PAX 22-33 and PAX 41-49 indicate sequence identity between strains in the regions of 22-33 and 41-49 of the pilin molecules.

TABLE V.1. Antipeptide antisera titers measured by direct ELISA when assayed against BSA-peptide conjugates and PAK pili.

| Peptide                 | Corresponding Antipeptide Antiserum Titers <sup>a</sup> |                      |
|-------------------------|---|----------------------|
|                         | BSA-peptide conjugates                                  | PAK pili             |
| 22-33                   | $1.2 \times 10^{-5}$                                    | $7.9 \times 10^{-3}$ |
| 34-40 <sup>c</sup>      | $2.2 \times 10^{-6}$                                    | -                    |
| 41-49                   | $2.0 \times 10^{-5}$                                    | $8.9 \times 10^{-4}$ |
| 58-70                   | $2.0 \times 10^{-5}$                                    | $7.9 \times 10^{-4}$ |
| 74-83                   | $2.2 \times 10^{-5}$                                    | -                    |
| 88-97                   | $4.5 \times 10^{-6}$                                    | $9.5 \times 10^{-3}$ |
| 105-114                 | $2.2 \times 10^{-6}$                                    | $1.1 \times 10^{-4}$ |
| 117-125                 | $7.4 \times 10^{-6}$                                    | $5.4 \times 10^{-3}$ |
| 128-144 R1 <sup>b</sup> | $3.5 \times 10^{-6}$                                    | $1.8 \times 10^{-5}$ |
| 128-144 R2 <sup>b</sup> | $7.1 \times 10^{-6}$                                    | $8.9 \times 10^{-6}$ |
| 128-144 O1 <sup>b</sup> | $4.5 \times 10^{-6}$                                    | $7.9 \times 10^{-6}$ |
| 128-144 O2 <sup>b</sup> | $2.1 \times 10^{-6}$                                    | $8.9 \times 10^{-6}$ |
| 137-144                 | $2.4 \times 10^{-6}$                                    | $1.0 \times 10^{-3}$ |

a) The antiserum endpoint titer was determined as the cutoff at an A<sub>405</sub> of 0.05 U.

b) The peptides as shown in Figure V.2 were coupled to BSA and their antigenicities assayed using an anti-PAK pilus antiserum. R1 and R2 represent two different rabbit antisera to the reduced peptide. O1 and O2 represent two different antisera to the oxidized peptide (disulfide bonded between cysteine residues 129 and 142).

c) This region was used as a control. It is a predicted interior region in the protein (Parker *et al.*, 1986).

binding to its homologous pili. The results are summarized in Tables V.1 and V.2. Anti-PAK peptide antisera obtained from KLH-peptide immunogens have antibody titers that were in the range of  $10^{-5}$  to  $10^{-6}$ , when the binding of the antipeptide antibodies to BSA-peptide conjugates was assayed (Table V.1). Of the eight predicted surface regions for PAK pilin, only one of the antisera raised against region 3 (anti-PAK 74-83) failed to react with PAK pili in direct ELISA. A control consisting of antipeptide antibodies to PAK 34-40, a region which is not predicted to be on the surface of the protein, also failed to bind PAK pili. The antibody titers, when assayed against PAK pili, were 10- to 1000- fold less than the antibody titers assayed against their respective BSA-peptide conjugates. However, this was not the case with the anti-PAK 128-144 antisera. Of the four anti-PAK 128-144 antisera, three of these reacted as strongly with the native protein as with the BSA-peptide conjugate, with antibody titers in the range of  $10^{-6}$ . Antipeptide antisera raised to synthetic peptides encompassing residues 22-33, 88-97, 117-125 and 137-144 (regions 1, 5, 7 and 8) gave weak responses in ELISA. Sera raised against synthetic peptides encompassing residues 41-49, 58-70 and 105-114 (regions 3, 4 and 6) gave slightly better results, with antibody titers in the range of  $10^{-4}$ .

Region 8 of the PAO pilin (encompassing residues 128-144), like its PAK counterpart, also produced the highest antibody titer ( $3.2 \times 10^{-6}$ ) of all the anti-PAO peptide antisera which were screened, as shown in Table V.2. Most of the PAO peptides gave rise to antibody titers in the range of  $10^{-5}$ , but two of these (anti-PAO 58-70 and 88-97) were only in the range of  $10^{-4}$ . When all eight of the anti-PAO peptide antibodies were assayed for binding to PAO pili in direct ELISA, it was found that six of these bound to PAO pili. Even though PAO 58-70 and 88-97 did not produce antibody titers as high as some of the other PAO peptides, both of these antipeptide antisera bound to PAO pili. Anti-PAX 41-49 gave only weak binding to PAO pili. Again, as observed with the anti-PAK peptide antisera, in all instances where anti-PAO peptide antisera bound to PAO pili, the antibody titers were about 3 -1000 fold lower than the titers assayed with the corresponding BSA-

TABLE V.2. Anti-PAO peptide antisera titers measured by direct ELISA when assayed against BSA-peptide conjugates and PAO pili.

| Antipeptide Antisera<br>Against PAO Pilin Regions | End-point Titers          |                         |
|---|---------------------------|-------------------------|
|   | BSA-peptide<br>Conjugates | PAO Pili                |
| 22 - 33   | $2.0 \times 10^{-5}$      | $\sim 1 \times 10^{-3}$ |
| 41 - 49   | $1.6 \times 10^{-5}$      | $\sim 1 \times 10^{-2}$ |
| 58 - 70   | $2.0 \times 10^{-4}$      | $6.3 \times 10^{-4}$    |
| 75 - 84   | $1.5 \times 10^{-5}$      | $1.6 \times 10^{-4}$    |
| 88 - 97   | $1.0 \times 10^{-4}$      | $1.0 \times 10^{-3}$    |
| 105 - 114   | $4.2 \times 10^{-5}$      | -                       |
| 117 - 125   | $4.2 \times 10^{-5}$      | -                       |
| 128 - 144   | $3.2 \times 10^{-6}$      | $1.8 \times 10^{-5}$    |

The procedures are similar to those for the PAK pili (see legend of TABLE V.1).

peptide conjugates. The anti-peptide antibody titers to native pili can be expected to be lower, since many of the antibodies raised against small peptides in polyclonal sera may not recognize the corresponding peptide regions in their native conformations within the protein molecule.

### ***3. Reactivities of anti-pilus antisera with PAK and PAO pilin peptides***

The BSA-peptide conjugates were used to screen for linear B-cell epitopes on the pilin molecules. Anti-pilus antisera to the respective PAK and PAO pili were assayed with the synthetic peptides, and the results are summarized in Table V.3. With the PAK peptides, only the regions of residues 22-33 and 88-97 were not bound by anti-PAK pilus antiserum. PAK 74-83 was the most antigenic of the eight PAK peptides. The synthetic peptide encompassing residues 128-144 was the most antigenic of the eight PAO peptides. With the exception of PAO 88-97, the other PAO peptides displayed weaker binding to the anti-PAO pilus antiserum. In a similar manner to PAK 88-97, which did not bind to anti-PAK pilus antiserum, PAO 88-97 did not show any binding to the anti-PAO pilus antiserum.

### ***4. Crossreactivities of anti-PAK and anti-PAO peptide antisera with heterologous PAK and ...PAO pili in direct ELISA***

The results of the crossreactivity experiments are summarized in Table V.4. Of the six anti-PAO peptide antisera that bound to PAO pili, five of these crossreacted with PAK pili. Likewise, of the seven anti-PAK peptide antisera that bound to PAK pili, four of these crossreacted with PAO pili. The crossreactivities were observed in similar regions, i.e., the N-terminal half of the pilin molecule (residues 22-33, 41-49 and 58-70) and in the C-terminal region (residues 128-144) which contains the disulfide bond. As expected, anti-PAX 22-33 and anti-PAX 41-49 bound to both PAK and PAO pili, due to sequence homology between the two strains. Surprisingly, both the anti-PAK and anti-PAO 58-70

TABLE V.3. Antigenicities of corresponding peptide regions of PAK and PAO pilins when reacted against their respective homologous whole pilus antisera.

| PAK peptide | Antigenicity <sup>a</sup>     | PAO peptide | Antigenicity                 |
|-------------|-------------------------------|-------------|------------------------------|
| 22 - 33     | -                             | 22 - 33     | + (4.0 x 10 <sup>-4</sup> )  |
| 41 - 49     | ++ (1.3 x 10 <sup>-5</sup> )  | 41 - 49     | + (2.3 x 10 <sup>-4</sup> )  |
| 58 - 70     | + (4.0 x 10 <sup>-5</sup> )   | 58 - 70     | + (5.2 x 10 <sup>-4</sup> )  |
| 74 - 83     | +++ (2.8 x 10 <sup>-6</sup> ) | 75 - 84     | + (9.2 x 10 <sup>-4</sup> )  |
| 88 - 97     | -                             | 88 - 97     | - (3.0 x 10 <sup>-2</sup> )  |
| 105 - 114   | ++ (2.0 x 10 <sup>-5</sup> )  | 105 - 114   | + (4.3 x 10 <sup>-4</sup> )  |
| 117 - 125   | + (2.7 x 10 <sup>-3</sup> )   | 117 - 125   | + (4.3 x 10 <sup>-4</sup> )  |
| 128 - 144   | ++ (4.3 x 10 <sup>-5</sup> )  | 128 - 144   | ++ (4.2 x 10 <sup>-5</sup> ) |

a) The (-) symbol represents end-point titers of 10<sup>-2</sup> or the absence of binding of peptide to antisera; the (+) symbols denote progressively higher end-point titers and stronger binding. The antigenicities of the peptides were determined using direct ELISA, where the wells of the microplate were coated with the respective BSA peptide conjugates and reacted with antisera raised against whole pili.



TABLE V.4. Crossreactivities of anti-PAK and anti-PAO antipeptide antisera with heterologous pili from PAK and PAO strains in direct ELISA.

| Anti-PAK Peptide Antisera | Crossreactivities with PAO Pili | Anti-PAO Peptide Antisera | Crossreactivities with PAK Pili |
|---------------------------|---------------------------------|---------------------------|---------------------------------|
| 22 - 33                   | + ( $1.1 \times 10^{-3}$ )      | 22 - 33                   | + ( $2.9 \times 10^{-3}$ )      |
| 41 - 49                   | + ( $1.4 \times 10^{-3}$ )      | 41 - 49                   | + ( $1.4 \times 10^{-3}$ )      |
| 58 - 70                   | ++ ( $1.7 \times 10^{-4}$ )     | 58 - 70                   | ++ ( $5.3 \times 10^{-4}$ )     |
| 74 - 83                   | -* ( $\sim 10^{-2}$ )           | 75 - 84                   | + ( $2.0 \times 10^{-3}$ )      |
| 88 - 97                   | -                               | 88 - 97                   | - ( $\sim 10^{-2}$ )            |
| 105 - 114                 | -                               | 105 - 114                 | -*                              |
| 117 - 125                 | -                               | 117 - 125                 | -* ( $\sim 10^{-2}$ )           |
| 128 - 144                 | +++ ( $2.5 \times 10^{-5}$ )    | 128 - 144                 | ++ ( $2.4 \times 10^{-4}$ )     |

The (-) symbol represents end-point titers of  $10^{-2}$  or the absence of binding of antipeptide antisera; the number of (+) symbols denote progressively higher end-point titers and stronger binding; (\*) these antipeptide antisera did not bind to homologous or heterologous pili.

antisera gave rise to unexpected crossreactivities, even though little sequence homology was observed in the aligned protein sequences of the two pilin proteins [only one of thirteen residues was identical (panel A, Figure V.3)]. To account for this crossreactivity, the possible sequence homology between residues 58-70 with the complete sequence of the heterologous variant protein was searched and the data is presented in Figure V.3 (panels B and C). Two tripeptide sequences of PAK 58-70 were found to be identical to regions of the PAO pilin sequence; residues 61-63 (T-G-T) and 66-68 (A-T-K) of PAK pilin share homology with residues 104-106 and 112-114 of PAO pilin (panel B, Figure V.3). These two regions are in close proximity to each other and could account for the ability of anti-PAK 58-70 to crossreact with PAO pili. The PAK 58-70 region also shared some homology with residues 61-73 and 71-84 of the PAO pilin. These homologies involved five identical residues out of a stretch of thirteen residues. The homology between the PAK 58-70 and PAO 61-73 regions was obtained by shifting the sequence by only 3 residues. The other two possible homologies (between PAK 58-70 and PAO 71-84, and between PAK 58-70 and PAO 101-116) involved insertions of amino acid spaces to achieve maximum sequence homology. The latter would suggest that crossreactivities result from critical residues being brought into close contact with each other via folding of the polypeptide backbone to give rise to a discontinuous epitope.

A homology search of the PAO 58-70 region with the complete PAK pilin sequence was also carried out. The PAO 58-70 region showed sequence homology with PAK 55-67 following a shift of 3 residues [five identical residues out of thirteen (panel C, Figure V.3)]. This homology is the same as that observed between the PAK 58-70 with the PAO 61-73 regions (Panel B, Figure V.3). A second region of homology was observed between the PAO 58-70 and the PAK 10-21 regions. Maximum sequence homology was observed between PAO 58-70 and PAK 111-123 (six identical residues out of thirteen, panel C, Figure V.3).

A. Aligned sequences of PAK and PAO pilin based upon overall protein homology

```

PAK 58-70      K-S-G-T-G-T-E-D-A-T-K-K-E-NH2
PAO 58-70      S-K-I-K-I-G-T-T-A-S-T-A-T
  
```

B. Regions of homologies between PAK 58-70 and the PAO pilin protein

```

PAK 58-70      K-S-G-T-G-T-E-D-A-T-K-K-E-NH2
PAO 61-73      K-I-G-T-T-A-S-T-A-T-E-T-Y

PAK 58-70      K-S-G-T-G-T-E-D-A-T-K-K-E-NH2
PAO 71-84      E-T-Y-V-G-V-E-P-D-A-N-K-L-G

PAK 58-70      K-S-G-T-G-T-.....E-D-A-T-K-K-E-NH2
PAO 101-116    T-F-Q-T-G-T-S-S-P-K-N-A-T-K-V-I
  
```

C. Regions of homologies between PAO 58-70 and the PAK pilin protein.

```

PAO 58-70      S-K-I-K-I-G-T-T-A-S-T-A-T-NH2
PAK 55-67      W-S-V-K-S-G-T-G-T-E-D-A-T

PAO 58-70      S-K-I-K-I-G-T-T-A-S-T-A-T-NH2
PAK 10-21      V-A-I-I-G-I-L-A-A-I-A-I

PAO 58-70      S-K-I-K-I-G-T-T-A-S-T-A-T-NH2
PAK 111-123    N-K-G-K-I-I-T-L-T-R-T-A-A
  
```

D. Regions of homologies between PAK 105-114 and the PAO pilin.

```

PAK 105-114    G-G-A-G-P-K-N-K-G-K-NH2
PAO 54-63      G-I-A-G-S-K-I-K-I-G

PAK 105-114    G-G-A-G-P-K-N-K-G-K-NH2
PAO 105-114    G-T-S-S-P-K-N-A-T-K
  
```

E. Regions of homologies between PAK 117-125 and the PAO pilin.

```

PAK 117-125    T-L-T-R-T-A-A-D-G-NH2
PAO 117-125    T-L-N-R-T-A-D-G-V
  
```

Figure V.3. Can sequence homologies explain crossreactivities? Sequence homology to residues 58-70 of PAK was examined in other regions of the heterologous PAO pilin (internal homologies) and for homology in the protein sequence of with PAO 58-70, PAK 105-114 (external homologies). A similar search was carried out using a commercially available program, Sequence Search (Synthetic Peptide Inc., University of Alberta, Edmonton, Canada). The program searches for short peptide homologies ranging from 25-100% to percent to any selected proteins. \* represent insertions of residues to maximize homology.

In addition, anti-PAO 75-84 was also able to bind to the PAK pili. However, anti-PAK 75-84 did not bind to PAK pili, nor was it able to crossreact to PAO pili. The surface profile plot (Figure V.1) showed that this region of the PAO pilin has a much higher surface potential than the corresponding PAK pilin. The two amino acid substitutions of Ala-Ala (PAK 76-77) to Glu-Pro in PAO seemed to have a pronounced effect on the surface accessibility of this region. The Glu substitution has the effect of increasing the hydrophilicity and the Pro substitution might enhance the accessibility of this region. Obviously, sequence homology cannot guarantee crossreactivity. Anti-PAK 105-114 and anti-PAK 117-125 failed to crossreact with PAO pili (Table V.4), even though these regions have 50-55% identity (Panels D and E, Figure V.3).

Regions that gave rise to strain-specific antibodies were PAK 88-97, 105-144 and 117-125 and PAO 88-97 (Table V.4). The region of residues 88-97 was expected to give rise to strain-specific antibodies, due to the lack of sequence homology between two pilins (2 residues of identity out of 10, Figure V.2). A search for maximum homology of the region encompassing residues 88-97 with heterologous pilin sequences only showed homology for a short tripeptide sequence (an A-D-G sequence in PAK 92-94 and PAO 122-124 and a G-A-G sequence in PAO 94-96 and PAK 106-108). It seems reasonable that a minimum number of identical residues is required for crossreactivity; and 2 or 3 residues of identity are not sufficient to create crossreactivity. The results suggested that a simple comparison of aligned protein sequences of different pilin strains would not necessarily give an indication for the production of crossreactive antibodies or strain-specific antibodies. A careful search of the region of interest with the sequence of the whole crossreacting protein is necessary to predict potential crossreactivity.

### C. Discussion

In order to evaluate the possible similarities and differences in the surface regions of PAK and PAO pili, predicted surface profiles were first examined as shown in Figure V.1. The prediction algorithms were based on hydrophilicity, accessibility and mobility parameters. The use of a combination of three parameters instead of a single parameter has been shown to produce better predictions of surface antigenic sites (Lee *et al.*, 1989; Parker *et al.*, 1986; Strynadka *et al.*, 1988). The PAK and PAO pilin molecules share approximately 49% homology between their amino acid sequences (Sastry *et al.*, 1985). The composite surface profile plots of both PAK and PAO pilins, revealed very similar profiles, and eight potential surface regions were predicted. In fact, analyses of a number of pilins from *P. aeruginosa* strains (CD4, P1 and K122-4) have also predicted eight overlapping potential surface regions (Pasloske *et al.*, 1988), with regions 3, 5, 6 and 8 showing the highest predicted surface potentials. Secondary structure predictions, reported by Paranchych and coworkers (Paranchych, 1989; Sastry *et al.*, 1985), did not reveal significant differences between the PAK and PAO pilins. Watts *et al.* (1983) reported that PAO and PAK pilins have identical circular dichroic spectra with 47%  $\alpha$ -helical content. The pilus is composed of pilin molecules joined together through subunit-subunit interactions in a helical fashion (Folkhard *et al.*, 1981; Watts *et al.*, 1983a). Thus, not all the predicted surface regions on the pilin subunit would be expected to be exposed after assembly of the pilin subunits in the pilus.

Peptides corresponding to the *Pseudomonas* pilin sequence were synthesized, covering 56% (81 of 144 residues) of the whole pilin molecule. Of the regions with highest surface potential regions 3, 5, 6 and 8 for PAK pilin, and regions 5, 6 and 8 for PAO pilin, anti-peptide antibodies directed against region 8 (residues 128-144) had the highest antibody titers in both instances. The region of residues 128-144 of both PAK and PAO pilins, have two cysteine residues which form a disulfide loop in the native molecule. The presence of a disulfide bond in the peptide could have given rise to a more stable

conformation which might resemble the native structure in the protein. This stabilization could result in the generation of antibodies with a higher affinity for the protein molecule. Examples of the use of such looped peptides to produce anti-peptide antibodies to lysozyme, hepatitis-B surface antigen and human chorionic gonadotropin have been demonstrated (Arnon *et al.*, 1971; Dressman *et al.*, 1984; Stevens *et al.*, 1986). Interestingly, immunization with the reduced form of this peptide also gave rise to good antibody titers, as shown by the PAK pilin study. However, it was possible that the peptide may have reoxidized during immunization, since its free sulfhydryl groups were not alkylated. An antiserum raised against an analog of this peptide with the cysteine-129 substituted by an alanine residue bound weakly to PAK pili in direct ELISA even though high antibody titers were obtained (Table IV.1, Chapter IV). This suggested that the disulfide bridge might be important in raising anti-peptide antibodies that bind to the native protein in this region (see Chapter IV). Antibodies raised against a short synthetic peptide, corresponding to the last eight residues of the C-terminal end of the PAK pilin (residues 137-144), also gave rise to high antibody titers, but bound poorly to the PAK pili. The linear peptide sequence can be very immunogenic but these antibodies may not be able to recognize the corresponding region in the protein molecule. The exposure of this region on pili seems to be important in the adhesion of *P. aeruginosa* to epithelial cells (see Chapter VI).

Anti-PAK 128-144 have been shown to crossreact with PAO pili (see Chapter IV). In this study, it was shown that anti-PAO 128-144 was also able to crossreact very well with PAK pili. This region of pilin is semi-conserved (nine of seventeen amino acids) and the disulfide bridge may induce a structural configuration to enable good recognition by heterologous anti-peptide antibodies. Alternatively, the anti-peptide antibodies were simply recognizing some of the conserved amino acid residues. Due to some sequence homology, it is not unusual to observe crossreactivity when an antiserum raised against a synthetic peptide is assayed against another variant of the same protein. Recently, it was demonstrated that antibodies raised against a peptide corresponding to a region of the A-

subunit of pertussis toxin was able to bind to the A-subunit of cholera toxin because of some sequence homology (seven of twelve amino acid residues) between the two proteins (Burns *et al.*, 1987). Detection of crossreactivity between tetanus and botulinum toxins by an antipeptide antibody has also been reported (Halpern *et al.*, 1989).

The binding of whole pilus PAK and PAO antiserum to the synthetic peptides was assayed using direct ELISA with the BSA-peptide conjugates (Table V.3). Anti-PAO pilus antiserum bound to seven of eight synthetic peptides, while anti-PAK pilus antiserum bound to six of eight synthetic peptides. The region of residues 88-97 failed to bind either antisera. Interestingly, it is to this same region that antipeptide antibodies provided strain specificity. Although antibodies raised against the whole protein generally recognize conformational epitopes, these results clearly show that the linear sequences in the native pilin molecule are immunogenic. These results are in contrast with those of Lerner and coworkers (Green *et al.*, 1982) who found that antibodies to the intact influenza virus hemagglutinin did not react with any of 20 synthetic peptides corresponding to amino acid sequences of hemagglutinin. Yet, antipeptide antibodies to 18 of these 20 peptides were able to react with hemagglutinin. As suggested by Lerner (1982), peptide immunization can generate antibody specificity (both crossreactive and strain-specific) that cannot be obtained in other ways.

The major antigenic determinant of the PAK pilin has been reported to be a conformational epitope situated between the region encompassing 82-110 (Watts *et al.*, 1983). This region of the molecule is also believed to be the T-cell recognition site (Smart *et al.*, 1988). Isolated T-cell clones that bind to PAK pili failed to recognize the synthetic PAK 88-97 peptide (B. Singh, K.K. Lee and R.S. Hodges, unpublished data). This suggested that the major immunogenic determinant consists of more than these 11 amino acid residues, and that a longer peptide is needed for binding. Two other peptides, PAK 100-110 and 92-110, which were synthesized also failed to be recognized by these T-cell clones (B. Singh, K.K. Lee and R.S. Hodges, unpublished data). The anti-PAK pilus

antiserum bound very well to the PAK 137-144 peptide but the anti-PAK 137-144 antipeptide antiserum bound poorly to the PAK pili. In the case of the anti-PAK 74-83 antipeptide antiserum, the binding was hardly detectable (better binding could be obtained if the antiserum was first concentrated). These two peptides could have assumed conformations which were quite different from the conformation on the pilin molecule. This emphasizes the importance of the method of peptide presentation to the immune system. The peptide must be presented in a manner to mimic its conformation in the native protein. Failure of antipeptide antiserum to recognize the native protein cannot be interpreted that the region is not surface exposed. The combination of antipeptide antisera and the anti-PAK pilus antiserum results verified the success of Surfaceplot in that all regions predicted to be on the surface were found to be exposed on native pili.

In conclusion, the results of these studies have pointed to the complexity of the immune system and the difficulty of predicting regions of a protein molecule which could give rise to strain-specific and crossreactive antibodies. An explanation for crossreactivity or specificity in the presence of reasonable sequence homology remains an important area of investigation to be solved in molecular immunology. These results also suggested the possibility of raising strain-specific antipeptide antisera which could be useful in diagnosing the *P. aeruginosa* strains involved in an infection, and of raising crossreactive antisera which may be useful in synthetic vaccine development. We have also demonstrated the importance of the disulfide-bridged region of PAK pilin in the pilus-mediated adherence of *P. aeruginosa* to BECs (Chapter VI). The 128-144 peptide, encompassing the C-terminal disulfide loop, is highly immunogenic when coupled to a carrier protein, and should present itself as a good candidate for raising crossreactive antiserum to block *Pseudomonas* adherence.



## Chapter VI. Investigation of the Cell-Surface Binding Domain of *P. aeruginosa* PAK Pilus

### A. Introduction

The NMePhe pilus of *P. aeruginosa* consists of a polymer of a thousand or more single subunits arranged in a helical fashion. There has been no firm evidence of other proteins associated with the pilus. This is very different from type 1, Pap and S pili, where other proteins have been shown to be associated with the pilus (Abraham *et al.*, 1987; Hanson and Brinton, 1988; Lindberg *et al.*, 1987; Maurer and Orndoff, 1987; Schmoll *et al.*, 1989). The adhesin, a molecule responsible for conferring the binding ability to the pilus, is one of these minor proteins. In the Pap pilus, the papG molecule is the adhesin and it is associated with at least two other proteins, papE and papF, at the tip of the pilus (Lund *et al.*, 1988). In the absence of other minor proteins associated with the NMePhe pilus of *P. aeruginosa*, it might be possible to delineate a region of the pilin molecule which confers the adhesion property to the pilus.

In order to elucidate the cell-binding domain of *P. aeruginosa* pilus, anti-peptide antibodies were raised to peptides corresponding to predicted surface regions of PAK pilin. The anti-peptide antibodies that bind to a particular sequence that contains part of the binding domain or is located near the binding domain should block the pilus from adhering to cell surface receptors either directly or indirectly (sterically). In addition, the synthetic peptides were used to probe directly for the receptor-binding domain of the pilus. One previous piece of evidence that suggested that the C-terminal portion of the PAK pilin was important for binding to cell-surface receptors came from the studies of Paranchych *et al.* (1985). They showed that a PAK fragment, corresponding to residues 121-144, inhibited the binding of PAK pili to BECs. This finding has now been extended with studies employing synthetic peptides which correspond to the C-terminal region of the PAK pilin.

## B. Results

### 1. *The effects of polyclonal anti-peptide antibodies on PAK pili binding to human buccal ...epithelial cells*

The antibodies raised against peptides corresponding to different regions of the PAK pilin were assayed for their abilities to bind to PAK pili, and also to examine their effects on pili binding to BECs. The results are summarized in Table VI.1. When Fab fragments generated from anti-peptide antibodies were incubated with pili prior to their addition to BECs, only antibodies raised against the C-terminal disulfide loop region were able to inhibit the adherence of PAK pili to BECs (Table VI.1 and Figure VI.1). All four antisera raised against PAK 128-144 peptides (reduced and oxidized) reduced the binding of PAK pili to BEC by 36 - 72% of that of the control (which consisted of pre-immune Fab fragments from one of the rabbits used for immunization). A murine monoclonal antibody, PK99H, directed against the C-terminal region of PAK pilin which served as a positive control, was also effective in reducing the adherence of PAK pili to BECs to 64% of the control. In addition, an anti-peptide antiserum raised against a shortened peptide of the C-terminal end (137-144) also provided about 64% inhibition of pili binding to BECs. Anti-PAK 117-125 failed to inhibit binding even though this region is adjacent to the disulfide bridge. Interestingly, an antiserum raised against an analog of the PAK 128-144 peptide, where cysteine-129 was replaced by an alanine residue, was also able to inhibit PAK pili binding by 47% of the control. These results are more easily visualized in Figure VI.1. Anti-peptide antibodies raised to regions at the N-terminal and the hypervariable central portion of PAK pilin failed to inhibit pili binding to these BECs. Only those antibodies directed against the C-terminal disulfide-bridged region were able to block the adhesion of pili to cell surface receptors.

| Peptides to which Fab<br>fragments were generated | % PAK pili Binding to BECs |
|---|----------------------------|
| 22-33   | 100.0 ± 2.5                |
| 34-40   | 82.1 ± 20.3                |
| 41-49   | 94.8 ± 8.9                 |
| 58-70   | 97.3 ± 4.6                 |
| 74-83   | 100.5 ± 8.5                |
| 88-97   | 101.5 ± 8.7                |
| 105-114   | 93.4 ± 18.9                |
| 117-125   | 99.5 ± 1.5                 |
| 128-144 R1  | 72.0 ± 4.9                 |
| 128-144 R2  | 62.3 ± 0.1                 |
| 128-144 O1  | 70.6 ± 2.5                 |
| 128-144 O2  | 35.7 ± 7.6                 |
| 137-144   | 36.4 ± 3.0                 |
| 128/A-129*  | 53.3 ± 0.5                 |
| PK99H   | 64.6 ± 2.5                 |
| Preimmune   | 100.0 ± 13.9               |
| Control   | 92.7 ± 11.3                |

TABLE VI.1. The effect of anti-peptide Fab fragments on the binding of PAK pili to human buccal epithelial cells (BECs). The preimmune Fab obtained from one of the rabbits used for immunization served as a negative control. PK99H is an anti-PAK pilin monoclonal antibody. All Fabs were diluted such that their final titer as measured by ELISA to PAK pili was  $10^3$ . The data represents the average of three independent sets of experiments. \* 128/A-129 is the peptide 128-144 with cysteine-129 replaced by an alanine residue.

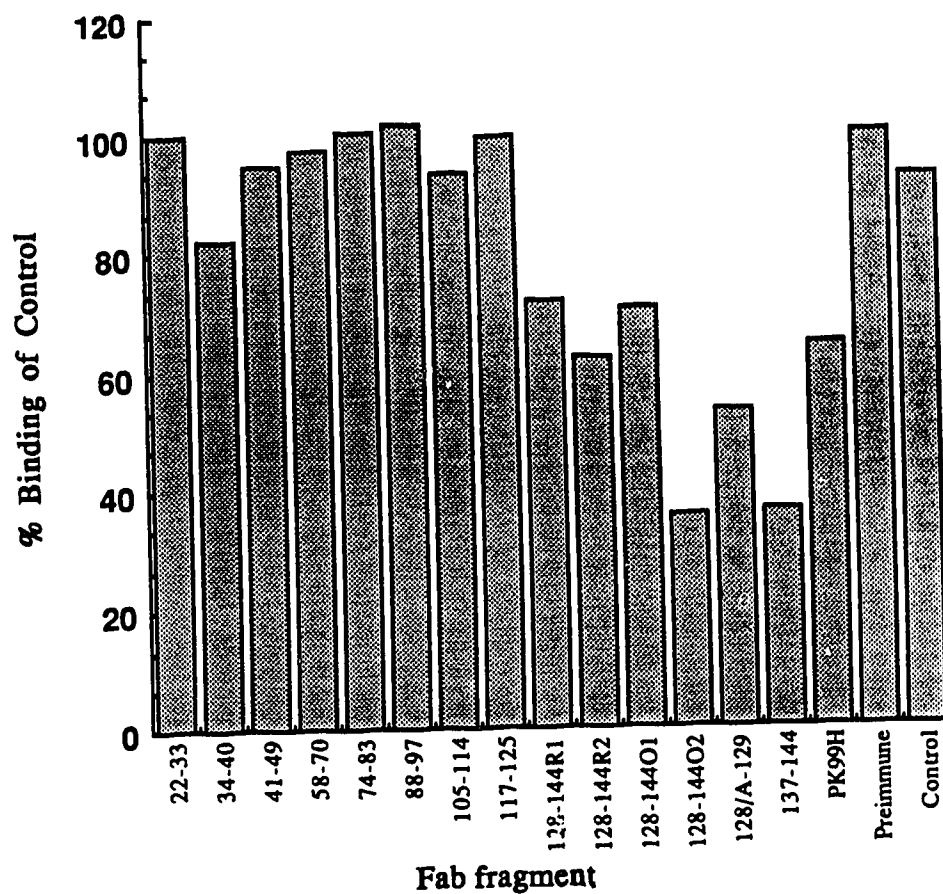


Figure VI.1. Inhibition of PAK pili binding to human buccal epithelial cells (BECs) by Fab fragments generated from anti-peptide antibodies. The binding of PAK pili is represented as a percentage of the control, in which no Fab fragments were present in the assay.

## 2. *The effects of murine monoclonal antibodies raised against PAK pili on pili binding to ...human buccal epithelial cells*

Four monoclonal antibodies raised against PAK pili (PK3B, PK34C, PK41C and PK99H), determined to be of the immunoglobulin G class, have been characterized for these studies (Doig *et al.*, 1990). The apparent association constants of these MAbs were determined by competitive ELISA and are summarized in Table VI.2. The assays were carried out with whole pili, fragments of the PAK pilin, or with synthetic peptides. PK41C did not bind to any of the PAK pilin fragments generated by chymotryptic digestion. It bound to PAK pili and crossreacted with the PAO pili. PK3B also failed to bind to any of these fragments. It specifically bound PAK pili but did not bind PAO pili. PK99H failed to bind to the PAK 31-53 and PAK 54-120 fragments. However, PK99H had a high affinity for the 121-144 chymotryptic fragment. This 121-144 fragment contained the disulfide bridge. Interestingly, PK99H was able to bind both the reduced and oxidized synthetic PAK 128-144 peptides. Furthermore, PK99H also bound to a short linear sequence at the extreme end of the C-terminal (residues 137-144). The peptide sequence prior to the disulfide bridge, residues 117-125, failed to interact strongly enough to allow the measurement of its binding affinity to PK99H. PK99H showed specificity for PAK pili only. PK34C bound strongly to the 121-144 fragment with an apparent association constant of  $5.9 \times 10^7 \text{ M}^{-1}$ . In contrast to PK99H, the short peptide of residues 137-144 was not bound by PK34C. PK34C only interacted with the PAK 128-144 peptide when it was oxidized suggesting the importance of the disulfide loop in forming the epitope for this particular antibody. In addition to the disulfide loop, part of the epitope of PK34C consists of some of the residues located prior to the disulfide bridge because the PAK 117-125 peptide also had an equally high affinity for the antibody, as evident by the apparent association constant. Another dissimilarity between PK34C and PK99H was that PK34C bound both PAK and PAO pili.

TABLE VI.2. Apparent association constants of PAK pili monoclonal antibodies to the PAK pilin fragments and to PAK and PAO pili determined from competitive ELISA data as described by Nieto *et al.* (1984).

| Fragment<br>PAK Pilin | PK99H                            | PK34C                            | PK3B     | PK41C     |
|-----------------------|----------------------------------|----------------------------------|----------|-----------|
| 1 - 30*               | ND                               | ND                               | ND       | ND        |
| 31 - 53*              | NE                               | NE                               | NE       | NE        |
| 54 - 120*             | NE                               | NE                               | NE       | NE        |
| 121 - 144*            | $9.9 \times 10^6 \text{ M}^{-1}$ | $5.9 \times 10^7 \text{ M}^{-1}$ | NE       | NE        |
| 117 - 125             | NE                               | $7.5 \times 10^5 \text{ M}^{-1}$ | ND       | ND        |
| 128 - 144 (reduced)   | $1.0 \times 10^8 \text{ M}^{-1}$ | NE                               | ND       | ND        |
| 128 - 144 (oxidized)  | $3.4 \times 10^7 \text{ M}^{-1}$ | $7.6 \times 10^5 \text{ M}^{-1}$ | ND       | ND        |
| 137-144               | $2.4 \times 10^6 \text{ M}^{-1}$ | NE                               | ND       | ND        |
| PAK pili              | 300 ml/g <sup>a</sup>            | 380 ml/g                         | 100 ml/g | 1000 ml/g |
| PAO pili              | NE                               | 5.6 ml/g                         | NE       | 6.1 ml/g  |

\* Chymotryptic fragments of PAK pilin.

a - affinity constants for MAb binding to purified pili are expressed in ml/g rather than as molar affinity constant because of the polydispersed size distribution of purified pili.

ND - not done

NE - no effect

The effects of the four monoclonal antibodies on the binding of *P. aeruginosa* to BECs were assayed. Both the PK41C and PK3B had no effect on the binding of PAK pili to BECs. The epitope of the PK41C appears to be located in the N-terminal of the PAK pilin, since both the PAK 1-30 fragment and the synthetic PAK 22-33 peptide were bound by this MAb (Doig *et al.*, 1990). PK3B failed to react with any of the PAK pilin fragments or synthetic peptides. The epitope may be a conformational epitope consisting of various parts of the pilin molecule brought together when the protein is folded (Doig *et al.* 1990).

Unlike PK3B and PK41C, both PK99H and PK34C were able to inhibit bacterial whole cell binding to BECs, and the data is presented in Table VI.3. In the data shown in Table VI.3, a solution of the Fab fragment of 100 mg/ml concentration and a ratio of bacteria to BECs between 1000:1 to 1500:1 were chosen, such that a significant level of inhibition could be assessed with a minimal amount of Fab needed in the assay mixture. Hence, a maximal inhibition of binding would not be expected (the percent inhibition is given in the parenthesis in Table VI.3). PK99H was only effective in blocking strain PAK, and to a small extent strain 492c. PK34C inhibited all pilus-producing *P. aeruginosa* strains to varying degrees. Normal mouse IgG had no effect on *P. aeruginosa* binding to BECs.

### 3. The ability of AcPAK 128-144 to mimic the PAK binding to cell surface receptors

The studies of Doig *et al.* (1988) have shown that the PAK whole cells bound to a single class of receptors on BECs and TECs (tracheal epithelial cells). These workers have also shown that purified PAK pili bound to BECs in a concentration-dependent manner. In addition, both PAK pili and anti-PAK pilus Fab fragments inhibited bacterial whole cell binding to BECs. A competitive inhibition pattern of the bacterial whole cell binding to BECs by PAK pili was indicative that both, bacterium and pili, bound to the same receptors on the cell surfaces. To delineate the region of PAK pilin responsible for this receptor-binding domain, a number of fragments of the PAK pilin and synthetic peptides were

TABLE VI.3. Effect of Fab fragment of MAbs PK99H and PK34C on the binding of *P. aeruginosa* to BECs

| Strain | Bacteria bound/BEC <sup>a</sup> |                                |                                |
|--------|---------------------------------|--------------------------------|--------------------------------|
|        | Control <sup>a</sup>            | PK99H                          | PK34C                          |
| PAK    | 35.2 ± 1.4                      | 25.6 (72.7) ± 1.0 <sup>c</sup> | 23.8 (67.5) ± 1.7 <sup>c</sup> |
| PAO    | 50.5 ± 2.0                      | 55.5 (110) ± 11.1              | 45.9 (91) ± 0.7 <sup>c</sup>   |
| HD1    | 38.0 ± 3.6                      | 31.0 (81.6) ± 3.5              | 31.3 (82.5) ± 1.1 <sup>c</sup> |
| 492c   | 30.9 ± 0.2                      | 23.8 (77.1) ± 0.5 <sup>c</sup> | 26.2 (84.8) ± 1.4 <sup>c</sup> |
| P1     | 36.3 ± 2.5                      | 34.7 (95.6) ± 5.9              | 29.5 (81.3) ± 0.2 <sup>c</sup> |
| K122-4 | 41.8 ± 1.5                      | 38.3 (91.8) ± 2.8              | 28.0 (67.1) ± 0.4 <sup>c</sup> |
| PAK/3  | 13.1 ± 1.4                      | 12.0 (91.9) ± 0.7              | 12.2 (93.3) ± 0.6              |

<sup>a</sup> The concentration of PK99H and PK34C Fab used in the inhibition assays was 100 µg/ml and had a titer of 10<sup>3</sup> by ELISA, using PAK pili as the antigen (coated at 1 µg per well). Given is the mean ± the standard deviation. The percent of control is given in parentheses.

<sup>b</sup> Control value when 100 µg of Fab fragments per ml produced from normal mouse IgG was added. No difference was noted between these values and those from tubes to which no Fab fragments were added.

<sup>c</sup> The significant difference ( $P < 0.05$ ) was determined by using the Student *t* test.



TABLE VI. 4. The effect of natural and synthetic peptide fragments of PAK pilin on the adherence of *Pseudomonas aeruginosa* PAK to BECs

| Fragment                          | Concentration ( $\mu\text{M}$ ) | Adhesion index<br>% of Control |
|-----------------------------------|---------------------------------|--------------------------------|
| PAK 121-144 <sup>a</sup>          | 25                              | 379 <sup>b</sup>               |
| PAK 54-120 <sup>a</sup>           | 25                              | 102                            |
| PAK 31-53 <sup>a</sup>            | 25                              | 110                            |
| PAK 134-144                       | 25                              | 104                            |
| PAK 116-144 reduced <sup>c</sup>  | 15 <sup>d</sup>                 | 287 <sup>e</sup>               |
| PAK 116-144 oxidized <sup>c</sup> | 15 <sup>d</sup>                 | 1060 <sup>e</sup>              |

a - chymotryptic fragments

b - determined at a ratio of 3061:1 (bacteria:BECs) and as direct competition assay

c - N<sup>α</sup>-acetylated synthetic peptides

d - the concentration of the peptides was normalized to an OD<sub>280</sub> of 0.183 (about 15  $\mu\text{M}$ )

e - determined at a ratio of 2240:1 (bacteria:BECs) and as a direct competition assay.

assessed for their abilities to inhibit bacterial whole cell binding to BECs. The results of these experiments are summarized in Table VI.4. The results are represented as a percentage of the control or adhesion index. The two PAK pilin fragments, residues 31-53 and 54-120, did not inhibit PAK binding to the epithelial cells. However, the fragment of residues 121-144 enhanced the binding by more than three fold. Synthetic peptides were used to extend further this result. The reduced PAK 116-144 peptide was also able to enhance PAK whole cell binding, as indicated by an approximate 3-fold increase in the adhesion index. However, the biggest increment in the enhancement of PAK whole cell binding to BECs (10-fold) was obtained when the disulfide bridge was restored to the PAK 116-144 peptide. The short PAK 137-144 peptide had no effect on the binding of bacteria to BECs.

Synthetic peptides, long enough to just cover the disulfide loop, were used to investigate the binding of the peptides to cell-surface receptors. Both the reduced and oxidized AcPAK 128-144 peptides were shown to bind to BECs in a concentration-dependent manner (Figure VI.2). Saturation of binding to BECs by the oxidized peptides was reached at about 30  $\mu\text{M}$ , but the reduced conformer did not reach a saturation point. The concentration at which the reduced and oxidized AcPAK 128-144 peptide occupy 50% of the receptor sites (apparent dissociation constant) was approximately 9.9  $\mu\text{M}$  and 6.40  $\mu\text{M}$ , respectively.

Inhibition assays were carried out with the synthetic AcPAK 128-144 peptides to assess their abilities to block PAK pili binding to BECs. Both the reduced and oxidized peptides were able to inhibit pili binding in preliminary studies. In subsequent experiments, the inhibition of PAK pili binding to BECs was assayed with a fixed concentration of the reduced AcPAK 128-144 peptides, together with varying concentrations of PAK pili. For each set of data points, different, but fixed concentrations of the reduced peptides were used. The nature of this inhibition was investigated using the reduced peptide because of the limited availability of the oxidized conformer. The binding

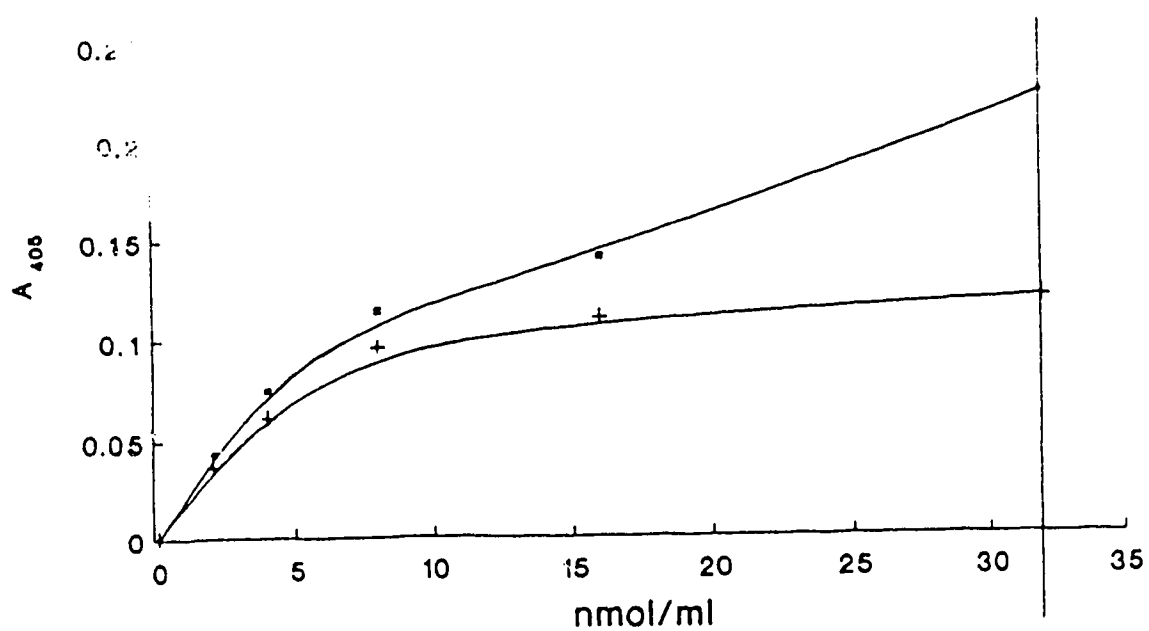


Figure VI.2. Binding of reduced (■) and oxidized (+) AcPAK 128-144 peptide to human BECs. Binding of the synthetic peptides to BECs was determined by a whole cell ELISA utilizing the monoclonal antibody, PK99H (which binds to reduced and oxidized AcPAK 128-144), to quantitate the amount of synthetic peptide bound to the surface of BECs.

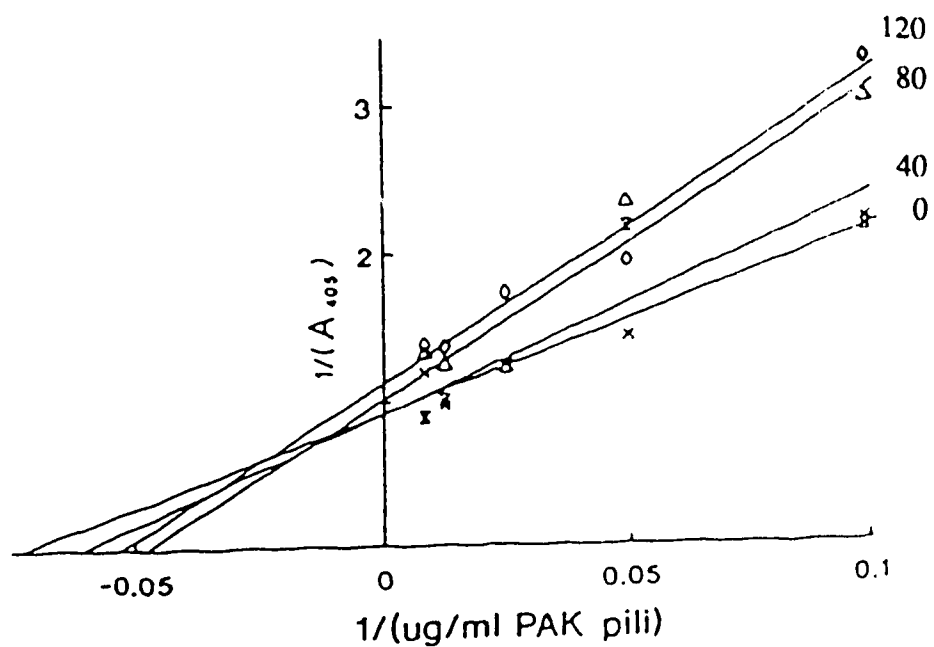


Figure VI.3. Modified Lineweaver-Burk plot of the binding of PAK pili to human BECs in the presence of 0 ( $\square$ ), 40 ( $\times$ ), 80 ( $\Delta$ ), and 120 ( $\circ$ ) nmole of peptide AcPAK 128-144 per ml.

assays were analyzed using modified Lineweaver-Burk plots, as shown in Figure VI.3. The variation of the maximum absorbance at 405 nm was relatively constant unlike the changes in the apparent association constants. This pattern of inhibition was similar to that of a competitive inhibition pattern.

#### 4. *Binding of alkaline phosphatase-peptide conjugate to BECs*

The successes of the synthetic peptide binding to cell surface receptors have led to the development of a more simple approach to assay this binding process. The synthetic peptide, PAK 121-144, was made with the benzoylbenzoyl photoreactive crosslinker and conjugated to a reporter molecule, alkaline phosphatase (AP). The binding of the AP-24mer to BECs is shown in Figure VI.4. The readings have been normalized to  $10^5$  BECs. The AP-24mer conjugate showed a concentration-dependent binding to the cells, and approached saturation at a concentration of about  $0.6 \mu\text{M}$ . Because of the limited availability of the conjugates, higher concentrations were not used. When the data was analyzed by transformation of the data into a double reciprocal plot, a straight line was obtained (Figure VI.5), suggesting a single binding site. From this data, an apparent dissociation constant of  $0.94 \mu\text{M}$  was obtained.

Interestingly, PAK pili, which had been coated onto the wells in the ELISA plates, were also bound by the AP-24mer conjugates. The binding data is shown in Figure VI.6. The AP-17mer was also able to bind to PAK pili but with a much lower  $A_{405}$  signal (data not shown). A control, using just the alkaline phosphatase alone, did not bind to the PAK pili. A double reciprocal analysis of the AP-24mer binding data (Figure VI.7) showed that the AP-24mer conjugate had an apparent association constant of  $0.24 \mu\text{M}$ . This ability of the synthetic peptides to interact with the pilus appears to mimic a kind of pilin-pilin interaction which may be involved in the assembly of homopolymeric pili. Such pilin-pilin interactions were also observed by Abraham and Beachey (1987), who found that a 13-

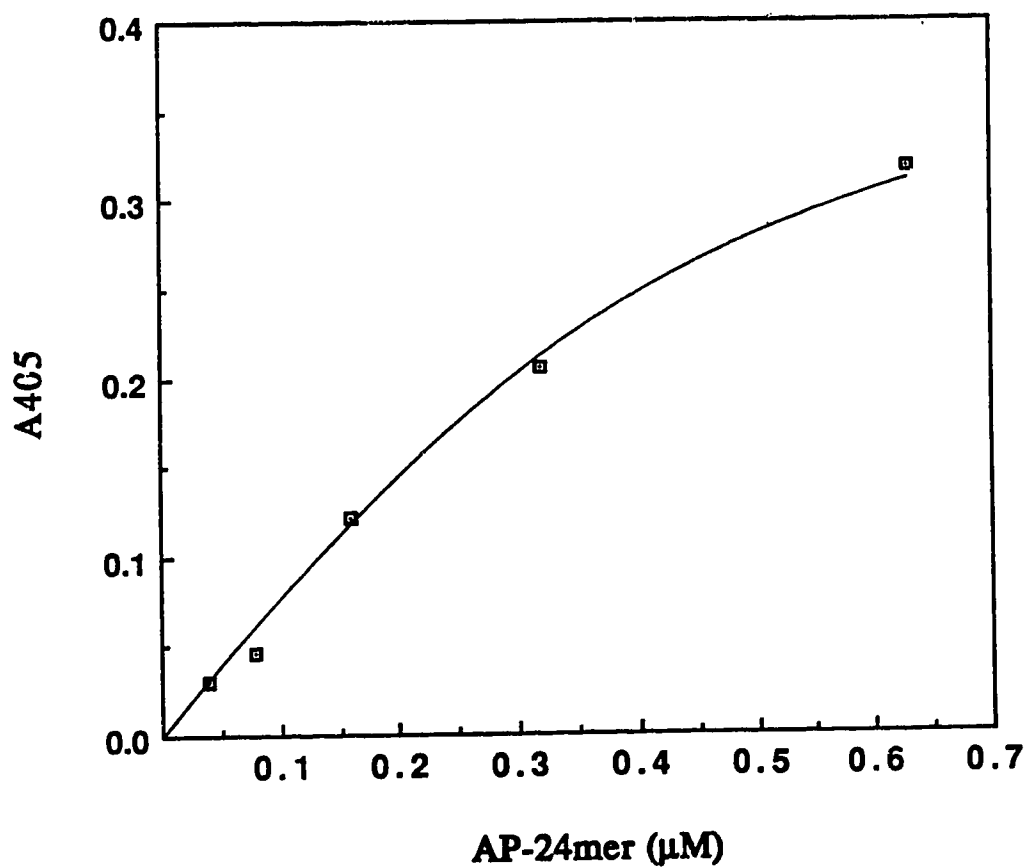


Figure VI.4. Binding of PAK 121-144 - alkaline phosphatase (AP-24mer) conjugate to BECs. These assays were carried out using an approach similar to whole cell ELISA, where varying concentrations of AP-24mer and the BECs were incubated at 37 °C. The A405 readings have been normalized to  $10^5$  BECs.

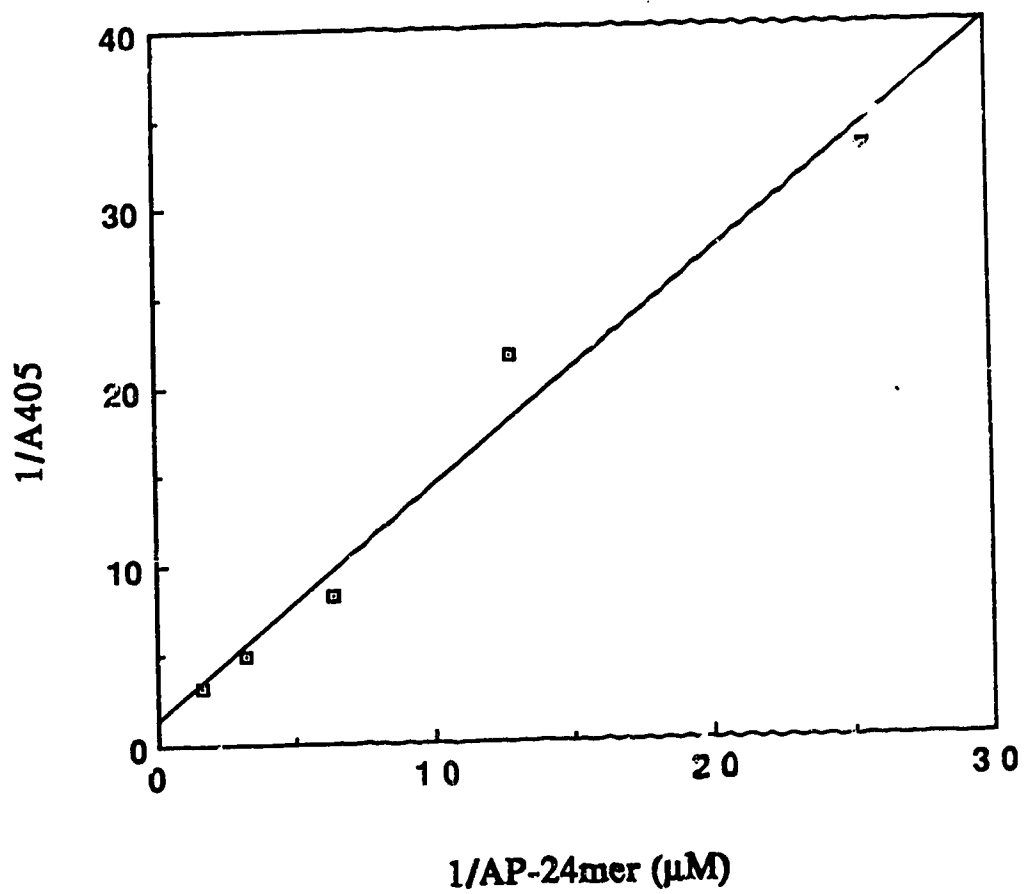


Figure VI.5. Double reciprocal plot of the binding data in Figure VI.4. The plot shows a straight line with a linear regression coefficient of 0.97.

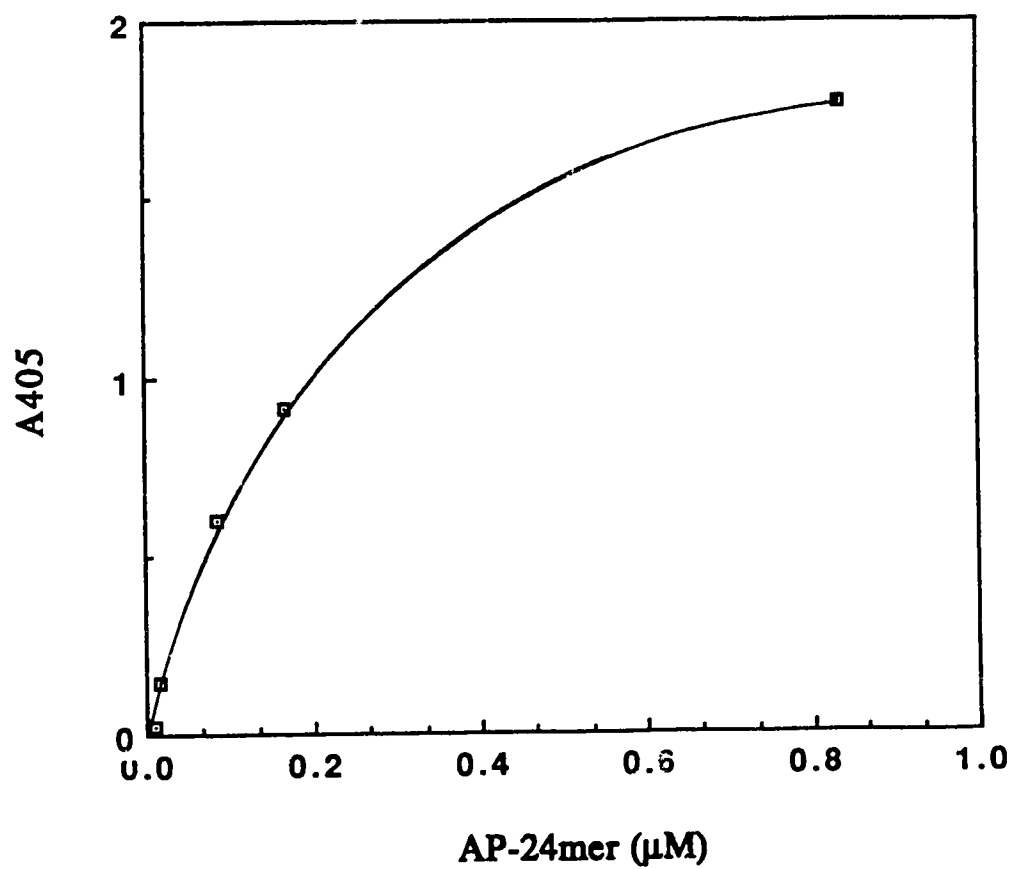


Figure VI.6. Binding of AP-24mer conjugate to PAK pili. The PAK pili were coated onto the wells in an ELISA plate and the conjugates were incubated at 37 °C for an hour with gentle agitation. Following several washes, 100 ul of p-nitrophenylphosphate (1mg/ml), were incubated for 30 min and the A405 readings were taken.



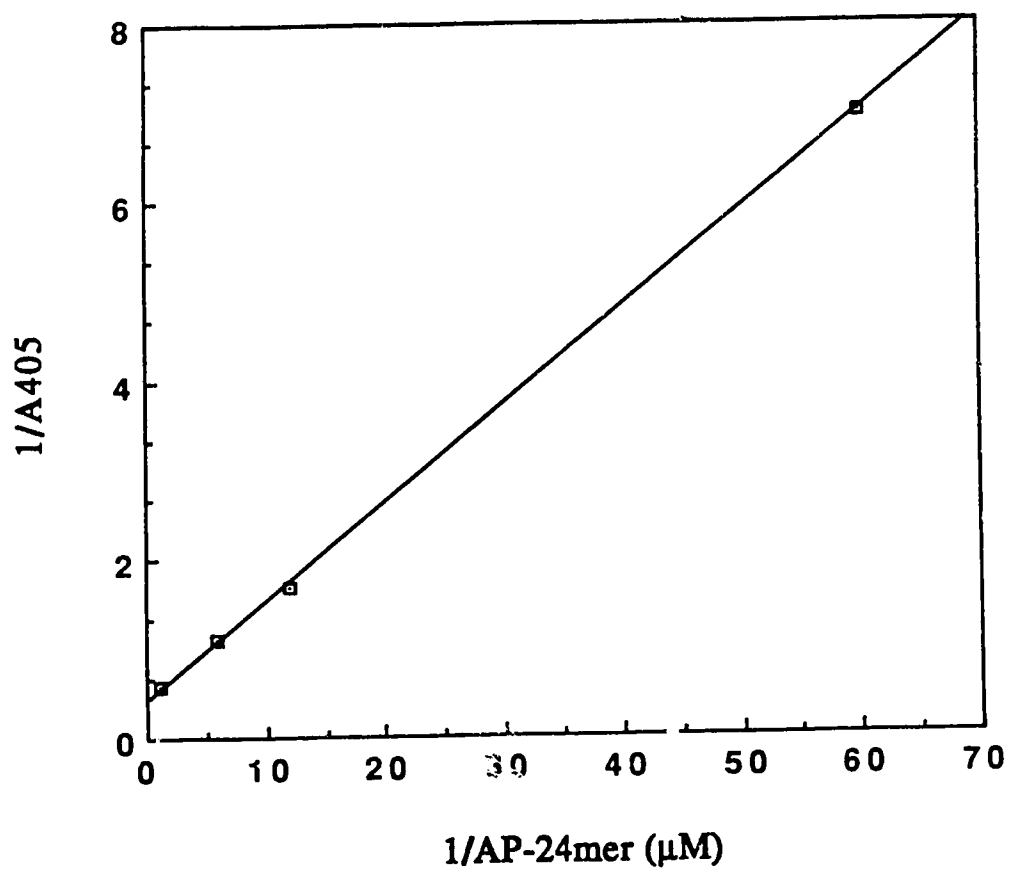


Figure VI.7. Double reciprocal plot of the binding data of Figure VI.6. The plot shows a linear line with a linear regression coefficient of 1.0.

residue synthetic peptide, corresponding to the N-terminal region of the type 1 fimbrial subunit of *E. coli*, was able to assemble into a fimbria-like structure which, when immunized in rabbits, generated antibodies which bound to type 1 fimbriae.

### C. Discussion

The experiments in the present studies were designed to delineate the region of PAK pilin containing a cell-surface receptor binding domain, since no other proteins are presently known to be associated with the NMePhe pilus of *P. aeruginosa*. The results of the anti-PAK peptide antibodies revealed the C-terminal disulfide-bridged region playing a role in the binding of PAK pilus to cell-surface receptors of the buccal epithelium. Antibodies directed against both the N-terminal and the central portion of PAK pilin have no inhibitory effect on PAK pili binding to BECs. Inhibition of PAK pili binding to BECs by Fab fragments generated from antipeptide antibodies showed that only those directed against the C-terminal disulfide loop region were able to block adhesion. Of the four Fabs directed against PAK 128-144, O2 antiserum provided the best inhibition. Fabs directed against a shorter C-terminal peptide, PAK 137-144, were also able to inhibit pili binding to BECs, even though the disulfide bridge was not present. The disulfide bridge did not seem to be required for generation of inhibitory antibodies (Fab fragments) because a cysteine to alanine substitution did not affect the inhibition of pili binding to BECs. Fabs directed against other regions of the pilin molecule (outside the C-terminal disulfide loop region) did not block the adherence of pili to BECs. These results suggested that the C-terminal region of PAK pilin (residues 128-144) forms the binding domain or part of the binding domain on the PAK pili.

This conclusion was supported by studies which showed that two monoclonal antibodies, directed against the C-terminal region of PAK pilin, were also able to block adherence. The PK41C monoclonal antibody, whose epitope is in the N-terminal region, failed to block *P. aeruginosa* binding to BECs. This was in agreement with the studies

with the polyclonal anti-peptide antibodies directed against the N-terminal of PAK pilin. The epitopes of the two inhibitory MAbs, PK99H and PK34C, are located at the C-terminal of the PAK pilin. The PK99H antibody was more specific than the PK34C in that PK99H only blocked PAK, and to a small degree 492c, whole cell binding to BECs. An unusual observation about PK99H was its high affinity for the reduced AcPAK 128-144 peptide even though the monoclonal antibodies were raised against native pili (with intact disulfide bridges). Two plausible explanations could account for the production of this hybridoma clone. The first explanation is that a small portion of the pilin monomers in the immunogen preparation possess cysteine residues which are in the reduced state. This small fraction of pilin monomers stimulated the production of the PK99H clone. The second explanation is that this clone was induced by pilin with oxidized cysteines since the PK99H also recognizes the oxidized AcPAK 128-144 peptides.

Earlier studies (Paranchych *et al.*, 1985) have also shown that a fragment of PAK pilin (121-144) was able to block the adherence of PAK pili to BECs. Even though the integrity of the disulfide bridge did not seem to be critical in generating anti-adhesion antibodies to PAK, it was previously shown that only the antibodies to oxidized AcPAK 128-144 were able to crossreact with PAO pili (see Chapter IV). The importance of the disulfide bridge was also illustrated by PK34C, which recognized a conformational epitope generated in part by an intact disulfide bond. The destruction of the disulfide loop also destroyed the epitope of the peptide for antibody recognition, which resulted in a loss of binding (Table VI.2). This antibody was able to block the binding of not only the PAK strain, but also the binding of all the *P. aeruginosa* strains tested. Thus, the integrity of the disulfide loop is very important in raising antibodies which are crossreactive with pili from other *P. aeruginosa* strains. The two cysteine residues on the C-terminal region are highly conserved in pilins from all *P. aeruginosa* strains. In addition, positions 131 (ser or thr), 137 (phe or tyr) and 139 (pro) are also highly conserved. The conservation of these residues within the disulfide-bridged region in the pilins of all *P. aeruginosa* strains

suggests a possible role these residues may play in maintaining a conformation conducive for receptor-binding function in the pilus. The exposure of the C-terminal disulfide-bridged region to the aqueous environment, and the importance of ser-131 in PAK pilin, were demonstrated by mutation of the PAK pilin gene (Pasloske, 1989). When ser-131 was mutated to gln-131, the binding of a PAK-specific phage, Pf (which attaches at the tip of the PAK pilus) was eliminated, suggesting the exposure of the C-terminal region at the tip of the PAK pilus.

The importance of the C-terminal region in the pilus-mediated adherence of *P. aeruginosa* was further illustrated by the binding of synthetic peptides to the cell surfaces of the buccal and tracheal epithelia. Both the reduced and oxidized AcPAK 128-144 peptides bound to the epithelial cells in a concentration-dependent manner, but only the oxidized peptides showed a saturable binding. Thus, a specific interaction was observed between the peptides and cell-surface receptors. These receptors appeared to be similar to the ones that are bound by PAK pili, because these peptides were able to compete with PAK pili for binding to BECs. This competitive inhibition demonstrated the occupation of the same sites on the cell surfaces.

It was interesting to note that in another study employing the AcPAK 116-144 peptide, an enhancement of bacterial whole cell binding to BECs was obtained. Studies by Paranchych *et al.* (1985) showed that the PAK 121-144 fragment inhibited binding of PAK to BECs. This discrepancy may be explained by the differences in the experimental conditions that were used in these studies. Previous studies by Paranchych *et al.* (1985) employed a low bacteria to BEC ratio and a high concentration of the peptide. In the present studies, a high bacteria to BEC ratio coupled with a low concentration of peptide were used and this allowed a better resolution of the pilus-receptor interaction. In order to reconcile these two differing observations, two interactions between the fragment and the receptor could be postulated since the PAK 121-144 peptide may consist of two predicted hydrophilic domains (regions 7 and 8 in Figure V.1, Chapter V; also see Sastry *et al.*,

1985): one of these interactions is a pilus-receptor interaction, and the other interaction is a pilin-pilin (subunit-subunit) interaction. A high concentration of the PAK 121-144 peptide used by Paranchych et al. (1985) may not have allowed for the resolution of the pilus-peptide (pilin-pilin) interaction thought to be observed in the present studies. The longer AcPAK 116-144 peptide completely covers the two hydrophilic domains of the C-terminal region. It can act as a bridge between the pilus and the receptor, with one domain interacting with the pilus and the other domain interacting with the receptor. The disulfide bridge is important in maintaining the function of these two domains because the destruction of the disulfide bond resulted in a loss of bacterial binding to the BECs.

Studies by Irvin and coworkers (Doig *et al.*, 1989; Irvin *et al.*, 1989) have shown that both the AcPAK 128-144 peptide and PAK pili bound to the detergent-solubilized BEC receptors which had been blotted onto nitrocellulose membrane. Polypeptide chains corresponding to molecular weights of 82, 55 to 51 and 40 kDa were observed. Furthermore, AcPAK 128-144 inhibited the binding of PAK pili to these proteins. These workers also showed that periodate oxidation destroyed the binding of both AcPAK 128-144 and PAK pili to these polypeptide chains, suggesting that the receptors are glycoproteins. Irvin *et al.* (1989) have also obtain immunofluorescence data to show that the binding of AcPAK 128-144 to TECs were localized to the cilia and luminal portions of the cell; these are the same regions to which *P. aeruginosa* whole cells were shown to bind.

The assays carried out in the above studies required the use of monoclonal antibodies and secondary antibody-enzyme conjugates to assay for binding. The times required for such assays are lengthy because of the long incubation periods. An attempt to simplify the assay has led to the use of synthetic peptides which have been conjugated directly to a reporter molecule, alkaline phosphatase. The AP-24mer conjugates (8:1 peptide to enzyme mole ratio) were able to bind to BECs with relatively high affinity (Figures VI.4 and VI.5). The relative dissociation constant of the AP-24mer was 0.94  $\mu\text{M}$  compared with 6.40  $\mu\text{M}$  for the oxidized AcPAK 128-144 peptide (the AP-17mer was also

assayed for binding to BECs, but the low A<sub>405</sub> signal obtained with this conjugate did not allow for an accurate measurement of its affinity for cell surface receptors). These peptides have also been conjugated to horseradish peroxidase (HRP). These HRP-peptide conjugates exhibited binding properties similar to that observed with the alkaline phosphatase-peptide conjugates, in that they also bound to the PAK pili. The binding of the HRP-peptide conjugates to BECs is presently being investigated (L. Kim, K.K. Lee, R.T. Irvin, and R.S. Hodges). Preliminary studies using the AP-24mer conjugates to bind receptors looked promising (data not shown). Solubilized membrane-bound receptors from BECs immobilized on nitrocellulose membrane were lighted up using this conjugate. The bands were assayed with the normal substrates used for alkaline phosphatase in immunoblots, i.e., nitro-blue tetrazolium chloride and 5-bromo-4-chloro-3-indolyl phosphate. Some of the bands obtained appeared to be similar to those observed by Irvin *et al.* (1989) and Doig *et al.* (1989). Inhibition studies with free peptides and PAK pili would have to be carried out to demonstrate the specificities of the conjugate-receptor interactions.

In light of the present findings, it appears that the pili-mediated adhesion of *P. aeruginosa* could be attributed to the structural pilin subunit. This mechanism is different from the pili-mediated adhesion of the *E. coli* Pap, S and type 1, where the adhesin molecule is one of the minor proteins, and not the structural pilin subunit itself. In the Pap pilus system, papG, F and E are associated at the tip of the pilus and PapG is the adhesin molecule (Lindberg *et al.*, 1987). PapE may be an important link between PapG and the pilus filament. PapF is required for bacterial binding to receptors and may have a role in the initiation of pilus assembly. PapD acts as a chaperone (Lindberg *et al.*, 1989) and its crystal structure has been recently deduced by Holmgren and Branden (1990). The receptor for the Pap pilus in the epithelium of the urinary tract is an  $\alpha$ -D-galactopyranosyl-(1-4)- $\beta$ -D-galactopyranose digalactoside moiety in the globoseries of glycolipids (Hultgren *et al.*, 1988). The receptor for the type 1 pilus consists of a mannose moiety on protein,

while in the S fimbriae,  $\alpha$ -sialyl-2,3- $\beta$ -galactose is the receptor (Korhonen *et al.*, 1984; Parkkinen *et al.*, 1986). The type 1 pilus also has at least 3 minor tip proteins, one of which is the adhesin molecule (Hanson and Brinton, 1988; Hanson *et al.*, 1988).

In the absence of known minor proteins associated with the *P. aeruginosa* pilus, does the pilus-mediated adhesion occur at the tip or does it occur laterally with multiple receptor binding sites contributed by the many pilin subunits which make up the filamentous rod? The pilus is a contractile organelle, and bacterial adhesion occurring at the tip would not be an unusual mechanism in the adherence of bacterium to host. The contraction of the pilus would then draw the bacterium and host cell together, enabling the bacterium to adhere firmly to the surface of the host cell, leading to subsequent stages in the infection process. Such an approach by the bacterium would also bypass any repulsion of charges on the membrane surfaces of both bacterium and host cell, which would prevent a successful adhesion of the bacterium to the host cell. Immunogold labelling electron microscopy has been used to try to visualize protrusion of the C-terminal region at the tip of the pilus. Such an experiment has not been successful. The gold labels were neither tip located nor were they laterally distributed along the pilus length. Normally, when the pilus is coated with anti-pilus antibodies, the fuzzy appearance of the pilus would be observed. However, the use of the anti-PAK 128-144 antisera (directed against reduced or oxidized peptides) failed to give such a fuzzy appearance to the PAK pili. Preliminary data have been obtained that showed the binding of the PK99H monoclonal antibody (whose epitope is located at the region of residues 128-144 of PAK pilin) at the tip of the PAK pilus (R.T.Irvin, personal communication).

As it stands right now, both polyclonal and monoclonal antibodies directed against the C-terminal region of PAK pilin are able to block adhesion of bacteria to BECs. The peptides corresponding to the sequence of this region bind to the cell surface receptors and can competitively inhibit PAK pili from binding to them. All these data point to the structural pilin subunit containing a receptor-binding domain.

## Chapter VII. Perspectives and Prospects

Despite the abundance of data presently available (Table I.1; see also Holder, 1988; Lieberman, 1985; and Pennington, 1990), the development of an anti-adhesion vaccine for *P. aeruginosa* infection has not been fully examined. Perhaps this lack of progress may have been due to an inadequate understanding of the mode and mechanism of adherence of these organisms. In order to explore and to capitalize on the potential of a peptide-based vaccine for *P. aeruginosa* infection, much research has been carried out to determine the mechanism of adherence of *P. aeruginosa* to host epithelial cells to locate the region of importance in the binding, to identify the protein involved, and to gauge the possibility of blocking this adherence process. Two adhesins are known to mediate the adherence of *P. aeruginosa* to host cells. Mucins or mucoid exopolysaccharides (MEP) mediate the adhesion of mucoid strains of *P. aeruginosa* (Ramphal and Pier, 1985; Ramphal *et al.*, 1984; Doig *et al.*, 1987). The pili-mediated attachment of nonmucoid strains to mammalian epithelial cells (Doig *et al.*, 1988; Ramphal *et al.*, 1984; Sato and Okinaga, 1987; Woods *et al.*, 1980). Purified pili from a particular strain were able to block adherence of homologous strains. Similarly, antibodies against pili were only able to block the binding of homologous strains (Ramphal *et al.*, 1987; Woods *et al.*, 1980). Ramphal *et al.* (1987) reported that an antiserum against MEP from a single mucoid strain inhibited the adherence of all six mucoid isolates tested (from CF patients), suggesting antigenic similarities of the MEP of mucoid strains. However, using more refined binding studies, Doig *et al.* (1987) found that alginates from various strains of *P. aeruginosa* possessed structural diversities. Alginate-based vaccines have had only limited success (Woods and Bryan, 1985). Immunization with purified alginate resulted in bacterial clearance which was associated with an increase in anti-alginate antibody titer. This protection was strain-specific in the chronic lung infection with *P. aeruginosa* in rats. However, it was also found that the anti-alginate antibodies formed immune complexes and resulted in tissue damage. This



undesirable damaging effect makes the alginate an unsuitable vaccine candidate. However, ongoing research is being carried out to improve the alginate vaccine (Garner *et al.*, 1990; Pier *et al.*, 1987; Pier *et al.*, 1990). It is believed that the appearance of the alginate producing mucoid strains emerge after initial colonization by nonmucoid *P. aeruginosa* strains (Dogget, 1969; Hoiby, 1974). Clearly, the prevention of colonization by pilus-mediated nonmucoid strains would be a better target for developing an anti-adhesion vaccine. The documented evidence that antibodies against pili could block adherence, albeit of homologous strains (Ramphal *et al.*, 1987; Woods *et al.*, 1980), offered hope for a pilus-based vaccine which would interrupt the initial colonization process.

To delineate the region of pilus involved in the pilus-mediated adherence, the project was designed to map the surface regions of pilin and from there determine which surface region/s contributed to the binding properties of pilus. This rationale was based on the premise that no other minor proteins are associated with the filamentous rod which could contribute to the adhesive property of pilus. Pili from strains PAK and PAO were selected for the studies because they have been characterized and purified (Paranchych *et al.*, 1980; Pasloske *et al.*, 1985; Sastry *et al.*, 1983; Sastry *et al.*, 1985).

The predicted surfaces of PAK and PAO pilins based on the Surfaceplot program (Parker *et al.*, 1986) yielded similar surface profiles and a possibility of eight surface regions on both PAK and PAO pilins (Figure V.1, Chapter V). In fact, when the prediction algorithms were applied to three other pilins, P1, CD4 and K122-4, similar surface profiles were observed (Pasloske *et al.*, 1988; unpublished data). In comparative studies carried out by Dalrymple and Mattick (1987), the conservation of certain regions of the NMePhe pilin is maintained in several genera, including *P. aeruginosa*, *N. gonorrhoeae*, *B. nodosus* and *M. bovis*. Since these organisms share the same class of NMePhe pili, they have very similar morphology, i.e., 5  $\mu\text{m}$  in length and 0.05  $\mu\text{m}$  in diameter. Within the same *Pseudomonas* species, pilin molecules from different strains would be expected to have similar structural features. The highly conserved N-terminal

region (residues 1-30) believed to be involved in pilin-pilin interaction is supported by the physicochemical studies of Watts *et al.* (1983). Mutation in the first few residues at the N-terminus and also the disruption of the methylation process of the N-terminal phenylalanine resulted in unassembled pilin subunits (Pasloske *et al.*, 1988). Other conserved residues in the pilin molecule may also participate in pilin-pilin interactions.

In the mapping studies, most of the predicted surface regions were located by antipeptide antisera raised against synthetic peptides corresponding to those regions predicted by the Surfaceplot program (Chapter V), thus showing its effectiveness. In one or two cases, the antipeptide antiserum failed to bind to pili. However, antiserum raised against whole protein was able to bind to these synthetic peptides, attesting to their surface location and to their immunogenicities and antigenicities (e.g. PAK 74-83). Regions on the surface need not be immunogenic, e.g., PAK 88-97 and PAO 88-97, when immunized as part of the native protein. However, immunization with the peptide conjugated to a protein carrier, resulted in good humoral response to this region of the protein. This is part of the elegance of using a peptide immunogen. Regions on a protein which are ordinarily immunorecessive can be made to induce antibody production with a specificity just to the peptide or region of interest. The limitation is that the ability of the antipeptide antibodies to bind to native protein may not be of a high affinity because of conformational constraints of that region of the protein. Thus, there are researchers who would make synthetic peptides based on secondary structure predictions because it is thought that antibodies bind to  $\beta$ -turns.  $\beta$ -turns structures tend to be found on the surface of proteins. The antigenic sites often have convex surface shapes, while the complementary binding sites on the antibodies have concave shapes (Geysen *et al.*, 1987). However, our understanding as to why peptides can generate antibodies which bind to proteins is still limited. Generally, peptides do not have well defined structures in solution and yet are able to generate antibodies which bind the native proteins. The perplexity of this 'ordered-disordered paradox' was again highlighted by recent crystallographic data on the binding of an antipeptide monoclonal

antibody to the peptide and its corresponding native protein (Stanfield *et al.*, 1990). A synthetic 19-residue peptide homolog of the C-helix of myohemerythrin (Mhr) was cocrystallized with a monoclonal antibody specific for the first five residues of this peptide. This region of the peptide was shown to be absent of any regular structure in solution by NMR and CD measurements. It was found that the peptide adopted a type II  $\beta$ -turn conformation when bound to the Fab fragment, showing that the antibody bound to the peptide in a well-defined secondary structure common in proteins. The binding of this monoclonal antibody to the native Mhr would be interesting because the same sequence on the protein has been shown to adopt an  $\alpha$ -helical structure in the native protein (Sheriff *et al.*, 1987), quite different from the solution structure or the Fab-bound structure. Furthermore, one of the essential residues (His-73) which contributed to the epitope was intimately involved in the coordination of an iron atom internally and would not be available for binding to the antibody. Some denaturation of the native protein would be anticipated for binding to occur, and in fact the apo-form of the protein did bind much better to the Fab than its native form. Further light on the mechanism of antigen-antibody binding in this example will have to wait until these researchers have successfully crystallized the Fab-apo Mhr complex, as well as the complexes of two other monoclonal antibodies to the 19-residue peptide.

Although it was possible to obtain crossreactive and strain-specific antibodies from the predicted surface regions, the ability to predict crossreactivity and strain-specificity in related proteins appears to be more than just a simple comparison of the primary amino acid sequences of the proteins. Structural features inherent in the primary sequence may have a role in determining whether the region of the molecule would be crossreactive or strain-specific in related proteins.

The conservation of residues in the semiconserved C-terminal region of *Pseudomonas* pilin is important in the functionality of this molecule. The region around residues 121-144 in PAK pilin is immunogenic but it is not the immunodominant region,

which is thought to be a conformational epitope located between residues 82-110 (Sastry *et al.*, 1985; Watts *et al.*, 1983). Anti-pilus antisera against PAK and PAO pili can recognize synthetic peptides corresponding to residues 128-144 of the protein. Immunization of mice with PAK pili gave rise to monoclonal antibodies which could bind the disulfide-bridged region of PAK pilin. This disulfide-bridged region contains a receptor-binding domain, as evident by the abilities of both polyclonal and monoclonal antibodies to bind this region, and subsequently block both pili and bacteria from binding BECs. The immunorecessiveness of this region would play an important role in that it would be less likely to be bound by host antibodies which would block its adherence function. It is a common ploy for microorganisms to divert the host defence system away from the important functional regions. The immunodominant region of PAK pilin is located away from the C-terminal region. Thus, polyclonal antipeptide antibodies directed against regions away from the C-terminal region, such as the region of residues 88-97, 105-114 and 117-125, did not block PAK pili binding to BECs. The antibodies, anti-PAK 128-144, PK99H and PK34C, bound and blocked adherence of both pili and bacteria to BECs. The two cysteine residues are conserved in all the known *P. aeruginosa* pilin sequences. In addition, there are other conserved residues in this region such as Ser-130, Phe-137 and Pro-139 (Figure I.1, Chapter 1) which may contribute to receptor-binding function.

The conservation of the two cysteines at the C-terminal region of the NMePhe pilin and their forming a putative disulfide bond has led to speculations of a possible role for such a disulfide bond in bacterial pilus function. Within this loop region lies a strain-specific immunodominant epitope of gonococcal pilin (Rothbard *et al.*, 1984). Although controversial, the hypervariable disulfide loop region may also contain part of the receptor-binding domain of gonococcal pilus (Nicholson *et al.*, 1987). As stated by Schoolnik *et al.* (1983), if each pilus subunit possesses a receptor-binding domain, one would expect a polyvalent ligand with a linear array of binding sites along its longitudinal axis. This region of the molecule could be involved in pilin-pilin interactions and, thus, would not be

exposed along its longitudinal axis. If so, only the distal pilin subunit would be exposed at the tip of the pilus, leading to a single receptor-binding domain for each assembled pilus. Based on prediction algorithms used by Schoolnik *et al.* (1984), the C-terminal disulfide bridge region is fairly hydrophilic and could be exposed to the aqueous environment. This exposure would then enable this region to act as a receptor-binding domain. As mentioned earlier, no minor proteins associated with the gonococcal pilus or with other NMePhe pili have been discovered. The pilin molecules do not undergo post-translational addition of carbohydrate, sulfate or phosphate groups which may contribute to binding activities. However, recent reports by Muir *et al.* (1988) and Parge *et al.* (1990) suggested that other proteins may be associated with the gonococcal pilus. These putative pilus-associated proteins have not been characterized nor are their functions on the pilus known. The studies carried out with the PAK pilin demonstrated that the C-terminal disulfide-looped terminal region (PAK 128-144) contains a receptor-binding domain for the PAK pilus. Polyclonal antibodies to this peptide blocked the adherence of pili to BECs. Monoclonal antibodies directed against this region of residues 121-144 block both homologous (PAK) and heterologous strains from binding to BECs. Moreover, the direct binding of the AcPAK 128-144 peptide to cell-surface receptors demonstrated unequivocally that this region of pilin is a receptor-binding domain on the PAK pilin. It will also be important to verify these results with the binding of synthetic peptides, corresponding to the C-terminal region of pilins from the other *P. aeruginosa* strains, to cell-surface receptors. Antibodies raised against these peptides can also be used to block *Pseudomonas* adherence to host cells.

The prospect of a synthetic peptide vaccine for *P. aeruginosa* infection from an anti-adhesive approach looks very promising. We have been able to locate a region of the *Pseudomonas* pilin which contains a receptor-binding domain and antibodies directed against this region can block bacterial adherence. Rowlands (1989) stated two basic requirements for a peptide vaccine: firstly, a sequence of amino acids capable of eliciting

antibodies which react with the native protein from which the sequence was derived (B-cell epitope); and secondly, a sequence of amino acids which could induce T-cell help for the B-cell. The first requirement has been met in the present research for a synthetic peptide vaccine for *P. aeruginosa* infection. However, the second issue has not been dealt with in this thesis. The humoral response requires cooperation between B and T lymphocytes. The B and T cells are specialized cells in the immune system. The proliferation and maturation of B-cells require not only the stimulatory signal from the antigen, but also from a T-helper cell. The T-cells are primed to proliferate and mature into helper cells after exposure to an antigen, in combination with major histocompatibility complex molecules on antigen-presenting cells. The T-cell epitopes are usually, but not always, different from those of B-cell epitopes. The reason for the use of large protein carriers such as KLH is that it has a number of T-cell epitopes which help stimulate a helper T-cell response. Enhancement of the immunogenicity of the vaccine could be achieved by the incorporation of B- and T- cell epitopes onto the same carrier molecule. Although the presence of the carrier may have undesirable side-effects and may abrogate some of the potential advantages of a totally synthetic vaccine (Kowlands, 1989), suitable human carrier proteins, such as tetanus and diphtheria toxoids, are applicable. The use of these toxoids in humans has been approved by the Food and Drug Administration. Alternatively, instead of using a monomeric presentation, polymers of the B-cell epitope could be employed to enhance the humoral response if a protein carrier is not desirable. In addition to the above approaches, a totally synthetic method of presenting peptides as regular polymeric arrays involving the use of a synthetic core consisting of polymers lysine residues, has been developed by Tam (1988). In this multiple antigen peptide (MAP) approach, peptide antigens are incorporated via the  $\alpha$ - and  $\xi$ - amino groups of the lysine residues in the core structure, to give rise to a macromolecular structure without the presence of a large protein carrier. Such an approach has been extended to include both B- and T- cell epitopes (Tam and Lu, 1989). Another issue with the efficacy of synthetic peptide vaccines is that short

linear peptides are often insufficient for generating good immunological responses in a divergent genotypic population. To ensure an immune response in an outbred population, the vaccine may have to be incorporated with a cocktail of helper T-cell epitopes. The issue of cell-mediated immunity has not been dealt with in this thesis. From previous studies (Smart *et al.*, 1988), the major T-cell epitope of the *P. aeruginosa* PAK pilin has been located in the region of residues 82-104. Further studies which have been carried out to pinpoint this sequence to a limited 15-residue sequence have not been successful (B. Singh, K.K. Lee, and R.S. Hodges, unpublished data), although studies are still being carried out to map the T-cell epitopes of PAK pilin (B. Singh, K.K. Lee, R.S. Hodges, and A. Holm). Delineation of the major T-cell epitope may enable us to enhance the immunogenicity of a pilus-based synthetic peptide vaccine.

The important contribution of each amino acid residue in the receptor-binding region of *P. aeruginosa* pilin should be examined. In this regard, studies are underway in this laboratory to synthesize single amino acid (alanine) substitutions in the region of residues 121-144 of PAK pilin, with the exception of the two cysteines to conserve the disulfide bridge in all the analogs. These analogs will be used in two ways. Firstly, they will be used to map the epitopes of the strain-specific PK99H MAb and the crossreactive PK34C MAb. In addition, the mapping of the epitopes of the crossreacting (17-O1) and the strain-specific (17-O2) polyclonal antibodies is presently being pursued in this laboratory (W.Y. Wong and R.S. Hodges). The data from these studies should provide insight into the residues that contribute to strain-specific and crossreacting antibodies. Secondly, the analogs will be used for binding studies to determine which residues, when substituted, would contribute to a significant loss of binding. This would enable us to know which of the residues in the C-terminal region contribute to receptor-binding function and how widely conserved these residues are in the pilins from different *P. aeruginosa* strains. By substituting all the residues not involved in adherence with alanine or glycine residues, perhaps a better crossreacting antibody could be obtained. Alternatively, a

cocktail vaccine using the C-terminal regions of all pilin types and conjugated to a carrier molecule may also be tested. In collaboration with Drs. Randy Read and Randy Irvin (Medical Microbiology and Infectious Disease, University of Alberta), crystallization of the AcPAK 128-144 and AcPAK 121-144 peptides and the co-crystallization of the monoclonal antibodies with these peptides are being undertaken to rationalize the structure of the peptides and its binding to the antigen-binding site of the antibodies. Such an approach should provide a more rational way to designing a *Pseudomonas* vaccine.

Another area of study which should be pursued is whether there are other minor protein components (besides the pilin subunits) associated with the PAK pilus. In the Pap pilus of *E. coli*, the adhesin molecule along with other pilus-associated proteins are located at the tip (Lindberg *et al.*, 1984; Lindberg *et al.*, 1987; Lund *et al.*, 1987), while in the type 1 pilus, the adhesin and other pilus-associated proteins are distributed along the shaft (Hanson *et al.*, 1988; Krogfelt *et al.*, 1990; Maurer and Orndoff, 1987). No other minor proteins associated with the *Pseudomonas* pilus have been found. The absence of available evidence does not necessarily negate their existence in the NMePhe pilus system. The approach to this problem of whether there are other pilus-associated proteins may lie in genetic studies to localize the pilin operon of *P. aeruginosa*. Three other genes involved in *P. aeruginosa* pilus expression have been reported (Nunn *et al.*, 1990). Further studies to delineate the pilus operon are underway. In this way, the genetic approach coupled with DNA sequencing studies and biochemical characterization of the gene products may shed some light on the NMePhe pilus system of *P. aeruginosa*.

Two interesting developments were initiated in the course of the present research project. The first involved a new monitoring procedure for reduced (free sulfhydryl groups) and oxidized (intrachain disulfide bonded) peptides using RPC. Peptides to be oxidized to form intrachain disulfide bond could be modified with N-ethylmaleimide (NEM) and separated by RPC. This development came about as a result of the inability to monitor clearly the reduced and oxidized AcPAK 128-144 peptide by RPC in the early



phase of the research. This new method provided good baseline resolution between reduced and oxidized conformers. This is particularly useful for peptides that are not resolved by RPC. This method is not as fast as the colorimetric Ellman assay (Ellman, 1959). Unlike the Ellman method which monitors the free sulfhydryls alone, this RPC method monitors the UV absorbance of both reduced and oxidized peptides. It was found to be highly sensitive and only small quantities of peptides (nanomolar range) were needed. It is possible to monitor both reduced and oxidized peptides using electrochemical detectors which are very sensitive detector systems (Allison and Shoup, 1983). The application of electrochemical detectors system for thiol-containing peptides has been limited. This sensitive detector system has been recently reviewed by Dou *et al.* (1990). The simplicity of the RPC method negates the unnecessary purchase of such detectors in routine monitoring and quantitation of reduced and oxidized peptides. This method is now routinely used in this laboratory to monitor the oxidation of peptide

The second development was the use of ligand-reporter conjugates to assay protein-receptor or protein-protein interactions. Although this approach is still in its infancy, the use of the alkaline phosphatase-PAK 121-144 conjugate (AP-24mer) to bind to pili and cell-surface receptors has shown great promise. This is not a new idea as such because many ligands have been conjugated to reporter molecules and used in other biological assays. The side-chains of the amino acids, such as the  $\xi$ -amino,  $\alpha$ - and  $\beta$ - carboxyls and the thiol groups, are useful for chemical modifications because the reactivities can be pH-controlled and many heterobifunctional reagents have been designed to react with these side-chains to generate hetero-oligomers. The chemical aspects and application of protein modification have been recently reviewed by Means and Feeney (1990). An excellent source of these bifunctional reagents is the Pierce Chemical Company catalogue. Some of the practical aspects of preparation of protein-conjugates have been reviewed by Thorpe and coworkers (Cumber *et al.*, 1985) and Koppel (1990). The conjugation method developed in the present study uses a simple photoreactive molecule attached at a defined

site on the peptide during synthesis of the peptide (Parker and Hodges, 1985). Because the photolytic crosslinking of the benzoylbenzoyl moiety is non-specific in nature in that it does not rely on functional side chains of amino acids, the peptide could easily be covalently crosslinked to the surface of the reporter molecule upon irradiation with UV light. The activity of the reporter molecule may be reduced because of steric hindrance due to a covalently-attached peptide close to the cleft of the active site. The attachment of peptide to reporter molecule was non-specific and as such a loss of activity could not be tightly controlled but the probability of this occurrence in a given population should be statistically low. Further reduction of the loss of enzymatic activity could be achieved by controlling the number of peptides to be conjugated to each reporter molecule. The application of this methodology was demonstrated in the binding of the AP-24mer to immobilized PAK pili on the wells of the ELISA plates and to cell-surface receptors on BECs. Thus, the study of protein-protein and ligand-receptor interactions of many biological systems could be carried out in this way if the region of interaction is contained within a linear sequence of the protein. One half of the bimolecular process could be immobilized to a solid support and the second half (ligand) conjugated to an enzyme or other reporter molecules. The binding process could be visualized and quantitated spectrophotometrically. Characterization of the binding could be determined with peptide analog inhibition assays and many such assays could be carried out in multi-well polystyrene plates. Another application could be the isolation of receptors. Receptors isolated by gel electrophoresis could be visualized by the AP-24mer conjugates. This assay could facilitate isolation of receptors which are membrane-bound or cytosol-localized, e.g., peptide hormone receptors.

Peptide inhibition studies using the AP-24mer binding to BECs and to PAK pili will have to be carried out to show the specificities of this assay. Quantitation of the molar ratios of peptide to alkaline phosphatase needs to be carried out to determine the optimum ratio which would give high affinity and high sensitivity of the conjugate with minimal loss of enzymatic activity or loss of binding. The question of the length of the spacer arm

should be considered. In the conjugates that were made, the length of the spacer arm between the peptide and the alkaline phosphatase was made up of the photoreactive benzoylbenzoyl moiety and the norleucine residue. The fact that the AP-17mer bound poorly to PAK pili and to BECs could be due to the close proximity between the binding domain on the peptide and the enzyme surface which resulted in steric hindrances between the peptide and the receptor. Thus, the appropriate length of the spacer arm should be established. The viability of this method should be tested in other biological systems. One such assay might be the immobilization of the anti-PAK 128-144 immunoglobulin or Fab to the wells of the ELISA plate and assaying the binding of the AP-24mer conjugate to these protein receptors. The further development and establishment of this methodology could provide other scientists involved in many areas of ligand-receptor and protein-protein interaction research with a new powerful tool to unravel some of the mechanisms of the biological world.

## Bibliography

- Abraham, S.N., J.D. Goguen, D. Sun, P. Klemm, and E.H. Beachey. (1987) *J. Bacteriol.* **169**: 5530-5536.
- Alexander, J.W., M.W. Fisher, E.G. MacMillan, and N.A. Altemeir. (1969) *Arch. Surg.* **99**: 249-255.
- Anderer, F. (1963) *Biochim. Biophys. Acta* **71**:246-248.
- Arnon, R., E. Maron, M. Sela, and C.B. Anfinsen. (1971) *Proc. Natl. Acad. Sci. USA* **68**: 1450-1455.
- Aronson, M., O. Medalia, L. Schöri, D. Mirebran, N. Sharon, and I. Ofek. (1979) *Rev. Infect. Dis.* **1**: 832-837.
- Atazzi, M.Z., C.S. McDaniel, and T. Manshour. (1988) *J. Protein Chem.* **7**: 655-666.
- Baker, N., and N.A. Marcus. (1982) *Curr. Microbiol.* **7**: 35-40.
- Baltimore, R.S. (1985) *Antibiot. Chemother.* **36**: 147-156.
- Barany, C. and R.B. Merrifield. (1979) *The Peptides* **2**: 1-284.
- Barlow, D.L., M.S. Edwards, and J.M. Thornton. (1986) *Nature* **322**: 747-748.
- Beachey, E.H. (1981) *J. Infect. Dis.* **143**: 325-345.
- Beard, M., J.S. Mattick, L.J. Moore, M.R. Mott, C.F. Mars, and J.R. Egerton. (1990) *J. Bacteriol.* **172**: 2601-2607.
- Bejarano, P.A., J.P.M. Langeveld, B.G. Hudson, and M.E. Noelken. (1989) *Infect. Immun.* **57**: 3783-3787.
- Berk, R.S., D. Brown, I. Coutinho, and D. Meyers. (1987) *Infect. Immun.* **55**: 1728-1730.
- Bodanszky, M. (1988) in "*Peptide Chemistry: a practical textbook*" Springer-Verlag, Berlin
- Bodey, G.P., R. Bolivar, V. Feinstein, and L. Jaleja. (1983) *J. Infect. Dis.* **5**: 279-313.
- Bradley, D.E. (1972) *Genet. Res.* **19**: 39-51.
- Brinton, C., A. Brown, K. Rogers, N. Guerina, S. Wood, J. Bryan, A. Labik, B. Polen and S. Lee, in "*Current Chemotherapy and Infectious Disease*", J.D. Nelson and C. Grassi (eds.), American Soc. Microbiology, Washington, D.C., pp. 1242-1245.
- Buchanan, T.M. (1977) in "*The gonococcus*" R.B. Roberts (ed.) J. Wiley & Sons, Inc. New York. pp 255-272.

- Burke, T.W.L., C.T. Mant, and R.S. Hodges. (1988) *J. Liq. Chromatogr.* **11**: 1229-1247.
- Burns, D.L., L.A. Smith, K.B. Seamon, K.A. Groover, and W. H. Habig. (1989) *Infect Immun.* **42**: 113-121.
- Cetin, E.T., K. Toreci, and O. Ang. (1965) *J. Bacteriol.* **89**: 1432-1433.
- Coburn, J., S.T. Dillon, B.H. Iglewski, and D.M. Gill. (1989) *Infect. Immun.* **57**: 997-998.
- Creighton, T.E. (1983) in "*Proteins: structures and molecular properties*" W.H. Freeman & Co., New York. pp 23.
- Cryz, S.J. (1987) *Pathol. Immunopathol. Res.* **6**:147-152.
- Cryz, S.J., E. Furer, J.C. Sadoff, and R. Germanier. (1986) *Infect. Immun.* **52**: 161-165.
- Cryz, S.J., E. Furer, and R. Germanier. (1983a) *Infect. Immun.* **39**: 1072-1079.
- Cryz, S.J., E. Furer, and R. Germanier. (1983b) *Infect. Immun.* **40**: 659-664.
- Cryz, S.J., E. Furer, J.C. Sadoff, R. Germanier, I Pastan, M.C. Willingham, and D.J.P. Fitzgerald. (1987) *Rev. Infect. Dis.* **9**: S644-S649.
- Cumber, A.J., J.A. Forrester, B.M.J. Foxwell, W.C.J. Ross, and P.E. Thorpe. (1985) *Meth. Enzymol.* **112**: 207-225.
- Darymple, B., and J.S. Mattick. (1987) *J. Mol. Evol.* **25**: 261-269.
- Diaz, F., L.L. Mosovich, and E. Neter. (1970) *J. Infect. Dis.* **121**: 269-274.
- Dogget, R.G. (1969) *Appl. Microbiol.* **18**: 936-937.
- Dogget, R.G., G.M. Harrison, and R.E. Carter, Jr. (1971) *Lancet* **i**: 236-237.
- Doig, P., W. Paranchych, P.A. Sastry, and R.T. Irvin. (1989) *Can. J. Microbiol.* **35**: 1141-1145.
- Doig, P., P.A. Sastry, R.S. Hodges, K.K. Lee, W. Paranchych, and R.T. Irvin. (1990) *Infect. Immun.* **58**: 124-130.
- Doig, P., N.R. Smith, T. Todd, and R.T. Irvin. (1987) *Infect. Immun.* **55**: 1517-1522.
- Doig, P.D., T.Todd, P.A. Sastry, K.K. Lee, R.S. Hodges, W. Paranchych, and R.T. Irvin. (1988) *Infect. Immun.* **56**: 1641-1646.
- Dou, L., J. Mazzeo, and I.S. Krull. (1990) *Biochromatography* **5**: 74-96.
- Dressman, G.R., J.T.Sparrow, R.C. Kennedy, and J.L. Melnick. (1984) in "*Modern approaches to vaccines: molecular and chemical basis of virus virulence and immunogenicity*" R.M. Channock and R.A. Lerner (eds) Cold Springs Harbour Press, New York. pp. 115-119.

- Dyson, H.J., R.A. Lerner, and P.E. Wright. (1988) *Ann. Rev. Biophys. Biophys. Chem.* **17**: 305-324.
- Egerton, J.R., P.T. Cox, B.J. Anderson, C. Kristo, M. Norman, and J.S. Mattick. (1987) *Vet. Microbiol.* **14**: 393-409.
- Eisenstein, B.I., I. Ofek, and E.H. Beachey. (1979) *J. Clin. Invest.* **63**: 1219-1228.
- Ellman, G.L. (1959) *Arch. Biochem. Biophys.* **82**: 70-77.
- Feurst, J.A., and A.C. Hayward. (1969) *J. Gen. Microbiol.* **58**: 227-237.
- Findlay, B.B., and S. Falkow. (1989) *Microbiol. Rev.* **53**: 210-230.
- Folkard, W., D.A. Marvin, T.H. Watts, and W. Paranchych. (1981) *J. Mol. Biol.* **149**: 79-93.
- Frost, L.S., M. Carpenter, and W. Paranchych. (1978) *Nature* **271**: 87-89.
- Galardy, R.E., L.C. Craig, J.D. Jamieson, and M.P. Printz. (1974) *J. Biol. Chem.* **249**: 3510-
- Galardy, R.E., L.C. Craig, and M.P. Printz. (1973) *Nature (London) New Biol.* **242**: 127-
- Garner, C.V., D. DesJardins, and G.B. Pier. (1990) *Infect. Immun.* **58**: 1835-1842.
- George, R.H. (1989) *Arch. Dis. Child.* **62**: 438-439.
- Geysen, H.M., J.A. Tainer, S.J. Rodda, T.J. Mason, H. Alexander, E.D. Getzoff, and R.A. Lerner. (1987) *Science* **235**: 1184-1190.
- Geysen, H.M., S.J. Rodda, T.J. Mason, G. Tribbick, and P.G. Schoofs. (1987) *J. Immunol. Meth.* **102**: 259-274.
- Gilleland, H.E., M.G. Parker, J.M. Matthews, and R.D. Berg. (1984) *Infect. Immun.* **44**: 49-54.
- Govan, J.R.W., and G.S. Harris. (1986) *Microbiol. Sci.* **3**: 302-308.
- Green, N., H. Alexander, A. Olson, S. Alexander, T.M. Shinnick, J.G. Sutcliffe, and R.A. Lerner. (1982) *Cell* **28**: 477-487.
- Guo, D.C., C.T. Mant, and R.S. Hodges. (1987) *J. Chromatog.* **386**: 205-222.
- Guo, D.C., C.T. Mant, A.K. Taneja, J.M.R. Parker, and R.S. Hodges. (1986) *J. Chromatog.* **357**: 499-517.
- Hagenmaier, H., and H. Frank. (1972) *Hoppe-Seylers Z. Physiol. Chem.* **353**: 1973-1976.
- Hancock, R.E.W. (1984) *Antibiot. Chemother.* **36**: 95-102.
- Hanson, M.S., and C.C. Brinton, Jr. (1988) *Nature* **332**: 265-268.

- Hanson, M.S., J. Hempel, and C.C. Brinton, Jr. (1988) *J Bacteriol.* **170**: 3850-3858.
- Henrichsen, J. (1972) *Bacteriol. Rev.* **36**: 478-503.
- Hermodson, M.A., K.C.S. Chen, and T.M. Buchanan. (1978) *Biochemistry* **17**: 442-445.
- Hirao, Y., and J.Y. Homma. (1978) *Jap. J. Exp. Med.* **48**: 41-51.
- Hirs, C.H.W., W.H. Stein, and S. Moore. (1954) *J. Biol. Chem.* **211**: 941-
- Hodges, R.S., T.W.L. Burke, and C.T. Mant. (1988) *J. Chromatogr.* **444**: 349-362.
- Hodges, R.S., R.J. Heaton, J.M.R. Parker, L. Molday, and R.S. Molday. (1988) *J. Biol. Chem.* **256**: 11768-11775.
- Hodges, R.S., P.D. Semchuk, A.K. Taneja, C.M. Kay, J.M.R. Parker, and C.T. Mant. (1988) *Peptide Res.* **1**: 19-30.
- Holder, I.A. (1988) *Serodiag. Immunother.* **2**: 7-16.
- Holder, I.A., and J.G. Naglich. (1986) *J. Trauma* **26**: 118-122.
- Holder, I.A., R. Wheeler, and T.C. Montie. (1982) *Infect. Immun.* **35**: 270-280.
- Hoiby, N. (1974) *Acta Pathol. Microbiol. Scand.* **B82**: 551-558.
- Holmgren, A., and C.I. Branden. (1989) *Nature* **342**: 248-251.
- Hooke, A.M., D.O. Sordelli, C. Cerquetti, and J.A. Bellanti. (1987) *Infect. Immun.* **55**: 99-103.
- Hope, D.B., V.V.S. Murti, and V. Du Vigneaud. (1962) *J. Biol. Chem.* **237**:1563-1566.
- Horvat, R.T., M. Clabaugh, C. Duval-Jobe, and J.L. Parmley. (1989) *Infect. Immun.* **57**: 1668-1674.
- Houghten, R.A. (1985) *Proc. Natl. Acad. Sci. USA* **82**: 5131-5135.
- Houghten, R.A., M.K. Pray, S.T. Degraw, and C.J. Kirby. (1986) *Int. J. Pept. Prot.* **27**: 673-678.
- Houwink, A.L., and W.V. Iterson. (1950) *Biochim. Biophys. Acta* **5**: 10-44.
- Hughes, G.J., and S. Frtger (1990) in "Laboratory methods in Biochemistry: amino acid analysis and protein sequencing" C. Fini, A. Floridi, V.N. Finelli, and B. Wittman-Liebold (eds) CRC Press Inc., Boca Raton, FL. pp 44-62.
- Hultgren, S.J., F. Lindberg, G. Magnusson, J. Kihlberg, J.M. Tennent, and S. Normark. (1989) *Proc. Natl. Acad. Sci. USA.* **88**: 4357-4361.
- Iglewski, B.H., and I. Kabat. (1975) *Proc. Natl. Acad. Sci. USA.* **72**: 2284-2298.

- Irvin, R.T., P. Doig, K.K. Lee, P.A. Sastry, W. Paranchych, T. Todd, and R.S. Hodges. (1989) *Infect. Immun.* **57**: 3720-3726.
- Isaacson, R.E., E.A. Dean, R.L. Morgan, and H.W. Moon. (1980) *Infect. Immun.* **29**: 824-826.
- Ishimoto, K., and S. Lory. (1989) *Proc. Natl. Acad. Sci. USA.* **86**: 19554-19557.
- Janin, J. (1979) *Nature* **277**: 491-492.
- Jarvis, W.R., J.W. White, V.P. Munn, J.L. Mosser, T.G. Emori, D.H. Culver, C. Thornsberry, and J.M. Hughes. (1984) *Mort. Morb. Wkly. Report* **33**: 9S-21S.
- Johanson, W.G., A.K. Pierce, T.P. Sanford, and G.D. Thomas. (1972) *Arch. Intern. Med.* **77**: 701-706.
- Johanson, W.G., D.E. Woods, and T. Chauchuri (1979) *J. Infect. Dis.* **139**: 667-673.
- Johanson, W.G., J.H. Higuchi, T.R. Chaudhuri, and D.E. Woods. (1980) *Am. Rev. Respir. Dis.* **121**: 55-63.
- Johnson, K., and S. Lory. (1987) *J. Bacteriol.* **169**: 5663-5667.
- Johnson, K., M.L. Parker, and S. Lory (1986) *J. Biol. Chem.* **261**: 15703-15708.
- Jones, G.W., and J.M. Rutter. (1972) *Infect. Immun.* **6**: 918-927.
- Karplus, P.A., and G.E. Schulz. (1985) *Naturwissenschaften* **72**: S212.
- Kent, S.B.H. (1988) *Ann. Rev. Biochem.* **57**: 957-990.
- Kent, S.B.H., and I. Clarke-Lewis. (1985) in "Synthetic peptides in biology and medicine" Alitalo, K., P. Partanen, and A. Vaheri (eds) Elsevier Sci. Pub., Amsterdam. pp29-58.
- Kluftinger, J.L., F. Lutz, and R.E.W. Hancock. (1989) *Infect. Immun.* **57**: 882-886.
- Koppel, G.A. (1990) *Bioconjugate Chem.* **1**: 13-23.
- Korhonen, T.K., V. Vaisanen-Rhen, M. Rhen, A. Pere, J. Parkkinen, and J. Finne. (1984) *J. Bacteriol.* **159**: 762-766.
- Kreger, A.S., D.M. Lyerly, L.D. Hazlett, and R.S. Berk. (1986) *Invest. Ophthalm. Vis. Sci.* **27**: 932-939.
- Kroghfelt, K., H. Bergmans, and P. Klemm. (1990) *Infect. Immun.* **58**: 1995-1998.
- Kroghfelt, K., M. Meldal, and P. Klemm. (1987) *Microbial Pathog.* **2**: 465-472.
- Kurioka and Liu, P.V. (1967) *J. Bacteriol.* **93**: 670-674.
- Laemmli, U.K. (1970) *Nature* **227**: 682-685.



- Lazure, C., S. Benjannet, J.A. Rochemont, N.B. Seidah, and M. Chretien. (1990) in "Laboratory methods in Biochemistry: amino acid analysis and protein sequencing" A. Fini, A. Florini, V.N. Finelli, and B. Wittman-Liebold. (eds) CRC Press Inc., FL pp 83-107.
- Lee, K.K., J.A. Black, and R.S. Hodges. (1990) in "Peptides: chemistry, biology and structure. Proceedings of the twelfth American Peptide Symposium" J.E. Rivier and G.R. Marshall (eds). ESCOM Sci. Pub., Leiden. pp 999-1002.
- Lee, K.K., P. Doig, R.T. Irvin, W. Paranchych and R.S. Hodges. (1989) *Mol. Microbiol.* 3: 1493-1499.
- Lee, K.K., P.A. Sastry, W. Paranchych, and R.S. Hodges. (1989) *Infect. Immun.* 57: 520-526.
- Lein, J., R. Chan, K. Lam, and J.R.W. Costerton. (1980) *Infect. Immun.* 28: 546-556.
- Lenard, J., and A.B. Robinson. (1967) *J. Amer. Chem. Soc.* 81: 181-182.
- Lerner, R.A. (1972) *Nature* 299: 592-596.
- Lieberman, M.M. (1985) *Surv. Synth. Path. Res.* 4: 312-322.
- Lieberman, M.M., M.S. Walker, E. Ayaala, and I. Chapa. (1986) *J. Surg. Res.* 40: 138-144.
- Lindberg, F., B. Lund, L. Johanan, and S. Normark. (1987) *Nature* 328: 84-87.
- Lindberg, F., J.M. Tennent, S.J. Hultgren, B. Lund, and S. Normark. (1989) *J. Bacteriol.* 171: 6052-6058.
- Lindberg, F.P., B. Lund, and S. Normark. (1984) *EMBO J.* 3: 1167-1173.
- Linker, A., and R.S. Jones (1961) *J. Biol. Chem.* 241: 3845-3851.
- Lory, S. (1989) *Ped. Pulmonol. Suppl.* 4: 83-84.
- Lory, S., and P.C. Tai. (1985) *Curr. Topics Microbiol. Immunol.* 118: 53-69.
- Lund, B., F. Lindberg, B.I. Marklund, and S. Normark. (1987) *Proc. Natl. Acad. Sci. USA* 84:5898-5902.
- Lund, B., F. Lindberg, B.I. Marklund, and S. Normark. (1988) *Proc. Natl. Acad. Sci. USA* 85: 1887-1894.
- Lunte, S.M., and P.T. Kissinger. (1985) *J. Liq. Chromatogr.* 8: 691-706.
- MacIntyre, S., T. McVeigh, and P. Owen. (1986) *Infect. Immun.* 51: 675-686.
- Male, D., B. Champion, and A. Cooke. (1987) in "Advanced Immunology" Lippincourt Co., London. Chapter 8.
- Mant, C.T., T.W.L. Burke, and R.S. Hodges. (1987) *Chromatographia* 24: 565-572.

- Mant, C.T., and R.S. Hodges. (1986) *LCGC Mag.* 4: 251-253.
- Mant, C.T., and R.S. Hodges (1990) in "*HPLC of biological macromolecules*" K.M. Gooding, and F.E. Regnier (eds). Marcel Dekker Inc., pp301-332.
- Marcus, H., A. Austria, and N.R. Baker. (1989) *Infect. Immun.* 57: 1050-1053.
- Matthews-Greer, J.M., and H.E. Gilleland. (1987) *J. Infect. Dis.* 155:1282-1291.
- Mattick, J.S., M.M. Mills, B.J. Anderson, B. Darylample, M.R. Mott, and J.R. Egerton. (1987) *J. Bacteriol.* 169: 33-41.
- Matsoukas, J.M., M.N. Scanlon, and G.J. Moore. (1984) *J. Med. Chem.* 27: 404-406.
- Maurer, L., and P.E. Orndoff. (1987) *J. Bacteriol.* 169:640-645.
- McEachran, D.W., and R.T. Irvin. (1985) *Can. J. Microbiol.* 31: 563-569.
- Means, G.E., and R.E. Feeney. (1990) *Bioconjugate Chem.* 1: 2-12.
- Miler, J.M., J.F. Spilsbury, R.J. Jones, E.A. Roe, and E.J.L. Lowbury. (1979) *J. Med. Microbiol.* 10: 19-27.
- Mitchell, A.R., S.B.H. Kent, M. Engelhard, and R.B. Merrifield. (1978) *J. Org. Chem.* 43: 2845-2852.
- Moore, R.A., W.A. Woodruff, and R.E.W. Hancock. (1986) *Antibiot. Chemother.* 39: 172-181.
- Morihara, K. (1963) *Biochim. Biophys. Acta* 73: 113124.
- Morihara, K., (1964) *J. Bacteriol.* 88: 745-757.
- Morihara, K., H. Tsuzuki, T. Oka, H. Inoue, and M. Ebata. (1965) *J. Biol. Chem.* 240: 3295-3304.
- Muir, L.L., R.A. Strugnell, and J.K. Davis. (1988) *Infect. Immun.* 56: 1743-1747.
- Nicholson, I.J., A.C.F. Perry, M. Virji, J.E. Heckels, and J.R. Saunders. (1987) *J. Gen. Microbiol.* 133: 825-833.
- Nunn, D., S. Bergman, and S. Lory. (1990) *J. Bacteriol.* 172: 2911-2916.
- Ofek, I., E.H. Beachey, B.I. Eisenstein, M.L. Alkan, and N. Sharon. (1979) *Rev. Infect. Dis.* 1: 832-837.
- Pace, C.N. (1990) *Trends Biotechnol.* 8: 93-100.
- Palleroni, N. (1975) in *Genetics and biochemistry of Pseudomonas*. P.H. Clarke and M.H. Richmond (eds) J. Wiley & Sons Ltd., London. pp 1-36.
- Paranchych, W. (1989) in *The Bacteria*" B.H. Iglewski and V.L. Clarke (eds.) Acad. Press, New York. vol. 11 pp.61-78.

- Paranchych, W., and L.S. Frost. (1988) *Adv. Microbiol. Physiol.* **29**: 53-114.
- Paranchych, W., L.S. Frost, and M. Carpenter. (1978) *J. Bacteriol.* **135**: 1179-1180.
- Paranchych, W., B.L. Pasloske, and P.A. Sastry. (1990) in "*Pseudomonas: biotransformations, pathogenesis and evolving biotechnology*" S. Silver, A.M. Chakrabarty, B.H. Iglewski, and S. Kaplan, (eds.), Amer. Soc. Microbiologist, Washington, D.C., pp. 343-351.
- Paranchych, W., P.A. Sastry, D. Drake, J.R. Pearlstone, and L.B. Smillie. (1985) *Antibiot. Chemother.* **36**: 49-57.
- Paranchych, W., P.A. Sastry, L.S. Frost, M. Carpenter, G.D. Armstrong, and T.H. Watts. (1979) *Can. J. Microbiol.* **25**: 1175-1181.
- Paranchych, W., P.A. Sastry, K. Volpel, B.A. Loh, and D.P. Speert. (1986) *Clin. Investig. Med.* **9**: 113-118.
- Parge, H.E., S.L. Bernstein, C.D. Deal, D.E. McRee, D. Christensen, M.A. Capozza, B.W. Kays, T.M. Fieser, D. Draper, M. So, E.D. Getzoff, and J.A. Tainer. (1990) *J. Biol. Chem.* **265**: 2278-2285.
- Parker, J.M.R., D.C. Guo, and R.S. Hodges. (1986) *Biochemistry* **25**: 5425-5432.
- Parker, J.M.R., and R.S. Hodges. (1985a) *J. Protein Chem.* **3**: 465-478.
- Parker, J.M.R., and R.S. Hodges. (1985b) *J. Protein Chem.* **3**: 479-489.
- Parker, J.M.R., C.T. Mant, and R.S. Hodges. (1987) *Chromatographia* **24**: 832-838.
- Parkkinen, J., G.N. Rogers, T. Korhonen, W. Dahr, and J. Finne. (1986) *Infect. Immun.* **54**: 37-42.
- Pasloske, B.L. (1989) *PhD Thesis*, University of Alberta, Edmonton, Canada.
- Pasloske, B.L.P., M.R. Carpenter, L.S. Frost, B.B. Findlay, and W. Paranchych. (1988) *Mol. Microbiol.* **2**: 185-195.
- Pasloske, B.L., D.S. Drummond, L.S. Frost, and W. Paranchych. (1989) *Gene* **81**: 25-34.
- Pasloske, B.L., B.B. Finlay, and W. Paranchych. (1985) *FEBS Lett.* **183**: 408-412.
- Pasloske, B.L., and W. Paranchych. (1988) *Mol. Microbiol.* **2**: 489-496.
- Pasloske, B.L., P.A. Sastry, B.B. Finlay, and W. Paranchych. (1988) *J. Bacteriol.* **170**: 3738-3741.
- Pasloske, B.L., D.G. Scraba, and W. Paranchych. (1989) *J. Bacteriol.* **171**: 2142-2147.
- Pavloskis, O.R., D.C. Edman, S.H. Leppla, B. Wretland, L.R. Lewis, and K.E. Martin. (1981) *Infect. Immun.* **32**: 681-689.

- Pavloskis, O.R., M. Pollack, L.T. Callahan, and B.H. Iglewski. (1977) *Infect. Immun.* **18**: 596-602.
- Pecha, B., D. Low, and P. O Hanley. (1989) *J. Clin. Invest.* **83**: 2102-2108.
- Pedersen, B.K., and A. Kharazmi. (1987) *Infect. Immun.* **55**: 986-989.
- Pedersen, K.B., L.O. Fioholm, and K. Bovre. (1972) *Acta Pathol. Microbiol. Scand.* **B80**: 911-918.
- Pedersen, S.S., F. Espersen, N. Hoiby, and G.H. Shand. (1989) *J. Clin. Microbiol.* **27**: 691-699.
- Pedersen, S.S., F. Espersen, N. Hoiby, and T. Jensen. (1990) *J. Clin. Microbiol.* **28**: 747-755.
- Pier, G.B. (1982) *J. Clin. Invest.* **69**: 303-308.
- Pier, G.B. (1989) *Ped. Pulmonol. Suppl.* **4**: 153.
- Pier, G.B., and S.E. Bennett. (1986) *J. Clin. Invest.* **77**: 491-495.
- Pier, G.B., W.J. Matthews Jr., and D.D. Eardley. (1983) *J. Infect. Dis.* **147**: 494-503.
- Pier, G.B., J.M. Saunders, P. Ames, M.S. Edwards, H. Auerbach, J. Goldfarb, D.P. Speert, and S. Hurwitch. (1987) *N. Eng. J. Med.* **317**: 793-798.
- Pier, G.B., H.F. Sidberry, and J.C. Sadoff. (1978) *Infect. Immun.* **22**: 919-925.
- Pier, G.B., C.J. Small, and H.B. Warren. (1990) *Science* **249**: 537-540.
- Pietta, P.G., and G.R. Marshall. (1970) *J. Chem. Soc.* **D11**: 650.
- Pitt, T.L. (1986) *J. Roy. Soc. Med.* **79**: S13-S18.
- Pollack, M.S. (1990) in "*Principles and practice of infectious diseases*" G.L. Mandell, R.G. Douglas, and J.E. Bennet (eds.) Churchill-Livingstone Inc., London. pp1673.
- Pollack, M.S., and L.S. Young. (1979) *J. Clin. Invest.* **63**: 276-286.
- Porter, R.R. (1959) *Biochem. J.* **73**: 119-126.
- Prince, A. (1986) *Am. Rev. Respir. Dis.* **134**: 644-645.
- Ramphal, R., and M. Pyle. (1983) *Infect. Immun.* **41**: 3339-3341.
- Ramphal, R., and G.B. Pier. (1985) *Infect. Immun.* **47**: 1-4.
- Ramphal, R., C. Quay, and G.B. Pier. (1987) *Infect. Immun.* **55**: 600-603.
- Ramphal, R., J.C. Sadoff, M. Pyle, and J.D. Silipigni. (1984) *Infect. Immun.* **44**: 38-40.
- Reichert, R., N. Das, and Z. Zam. (1983) *Curr. Eye Res.* **2**: 289-293.

- Rivier, J., R. McClintock, R. Galyean, and H. Anderson. (1984) *J. Chromatogr.* **288**: 303-328.
- Rothbard, J.B., R. Fernandez, and G.K. Schoolnik. (1984) *J. Exp. Med.* **160**: 208-221
- Rothbard, J.B., R. Fernandez, L. Wang, N.N.H. Teng, and G.K. Schoolnik. (1985) *Proc. Natl. Acad. Sci. USA* **82**:915-919.
- Rowlands, D.J. (1989) *Biochem. Soc. Trans.* **17**: 945-947.
- Rutter, J.M., and G.W. Jones. (1973) *Nature* **242**: 531-532.
- Sadoff, J. (1989) *Ped. Pulmonol. Suppl.* **4**: 88.
- Saiman, L., K. Ishimoto, S. Lory, and A. Prince. (1990) *J. Infect. Dis.* **161**: 541-548.
- Sastry, P.A., B.B. Finlay, B.L. Pasloske, W. Paranchych, J.R. Pearlstone, and L.B. Smillie. (1985) *J. Bacteriol.* **164**: 571-577.
- Sastry, P.A., J.R. Pearlstone, L.B. Smillie, and W. Paranchych. (1983) *FEBS Lett.* **151**: 253-255.
- Sastry, P.A., J.R. Pearlstone, L.B. Smillie, and W. Paranchych. (1985) *Can. J. Biochem. Cell Biol.* **63**: 1006-1011.
- Sato, H., and K. Okinaga. (1987) *Infect. Immun.* **55**: 1774-1778.
- Satterwhite, T.K., H.L. Dupont, D.G. Evans, and D.J. Evans. (1978) *Lancet* **2**: 181-184.
- Schmoll, T., H. Hoschutzky, J. Morschhauser, F. Lottspeich, K. Jahn, and J. Hacker. (1989) *Mol. Microbiol.* **3**: 1735-1744.
- Schoolnik, G.K., J.Y. Tai, and E.C. Gotschlich. (1983) *Prog. Allergy* **33**: 314-331.
- Schoolnik, G.K., R. Fernandez, J.Y. Tai, J.B. Rothbard, and E.C. Gotschlich. (1984) *J. Exp. Med.* **159**: 1351-1370.
- Schulze-Gahmen, U., H-D. Klenk, and K. Beyreuther. (1986) *Eur. J. Biochem.* **159**: 283-289.
- Sela, M. (1969) *Science* **166**: 1365-1374.
- Sellwood, R., R.A. Gibbons, G.W. Jones, and J.M. Rutter. (1975) *J. Med. Microbiol.* **8**: 405-411.
- Shanson, D.C. (1989) in "*Microbiology in Clinical Practice*", 2nd Edition D.C. Shanson (ed.), Wright, London, pp. 151-167.
- Sheriff, S., W.A. Hendrickson, and J.L. Smith. (1987) *J. Mol. Biol.* **197**: 273-296.
- Smart, W., P.A. Sastry, W. Paranchych, and B. Singh. (1988) *Infect. Immun.* **56**: 18-25.
- Smith, H. (1984) *J. Appl. Bacteriol.* **47**: 395-404.

- Sokol, P. (1987) *Infect. Immun.* **55**: 2021-2025.
- Spackman, D.H., W.H. Stein, and S. Moore. (1958) *Anal. Chem.* **30**: 1190-1208.
- Spencer, R.L., and F. Wold. (1969) *Anal. Biochem.* **32**: 185-190.
- Stanfield, R.L., T.M. Frieser, R.A. Lerner, and I.A. Wilson. (1990) *Science* **248**: 712-719.
- Stevens, V.C., W-S. Chou, J.E. Powell, A.C. Lee, and J. Smoot. (1986) *Immunol Lett.* **12**: 11-18.
- Steward, M.W., and C.R. Howard. (1987) *Immunol. Today* **8**: 51-58.
- Steward, J.M., and J. Young. (1984) in "Solid-phase peptide synthesis" J.M. Steward and J. Young (eds) Pierce Chem. Co.
- Strynadka, N.C.J., M.J. Redmond, J.M.R. Parker, D.G. Scraba, and R.S. Hodges. (1988) *J. Virol.* **62**: 3474-3483.
- Swanson, J. (1973) *J. Exp. Med.* **137**: 571-589.
- Tam, J.P. (1988) *Proc. Natl. Acad. Sci. USA* **85**: 5409-5413.
- Tam, J.P., and Y.A. Lu. (1989) *Proc. Natl. Acad. Sci. USA* **86**: 9084-9088.
- Towbin, H., T. Staehelin, and J. Gordon. (1979) *Proc. Natl. Acad. Sci. USA.* **76**: 4350-4354.
- Tramont, E., J. Boslego, J. Sadoff, W. Zollinger, C. Brinton, J. Bryan, and A. Labik. (1980) in "Current Chemotherapy and Infectious Disease". J.D. Nelson and C. Grassi. (eds.), American Soc. Microbiology, Washington, D.C., pp. 1240-1242.
- Tsay, G.C., and M.S. Collins. (1984) *Infect. Immun.* **45**: 217-221.
- Ulmer, A.J., J. Pryjma, Z. Tarmok, M. Ernest, and H.-D. Flad. (1990) *Infect. Immun.* **58**: 808-815.
- Van Ness, B., J.B. Howard, and J.W. Bodley. (1980) *J. Biol. Chem.* **255**: 10710-10716.
- Vishwanath, W., and R. Ramphal. (1985) *Infect. Immun.* **48**: 331-335.
- Voller, A., D. Bidwell, G. Huldtt, and E. Engvall. (1973) *Bull. WHO* pp 209-211.
- Watts, T.H., C.M. Kay, and W. Paranchych. (1982) *Can. J. Biochem.* **69**: 867-872.
- Watts, T.H., C.M. Kay, and W. Paranchych. (1983) *Biochemistry* **22**: 3640-3646.
- Watts, T.H., E.A. Worobec, and W. Paranchych. (1982) *J. Bacteriol.* **152**: 687-691.
- Watts, T.H., P.A. Sastry, R.S. Hodges, and W. Paranchych. (1983) *Infect. Immun.* **42**: 113-121.